การศึกษาการใช้แผ่นรับภาพของเครื่องถ่ายภาพทางรังสีระบบคอมพิวเตอร์เพื่อวัดความกว้างของลำรังสีจากเครื่องเอกซเรย์คอมพิวเตอร์

นายศิรภัทร ศิระโรจนกุล

วิทยานิพนธ์นี้เป็นส่วนหนึ่งของการศึกษาตามหลักสูตรปริญญาวิทยาศาสตรมหาบัณฑิต
สาขาวิชาฉายาเวชศาสตร์ ภาควิชารังสีวิทยา
คณะแพทยศาสตร์ จุฬาลงกรณ์มหาวิทยาลัย
ปีการศึกษา 2551

THE STUDY OF COMPUTED TOMOGRAPHY DOSE PROFILE WIDTH USING COMPUTED RADIOGRAPHY IMAGING PLATE

Mr.Sirapath Sirarojnkul

A Thesis Submitted in Partial Fulfillment of the Requirements
for the Degree of Master of Science Program in Medical Imaging
Department of Radiology
Faculty of Medicine
Chulalongkorn University
Academic Year 2008

Thesis Title	THE STUDY OF COMPUTED TOMOGRAPHY DOSE PROFILE WIDTH USING COMPUTED RADIOGRAPHY IMAGING PLATE
By	Mr.Sirapath Sirarojnkul
Field of Study	Medical Imaging
Advisor	Associate Professor Sivalee Suriyapee

Accepted by the Faculty of Medicine, Chulalongkorn University in Partial Fulfillment of the Requirements for the Master's Degree

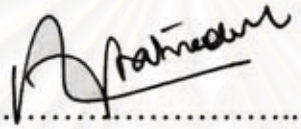

..... Dean of the Faculty of Medicine
(Associate Professor Adisorn Patradul, M.D.)

THESIS COMMITTEE

.....Chairman
(Associate Professor Anchali Krisanachinda, Ph.D.)

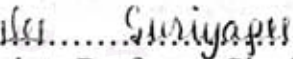

.....Thesis Advisor
(Associate Professor Sivalee Suriyapee)

.....Examiner
(Assistant Professor Kiat Arjhansiri, M.D.)

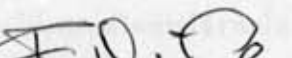

.....External Examiner
(Professor Franco Milano, Ph.D.)

ศิรภัทร ศิระโรจนกุล: การศึกษาการใช้แผ่นรับภาพของเครื่องถ่ายภาพทางรังสีระบบคอมพิวเตอร์เพื่อวัดความกว้างของลำรังสีจากเครื่องเอกซเรย์คอมพิวเตอร์ (THE STUDY OF COMPUTED TOMOGRAPHY DOSE PROFILE WIDTH USING COMPUTED RADIOGRAPHY IMAGING PLATE) อ.ที่ปรึกษาวิทยานิพนธ์หลัก: รศ.ศิวลี สุริยาปี; 91 หน้า

การควบคุมคุณภาพของเครื่องเอกซเรย์คอมพิวเตอร์นั้น ในปัจจุบันได้ใช้ฟิล์มเพื่อทำการตรวจสอบความกว้างของลำรังสีจากเครื่องเอกซเรย์คอมพิวเตอร์ แต่ในทางรังสีวิทยา ปัจจุบันนี้ฟิล์มได้ลดบทบาทลงไป จุดประสงค์ในการศึกษานี้คือ การศึกษาการใช้แผ่นรับภาพของเครื่องถ่ายภาพทางรังสีระบบคอมพิวเตอร์หาค่าพารามิเตอร์และเทคนิคที่เหมาะสมในการใช้งาน เพื่อวัดความกว้างของลำรังสีจากเครื่องเอกซเรย์คอมพิวเตอร์และเปรียบเทียบผลที่ได้กับวิธีการที่ใช้ฟิล์ม

แผ่นรับภาพของเครื่องถ่ายภาพทางรังสีระบบคอมพิวเตอร์ของบริษัทฟูจิ และฟิล์มวัดปริมาณรังสีรุ่น เอกส์ โอแมต วี ของบริษัทโกดัก เป็นเครื่องมือเก็บข้อมูลความกว้างของลำรังสีจากเครื่องเอกซเรย์คอมพิวเตอร์ รุ่น จีอี ไลท์สปีด อาร์ที เพื่อหาความสัมพันธ์ระหว่างค่าความดำของภาพกับปริมาณรังสีที่ได้รับ เครื่องมืออ่านข้อมูลประกอบด้วย เครื่องอ่านแผ่นรับภาพ รุ่น เอฟซีอาร์ เอกส์จี 5000 ของบริษัทฟูจิ เครื่อง ไวดาร์ โดสสิมิตรี โปร วีเอกส์อาร์16 อ่านค่าความดำของฟิล์ม เครื่องวัดค่าปริมาณรังสี อันฟอส เอกส์ไอวัดปริมาณรังสี ในการศึกษานี้ ใช้แท่งเซอโรเบนด์กับแผ่นตะกั่ว เพื่อกรองและจำกัดทิศทางของลำรังสีในขณะศึกษาด้วยแผ่นรับภาพของเครื่องถ่ายภาพทางรังสีระบบคอมพิวเตอร์

กราฟความสัมพันธ์ของความดำของฟิล์มกับปริมาณรังสี ที่ 120 กิโลโวลเทจ แสดงผลความสัมพันธ์เป็นเส้นตรงในช่วงปริมาณรังสีสูง ส่วนแผ่นรับภาพของเครื่องถ่ายภาพทางรังสีระบบคอมพิวเตอร์นั้นมีความสัมพันธ์กันเป็นเส้นตรงในช่วงแรก และเกิดการอิ่มตัวของความดำเมื่อได้รับรังสีจากการตั้งค่ามากกว่า 20 มิลลิแอมแปร์วินาที ในการศึกษานี้จึงทำการเก็บข้อมูลที่ 10 มิลลิแอมแปร์วินาที ค่าความกว้างของลำรังสีวัดที่จุดซึ่งมีค่าเป็นครึ่งหนึ่งของค่าความดำสูงสุดของภาพ โดยกำหนดให้ลำรังสีมีความกว้าง 5, 10, 15 และ 20 มิลลิเมตร ภาพที่เก็บโดยฟิล์มเมื่อทำการวัดในภาพที่สร้างจากค่าความดำของฟิล์ม ได้ค่าความกว้างของลำรังสี 7.7, 11.7 ,17.1 และ 20.5 มิลลิเมตร ตามลำดับ เมื่อทำการสร้างภาพจากรังสีโดยเปลี่ยนจากค่าความดำของฟิล์มเป็นปริมาณรังสี จากความสัมพันธ์ระหว่างค่าความดำกับปริมาณรังสี ค่าความกว้างเปลี่ยนเป็น 6.9, 11.3 ,16.5 และ 20 มิลลิเมตร สำหรับแผ่นรับภาพของเครื่องถ่ายภาพทางรังสี เมื่อทำการวัดในภาพที่สร้างจากค่าความดำของภาพที่ละดิจูดเท่ากับ 1 เซนซิติวิตี้เท่ากับ 5 ได้ค่าความกว้าง 7.8, 11.6 ,16.95 และ 20.1 มิลลิเมตร และเมื่อทำเป็นปริมาณรังสีที่ละดิจูดเท่ากับ 4 เซนซิติวิตี้เท่ากับ 200 ค่าความกว้างของลำรังสีที่วัดได้คือ 7.65, 11.3 ,16.5 และ 19.95 มิลลิเมตร

ผลการทดลองสรุปได้ว่า แผ่นรับภาพของเครื่องถ่ายภาพทางรังสีนั้นสามารถใช้แทนฟิล์มได้เมื่อตั้งค่าพารามิเตอร์ที่เหมาะสมตามการใช้งาน แต่ในการใช้งานนั้นต้องใช้อุปกรณ์กรองรังสีเพื่อป้องกันไม่ให้แผ่นรับภาพของเครื่องถ่ายภาพทางรังสีได้รับรังสีมากเกินไป สำหรับพารามิเตอร์ที่ดีที่สุดในการหาค่าความกว้างของลำรังสีที่สร้างโดยค่าความดำนั้นคือ ละดิจูดเท่ากับ 1 เซนซิติวิตี้เท่ากับ 5 ส่วนภาพที่สร้างโดยค่าปริมาณรังสีนั้นพารามิเตอร์ที่ดีที่สุดคือ ละดิจูดเท่ากับ 4 เซนซิติวิตี้เท่ากับ 200

ภาควิชา .....รังสีวิทยา..... ลายมือชื่อนิสิต....ศิรภัทร ศิระโรจนกุล.....

สาขาวิชา .....ฉายาเวชศาสตร์..... อ.ที่ปรึกษาวิทยานิพนธ์หลัก.ศิวลี สุริยาปี.....

ปีการศึกษา.....2551.....

5074831830 MAJOR MEDICAL IMAGING
KEYWORD: COMPUTED TOMOGRAPHY (CT), COMPUTED RADIOGRAPHY IMAGING PLATE (CR IP), PHOTOSTIMULABLE PHOSPHOR (PSP), CT DOSE PROFILE WIDTH.

SIRAPATH SIRAROJNKUL: THE STUDY OF COMPUTED TOMOGRAPHY DOSE PROFILE WIDTH USING COMPUTED RADIOGRAPHY IMAGING PLATE: THESIS ADVISOR: ASSOC. PROF. SIVALEE SURIYAPEE, 91 pp.

The quality control of the CT scanner is usually performed by using the film for the dose profile, but film processing is becoming less available in department of radiology. The purpose of this study is to measure the computed tomography (CT) profile width using computed radiography imaging plate (IP) and compared the profile with the measurement from verification film. The suitable parameters of image plate were selected for optimal exposure.

Fuji CR IP and Kodak X-Omat V film were exposed to GE LightSpeed RT to study the relation between pixel value or optical density and exposure at 120 kVp, 10-40 mAs, 10 mm collimator. IP was read by Fuji FCR-XG5000 CR reader. Optical density was read by Vidar DosimertyPro VXR-16. The exposure was measured by Unfors Xi semiconductor detector. Cerrobend block combined with lead plate were used to filter the energy of the x-ray beams. The dose profile widths were measured for 5, 10, 15 and 20 mm for both film and IP.

The characteristic curves irradiated with computed tomography scanner plotted in semi- log scales between exposure and pixel value showed linearity for film in the high exposure range. For IP, the pixel value saturated at 20 mAs, so the dose of about 10 mAs was selected to study the width of profile. The full width at half maximum measured by film of 5, 10, 15 and 20 mm. collimator beam were 7.7, 11.7, 17.1, and 20.5 mm, respectively, for the plotted of pixel value. When changing the pixel value to exposure, the full widths at half maximum were 6.9, 11.3, 16.5, and 20 mm, respectively. For IP, CT dose profiles were plotted by pixel value and exposure. By pixel value, the CT dose profile widths were 7.8, 11.6, 16.95 and 20.1 mm at L = 1 S = 5, and by exposure were 7.65, 11.3, 16.5 and 19.95 mm at L = 4 S = 200.

IP can be used to measure the CT profile width comparable to film. However, the filter needed to be used to avoid the overexposure of IP in CT scanner. For plotting the profile in pixel value, the best parameter was L = 1 S = 5 because the scatter was taken out and it has high contrast. For the CT dose profile width plotted by exposure, the best parameter is L = 4 S = 200. If S value was increased, the dose profile width was narrower. The deviation from collimator width was less when using exposure instead of pixel values or optical density for both film and IP.

Department Radiology Student's Signature Sirapath Sirarojnkul
Field of Study Medical Imaging Advisor's Signature Sivalee Suriyapee
Academic Year 2008

ACKNOWLEDGEMENTS

The success of this thesis could be attributed to the extensive support and assistance from my major advisor, Assoc. Prof. Sivalee Suriyapee and my co-advisor, Mr.Sornjarod Oonsiri, Mrs Petchaleeya Suwanpradit. I deeply thank them for their valuable advice and guidance in this research.

I wish to thank Assistant Professor Kiat Arjhansiri for my thesis committee and Professor Franco Milano, Florence University, Italy, for their kindness, helpful and valuable suggestion.

I would like to thank Assoc. Prof. Somjai Wangsuphachart, Chief of Department of Radiology, Faculty of Medicine, Chulalongkorn University for her kindness, helpful and valuable suggestion.

I would like to thank Assoc. Prof. Katsumi Tsujioka for his guideline for the measurement and introduced for ImageJ .

I would like to thank Ms.Chotika Jampangern, Mr.Taweap Sanghangthum, Mr.Isra Israngkul Na Ayuthaya, Ms.Pantiwa Insang and medical staff in Division of Radiation Oncology, Department of Radiology, King Chulalongkorn Memorial Hospital for their kindness in examining the research instrument and providing suggestions for improvement.

I would like to thank medical staffs in the computed tomography room and x – ray room No. 3, Department of Radiology, King Chulalongkorn Memorial Hospital for their kindness in examining the research instrument.

I am grateful to all the lecturers and staff of Medical Imaging, Chulalongkorn University, for supplying me academic knowledge on Medical Imaging.

Finally, I am grateful to my family for their financial support, entirely care, and love. The usefulness of this thesis, I dedicate to my father, my mother and all the teachers.

CONTENTS

LIST OF TABLES

Table **Page**

LIST OF FIGURES

Figure **Page**

Figure **Page**

Figure **Page**

LIST OF ABBREVIATIONS

Abbreviation	Term
°c	Degree celcius
μ	Attenuation coefficient
2D	Two dimensions
3D	Three dimensions
A	Atomic mass
ADC	Analog-to-digital converter
AgBr	Silver bromide
$AgNO_3$	Silver halide
BaFBr	Barium-fluoro-bromide
CCD	Charge-coupled-device
cGy	Centigray
cm	Centimeter
cm^3	Cubic centimeter
CR	Computed radiography
CT	Computed tomography
CV	Coefficient of variation
DICOM	Digital Imaging and Communications in Medicine
EDR	Exposure data recognizer
ESR	Electron spin resonance
Eu	Europium
FOV	Field of view
FWHM	Full width at half maximum

Abbreviation	Term
g/cm^3	Gram per cubic centimeter
I	Iodine
ICRP	International Commission on Radiological Protection
IP	Imaging plate
keV	Kiloelectronvolt
kV	Kilovoltage
kVp	Kilovoltage-peak
L	Latitude
mAs	Milliampere-second
MeV	Megaelectronvolt
mGy	Milligray
mm	Millimeter
mmAl	Millimeter-aluminum
MSCT	Multi-slice computed tomography
mSv	Millisievert
nC	Nanocoulomb
OD	Optical density
PA	Postero-anterior
PACS	Picture Archiving and Communication System
PMT	Photomultiplier tube
PSL	Photostimulated luminescence
PSP	Photostimulable phosphor

Abbreviation	Term
QC	Quality control
R	Roentgen
S	Sensitivity
SD	Standard deviation
Sv	Sievert
Z	Atomic number

CHAPTER I

INTRODUCTION

1.1 Background and rationale [1]

A Computed Tomography (CT) scan samples of a thin slab of tissue; ideally only the imaged slab is irradiated, and its thickness equals to the selected slice width. Inaccuracies arise from scanner & sign limitations and calibration of collimator settings. Most systems collimate the z axis dimension of the x-ray beam at both the source (patient collimation) and detectors (postpatient collimation) figure 1.1 shows the position of prepatient and postpatient collimator . Width of the imaged slice (from sensitivity profile) is determined by both sets of collimators. Width of the tissue irradiated (from dose profile) is a function only of the prepatient collimator.

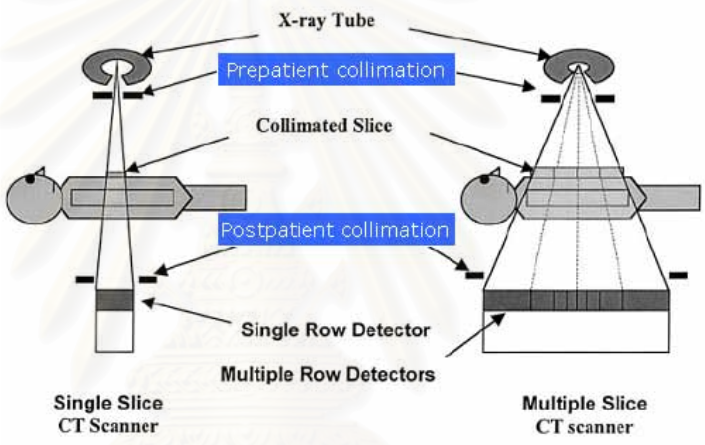

Figure 1.1 Pre-patient and post-patient collimator, prepatient collimator is used to adjust the beam width irradiated to patient , postpatient collimator is used to adjust the beam width on detector.

The quality control of the CT scanner is performed by using the film for the dose profile, but film processing are becoming less available in department of radiology, however, some published work showed the method of using computed radiography imaging plate for measuring the beam profile with variety of processing conditions.

If film or the imaging plate were irradiated by the x-ray source, the intensity from that source will effect to the optical density for the film or the pixel value for imaging plate, this result related to the exposure which was given to them, more exposure will get more density.

The optical density measured from the irradiated film has the linear relationship with the log exposure. The characteristic curve (H&D curve) of film and exposure is a straight line in a selected range of exposure. If film is irradiated in appropriate exposure quantity, the good image of beam profile would be obtained. However, the film response depends on the film processing condition. To reduce the uncertainty of film response, the quality control of film processor should be performed before using and the calibration of film densitometer needed to be undertaken.

The characteristic curve of the imaging plates is different from film, the characteristic curve is plotted between the pixel values and log exposure, If the imaging plate gets too much exposure, the saturation of the signal will be displayed. The pixel value will not increase when we increase the exposure. To use the imaging plate, the parameter setting and exposure technique which affect the pixel values must be selected for suitable dose profile image.

The dose profile (or radiation profile, beam profile) describes the distribution of radiation energy within a continuous medium along a line parallel to the scanner rotational axis. Like any x-ray field, radiation energy peaks in the center of the field and falls off diffusely at the edges shown in figure 1.2. Edge fall off is due to scatter within the field and collimator penumbra. The magnitude of penumbra depends on the z dimension of the focal spot (parallel to scan rotation axis) and focus collimator-patient geometry. The z-axis dimensions for rotating anode x-ray tube foci are typically less than 2 mm, but may be much larger in a stationary anode tube (rarely used in modem systems). Penumbra is typically much worse in the latter. The dose profile was obtained by measuring the full width at half maximum (FWHM), the FWHM of the CT dose profile is the distance between the two locations with the half of the maximum density.

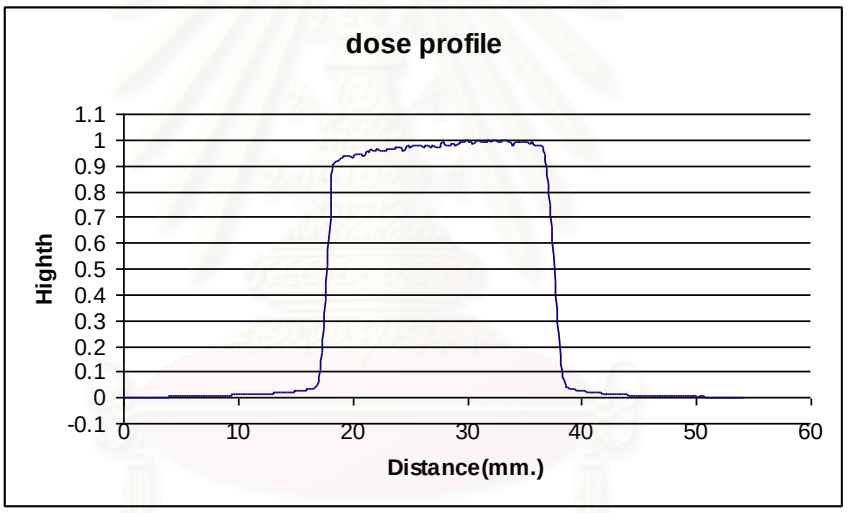

Figure 1.2 The shape of dose profile

For this study, the Fuji CR imaging plate which used at King Chulalongkorn Memorial Hospital will be employed for the measurement of the CT dose profile and compared with the measurement by film.

If a dose profile width collected by our CR imaging plates was acceptable , the result could be used to find dose profile width in the future when dark rooms are out of service or film is roll out. The accurate dose profile could indicate the setting of the pre-patient collimator to be aware of an overexposure.

1.2 Objective

1. To measure the computed tomography dose profile width using computed radiography imaging plate.
2. To determine difference of computed tomography dose profile width measured by computed radiography imaging plate and verification film.

CHAPTER II

REVIEW OF RELATED LITERATURES

2.1 Theory

2.1.1 Computed tomography [2]

2.1.1.1 Basic principle

The mathematical principles of CT were first developed by Radon in 1917. Radon's treatise proved that an image of an unknown object could be produced if one had an infinite number of projections through the object. We can understand the basic idea behind tomographic imaging with an example taken from radiography.

With plain film imaging, the three-dimensional (3D) anatomy of the patient is reduced to a two-dimensional (2D) projection image. The density at a given point on an image represents the x-ray attenuation properties within the patient along a line between the x-ray focal spot and the point on the detector corresponding to the point on the image. Consequently, with a conventional radiograph of the patient's anatomy, information with respect to the dimension parallel to the x-ray beam is lost. This limitation can be overcome, at least for obvious structures, by acquiring both a postero-anterior (PA) projection and a lateral projection of the patient. For example, the PA chest image yields information concerning height and width, integrated along the depth of the patient, and the lateral projection provides information about the height and depth of the patient, integrated over the width dimension, they are shown in figure 2.1. For objects that can be identified in both images, such as a pulmonary nodule on PA and lateral chest radiographs, the two films provide valuable location information. For more complex or subtle pathology, however, the two projections are not sufficient. Imagine the instead of just two projections, a series of 360 radiographs were acquired at 1-degree angular intervals around the patient's thoracic cavity. Such a set of images provides essentially the same data as a thoracic CT scan. However, the 360 radiographic images display the anatomic information in a way that would be impossible for a human to visualize: cross-sectional images. If these 360 images were stored into a computer, the computer could in principle reformat the data and generate a complete thoracic CT examination.

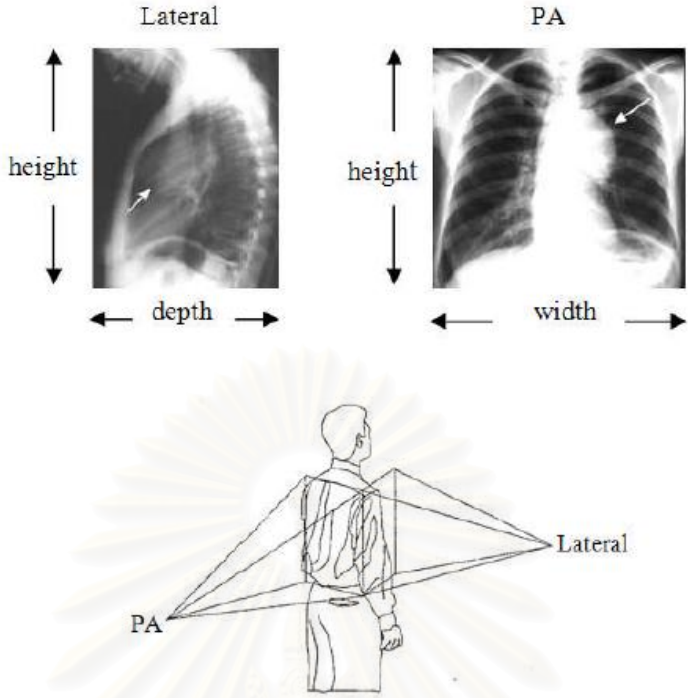

Figure 2.1 Postero-anterior and lateral chest radiographs.

The tomographic image is a picture of a slap of the patient's anatomy. The 2D CT image corresponds to a 3D section of the patient, so that even with CT, three dimensions are compressed into two. However, unlike the case with plain film imaging, the CT slice-thickness is very thin (1 to 10 mm) and is approximately uniform. The 2D array of pixels (picture elements) in the CT image corresponds to an equal number of 3D voxels (volume elements) in the patient. Voxels have the same in-plane dimensions as pixels, but they also include the slice thickness dimension. Each pixel on the CT image displays the average x-ray attenuation properties of the tissue in the corresponding voxel, it is shown in figure 2.2.

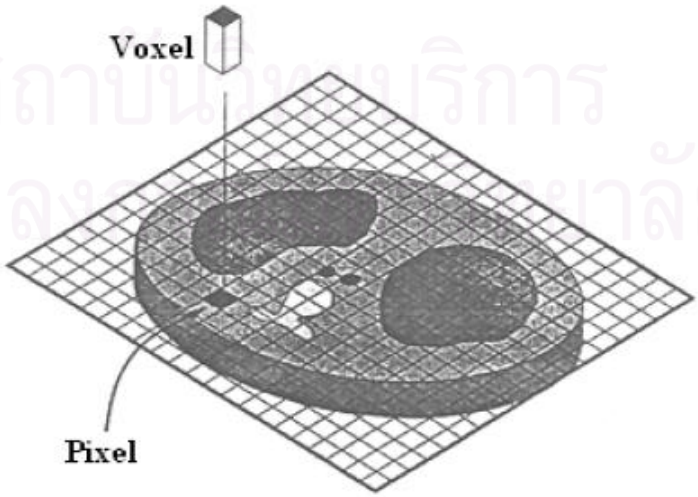

Figure 2.2 Pixel and voxel of a digital image.

2.1.1.2 Tomographic acquisition

A single transmission measurement through the patient made by a single detector at a given moment in time is called a ray. A series of rays that pass through the patient at the same orientation is called a projection or view. There are two projection geometries that have been used in CT imaging, they are shown in figure 2.3. The more basic type is parallel beam geometry, in which all of the rays in a projection are parallel to each other. In fan beam geometry, the rays at a given projection angle diverge and have the appearance of a fan. All modern CT scanners incorporate fan beam geometry in the acquisition and reconstruction process. The purpose of the CT scanner hardware is to acquire a large number of transmission measurements through the patient at different positions. The acquisition of a single axial CT image may involve approximately 800 rays taken at 1,000 different projection angles, for a total of approximately 800,000 transmission measurements. Before the axial acquisition of the next slice, the table that the patient is lying on is moved slightly in the cranial-caudal direction (the z-axis of the scan), which positions a different slice of tissue in the path of the x-ray beam for the acquisition of the next image.

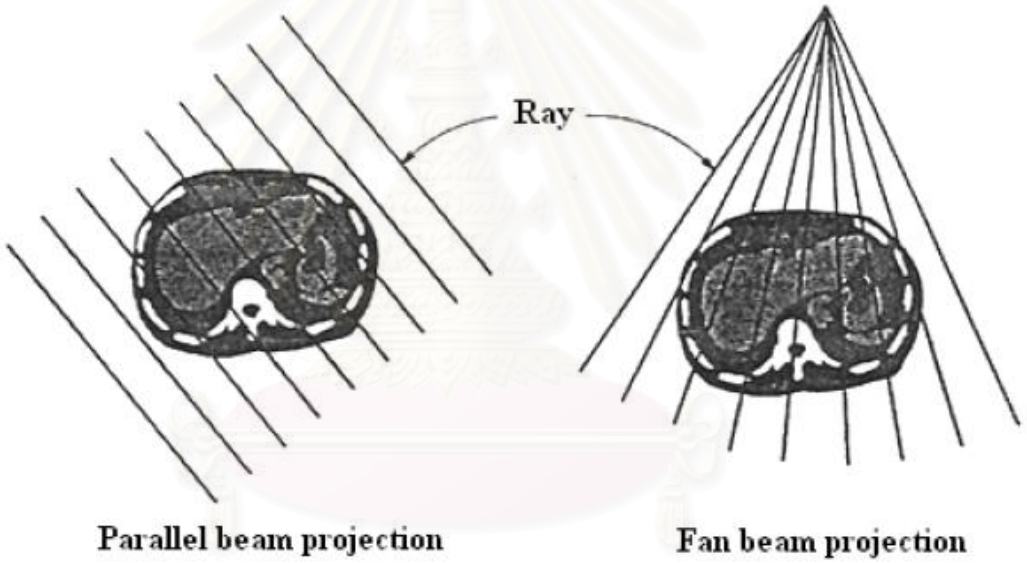

Figure 2.3 Two types of computed tomography beam projection.

2.1.1.3 Tomographic reconstruction

Each ray that is acquired in CT is a transmission measurement through the patient along a line, where the detector measures an x-ray intensity, I_t. The unattenuated intensity of the x-ray beam is also measured during the scan by a reference detector, and this detects x-ray intensity I_0. The relationship between I_t and I_o is given by

$$I_t = I_0 e^{-\mu t} \qquad (1)$$

Where t is the thickness of the patient along the ray and μ is the average linear attenuation coefficient along the ray. Notice that I_t and I_o are machine-dependent values, but the product μt is an important parameter relating to the anatomy of the

patient along a given ray. When the equation is rearranged, the measured values I_t and I_o can be used to calculate the parameter of interest:

$$\ln(\frac{I_0}{I}) = \mu t \qquad (2)$$

Where ln is the natural logarithm (to base *e*, *e* = 2.78…), *t* ultimately cancels out, and the value μ for each ray is used in the CT reconstruction algorithm. This computation, which is a preprocessing step performed before image reconstruction, reduces the dependency of the CT image on the machine-dependent parameters, resulting in an image that depends primarily on the patient's anatomic characteristics. This is very much a desirable aspect of imaging in general, and the high clinical utility of CT results, in part, from this feature. By comparison, if it is overexposed (I_o too high) it appears too dark. The density of CT images is independent of I_o, although the noise in the image is affected.

After preprocessing of the raw data, a CT reconstruction algorithm is used to produce the CT images. There are numerous reconstruction strategies; however, filtered back projection reconstruction is most widely used in clinical CT scanners. The back projection method builds up the CT image in the computer by essentially reversing the acquisition steps. During acquisition, attenuation information along a known path of the narrow x-ray beam is integrated by a detector. During back projection reconstruction, the μ value for each ray is smeared along this same path in the image of the patient. As the data from a large number of rays are back projection onto the image matrix, areas of high attenuation tend to reinforce each other, and areas of low attenuation also reinforce, building up the image in the computer.

2.1.1.4 Computed tomography number

After CT reconstruction, each pixel in the image is represented by a high precision floating point number that is useful for computation but less useful for display. Most computer display hardware makes use of integer images. Consequently, after CT reconstruction, but before storing and displaying, CT images are normalized and truncated to integer values. The number CT(*x*,*y*) in each pixel, (*x*,*y*), of the image is converted using this equation

$$CT(x, y) = \frac{\mu_{(x,y)} - \mu_{water}}{\mu_{water}} \times 1000 \qquad (3)$$

Where $\mu_{(x,y)}$ is the attenuation coefficient of the $\mu_{(x,y)}$ pixel before conversion, μ_{water} is the attenuation coefficient of water, and $CT_{(x,y)}$, is the CT number (Hounsfield unit) that ends up in the final clinical CT image. The value of μ_{water} is about 0.195 for the x-ray beam energies typically used in CT scanning. This normalization results in CT numbers ranging from about - 1,000 to + 3,000, where - 1,000 corresponds to air, soft tissues range from - 300 to - 100, water is 0, and dense bone and areas filled with contrast agent range up to + 3,000.

CT images are produced with a highly filtered, high-kV x-ray beam, with an average energy of about 75 keV. At this energy in muscle tissue, about 91% of x-ray interactions are Compton scatter. For fat and bone, Compton scattering interactions are 94% and 74%, respectively. Therefore, CT numbers and hence CT images derive

their contrast mainly from the physical properties of tissue that influence Compton scatter. Density (g/cm^3) is a very important discriminating property of tissue (especially in lung tissue, bone, and fat), and the linear attenuation coefficient, μ, tracks linearly with density. Other than physical density, the Compton scatter cross section depends on the electron density (ρ_e) in tissue: $\rho_e = NZ/A$, where N is Avogadro's number (6.023×10^2, a constant), Z is the atomic number, and A is the atomic mass of the tissue. The main constituents of soft tissue are hydrogen (Z = 1, A = 1), carbon (Z = 6, A = 12), nitrogen (Z =7, A = 14), and oxygen (Z = 8, A = 16).

Carbon, nitrogen, and oxygen all have the same Z/A ratio of 0.5, so their electron densities are the same. Because the Z/A ratio for hydrogen is 1.0, the relative abundance of hydrogen in a tissue has some influence on CT number. Hydrogenous tissue such as fat is well visualized on CT. Nevertheless, density (g/cm^3) plays the dominant role in forming contrast in medical CT.

CT numbers are quantitative, and this property leads to more accurate diagnosis in some clinical settings. For example, pulmonary nodules that are calcified are typically benign, and the amount of calcification can be determined from the CT image based on the mean CT number of the nodule. Measuring the CT number of a single pulmonary nodule is therefore common practice, and it is an important part of the diagnostic work-up. CT scanners measure bone density with good accuracy, and when phantoms are placed in the field along with the patient, quantitative CT techniques can be used to estimate bone density, which is useful in assessing fracture risk. CT is also quantitative in terms of linear dimensions, and therefore it can be used to accurately assess tumor volume or lesion diameter.

2.1.1.5 Geometry and historical development

A) The first generation

CT scanners represent a marriage of diverse technologies, including computer hardware, motor control systems, x-ray detectors, sophisticated reconstruction algorithms, and x-ray tube/generator systems. The first generation of CT scanners employed a rotate/translate, pencil beam system. Only two x-ray detectors were used, and they measured the transmission of x-rays through the patient for two different slices. The acquisition of the numerous projections and the multiple rays per projection required that the single detector for each CT slice be physically moved throughout all the necessary positions. This system used parallel ray geometry. Starting at a particular angle, the x-ray tube and detector system translated linearly across the field of view (FOV), acquiring 160 parallel rays across a 24 cm FOV. When the x-ray tube/detector system completed its translation, the whole system was rotated slightly, and then another translation was used to acquire the 160 rays in the next projection. This procedure was repeated until 180 projections were acquired at 1 degree intervals.

B) The second generation

The next incremental improvement to the CT scanner was the incorporation of a linear array of 30 detectors. This increased the utilization of the x-ray beam by 30 times, compared with the detector used per slice in first-generation systems. A relatively narrow fan angle of 10 degree was used. In principle, a reduction in scan

time of about 30-fold could be expected. However, this reduction time was not realized, because more data were acquired to improve image quality.

C) The third generation

The number of detectors used in the third-generation scanners was increased substantially (to more than 800 detectors), and the angle of the fan beam was increased so that the detector array formed an arc wide enough to allow the x-ray beam to interrogate the entire patient. Because detectors and the associated electronics arc expensive, this led to more expensive CT scanners. However, spanning the dimensions of the patient with an entire row of detectors eliminated the need for translation motion. The multiple detectors in the detector array capture the same number of ray measurements in one instant as was required by a complete translation in the earlier scanner systems. The mechanically joined x-ray tube and detector array rotation together around the patient without translation. The motion of third generation CT is rotate/translate, referring to the rotation of the x-ray tube and the rotation of the detector array. By elimination of the translational motion, the scan time is reduced substantially.

D) The fourth generation

The fourth-generation CT scanners were designed to overcome the problem of ring artifacts. With the fourth-generation scanners, the detectors are removed from the rotating gantry and are placed in a stationary 360-degree ring around the patient, requiring many more detectors. Modern fourth-generation CT systems use about 4,800 individual detectors. Because the x-ray tube rotates and the detectors are stationary, fourth-generation CT is said to use a rotate/stationary geometry. During acquisition with a fourth-generation scanner, the divergent x-ray beam emerging from the x-ray tube forms a fan-shaped x-ray beam. However, the data are processed for fan beam reconstruction with each detector as the vertex of a fan, the rays acquired by each detector being fanned out to different positions of the x-ray source.

E) The fifth generation

A novel CT scanner has been developed specifically for cardiac tomographic imaging. This cine-CT scanner does not use a conventional x-ray tube; instead, a large arc of tungsten encircles the patient and lies directly opposite to the detector ring. The x-rays arc produced from the focal track as a high-energy electron beam strikes the tungsten. There are no moving parts to this scanner gantry. The electron beam is produced in a cone-like structure (a vacuum enclosure) behind the gantry and is electronically steered around the patient so that it strikes the annular tungsten target. Cine-CT systems, also called electron beam scanners, are marketed primarily to cardiologists. They are capable of 50-msec scan times and can produce fast-frame-rate CT movies of the beating heart.

F) The sixth generation

In the early 1990s, the design of the third- and fourth-generation scanners evolved to incorporate slip ring technology. A slip ring is a circular contract with sliding brushes that allows the gantry to rotate continually, untethered by wires. The

use of slip-ring technology eliminated the inertial limitations at the end of each slice acquisition, and the rotating gantry was free to rotate continuously throughout the entire patient examination. This design made it possible to achieve greater rotational velocities than with systems not using a slip ring, allowing shorter scan times. Helical CT (also inaccurately called spiral CT) scanners acquire data while the table is moving; as a result, the x-ray source moves in a helical pattern around the patient being scanned. Helical CT scanners use either third- and fourth-generation slip-ring designs. By avoiding the time required to translate the patient table, the total scan time required to image the patient can be much shorter. Consequently, helical scanning allows the use of less contrast agent and increase patient throughput. In some instances the entire scan can be performed within a single breath-hold of the patient, avoiding inconsistent levels of inspiration. The advent of helical scanning has introduced many different considerations for data acquisition. In order to produce reconstructions of planar sections of the patient, the raw data from the helical data set are interpolated to approximate the acquisition of planar reconstruction data. The speed of the table motion relative to the rotation of the CT gantry is a very important consideration, and the pitch is a parameter that describes this relationship.

G) The seventh generation

X-ray tubes designed for CT have impressive heat storage and cooling capabilities, although the instantaneous production of x-rays (i.e., x-rays per mAs) is constrained by the physics governing x-ray production. An approach to overcoming x-ray tube output limitations is to makes better use of the x-rays that are produced by the x-ray tube. When multiple detector arrays were used, the collimator spacing was wider and therefore more of the x-ray that was produced by the x-ray tube was used in producing image data. With conventional, single detector array scanners, opening up the collimator increases the slice thickness, which was good for improving the utilization of the x-ray beam but reduce spatial resolution in the slice thickness dimension. With the introduction of multiple detector arrays, the slice thickness was determined by the detector size and not by the collimator.

2.1.2 Slice thickness

2.1.2.1 Single detector array scanners

The slice thickness in single detector array CT system is determined by the physical collimation of the incident x–ray beam with two lead jaws. As a gap between two lead jaws widen, the slice thickness increases. The width of the detectors place an upper limit on slice thickness. Open the collimator beyond the point do not increase slice thickness, but would be increase the dose to patient and scatter radiation.

CT imaging as literally having the geometry of slab of tissue, but this is not actually the case. The contrast of a small highly attenuated ball is greater if the bearing is in the center of CT slice and the contrast decrease as the bearing moves toward the edge of the slice, shown in figure 2.4, this effect describes the slice sensitivity profile. Helical scans have a slightly broader slice sensitivity profile due to translation of the patient during the scan. The nominal slice thickness is that width is set on the scanner control panel. The nominal slice width is thought of having a rectangular slice sensitivity profile.

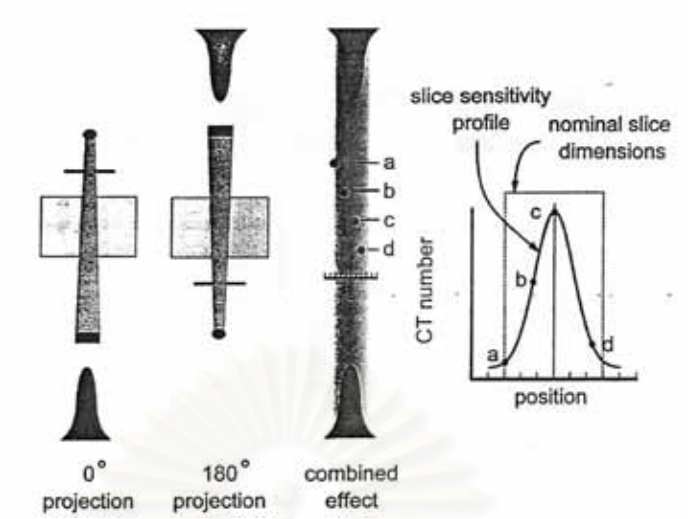

Figure 2.4 The acquisition process of single detector array scanner.

2.1.2.2 Multiple detector array scanners

The slice thickness of multi detector array CT scanners is determined not by the collimation, but rather by the width of the detectors in the slice thickness dimension. The width is changed by binning different number of individual detectors element together. The signals generated by adjacent detector elements are summed. Multiple detector arrays can be used both in conventional axial scanning and in helical scanning protocols. In axial scanning with no table movement, the width almost completely dictates the thickness of slice. For two slices at the edge of the scan, the inner side of the slice is determined by the edge of the detector, but outer edge of the slice is determined either by the collimation penumbra or the outer edge of detector, depend on the collimator adjustment, shown in figure 2.5. In helical mode, each detector array contributes to every reconstructed image, the slice sensitivity profile for each detector need to be similar to reduce artifacts.

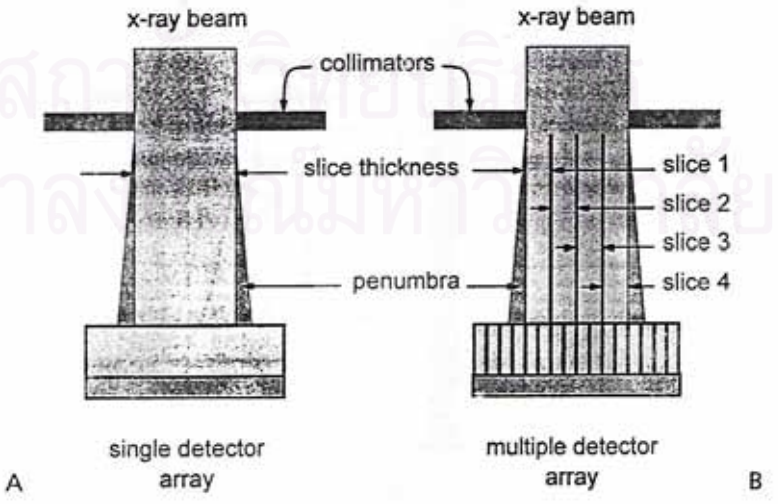

Figure 2.5 Comparison of the acquisition process between A) single detector array scanners and B)multiple detector array scanners (axial mode).

2.1.2.3 Detector pitch and collimation pitch

Pitch is a parameter that comes to play when the helical scan protocols are used. In the helical CT with one detector array, the pitch is determined by the collimator (collimator pitch) and is defined as

$$\text{collimator pitch} = \frac{\text{table movement per 360 degree rotation of gantry}}{\text{collimator width at isocenter}} \qquad (4)$$

The collimator pitch represents the traditional notation of pitch (figure 2.6) for single detector array scanners, a pitch of 1.0 implies that the number of CT view acquired, when averaged over long axis of the patient, is comparable to the number acquired with contiguous axial CT. the pitch less than 1.0 may result some slight improvement in image quality and higher relation dose to patient. The pitch greater than 1.0 is faster scan time, less patient motion, but decreases the image quality.

CT acquisition around 360 degrees are typical for images of the highest fidelity, the minimum requirement to produce an adequate CT image is scan of 180 degrees plus the fan angle. Which fan angle commonly at about 60 degrees, this means that (180+60)/360 = 0.66 of the full circle is required. This implied that upper limit on pitch should be about 1:0.66, or 1.5, because 66% of data in a 1.5 pitch scan remain contiguous.

Scanners that have multiple detector arrays required a different definition, the detector pitch is also useful concept for multiple detector array scanner, and it defined as

$$\text{detector pitch} = \frac{\text{table movement per 360 degree rotation of gantry}}{\text{detector width}} \qquad (5)$$

The need to define detector pitch and collimator pitch arises because beam utilization between single and multiple detector array scanners is different, for N detector arrays the collimator pitch is

$$\text{collimator pitch} = \frac{\text{detector pitch}}{N} \qquad (6)$$

For scanner with four detector arrays, detector pitches running from 3 to 6 are used. A detector pitch of 3 for a four detector arrays is equivalent to a collimator pitch of 0.75 (3/4) and pitch of 6 is 1.5(6/4).

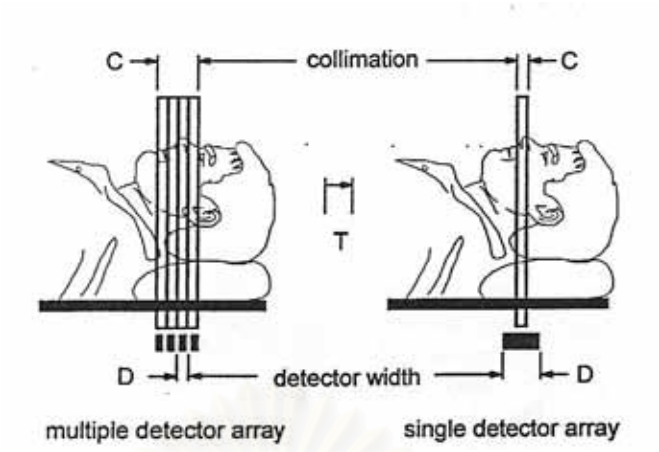

Figure 2.6 The collimator width (C) and the detector width (D), when the table moving with transition distance during the 360 degrees gantry rotation (T), collimator pitch defined as T/C , and detector pitch defined as T/D. for the four detector arrays scanner, collimator pitch of 1.0 is equal to the detector pitch of 4.0

2.1.3 Computed radiography

2.1.3.1 History of computed radiography (CR)

As early as 1975 the Eastman Kodak company patented a device that used thermoluminescent infrared stimulating phosphor thereby releasing a stored image. Unfortunately, it design application was towards improving a nearly antiquated microfilm storage system. The FUJI photo film company recognized the far reaching possibilities of this new discovery and in 1980 patent the first process that made use of photostimulable phosphors to record a reproducible radiographic image. The basic common finding of both applications was that some phosphors (call storage phosphor) could capture an image from absorbed electromagnetic or particulate radiation. Part of the energy stored in the phosphor was afterwards released when stimulated by high frequency helium neon laser. By detecting the phosphor's luminescence using photomultiplier tube (PMT) to generate an electrical signal that was ultimately reconstructed into a digital radiographic image – computerized imaging was started.

2.1.3.2 Fundamentals of computed radiography

The fundamental difference between computed radiography and analog imaging is of film – screen with photostimulable phosphor plates. Digital plates require a plate reader, a port linkage to patient text data (for the example RIS or HIS), and connection to output device such as printer, or onto PACS network. The technologist need a CR imaging system that includes storage phosphor cassettes, storage phosphor readers, bar code scanner, remote operator panel for entering patient data, and clinical workstation for reviewing or printing from PACS. Currently CR is more popular system over conventional radiography because existing radiographic equipment (x- ray system, x- ray tables, portable machines, etc) does not have to be modified. These pieces of equipment alone do not constitute the full requirement to operate CR system. It should be remembered that major reason for investing in CR imaging is that it is the point for general diagnostic imaging into PACS. The

advantage of CR imaging over conventional analog imaging is huge and well worth to upgrade. Shown in figure 2.7 [3].

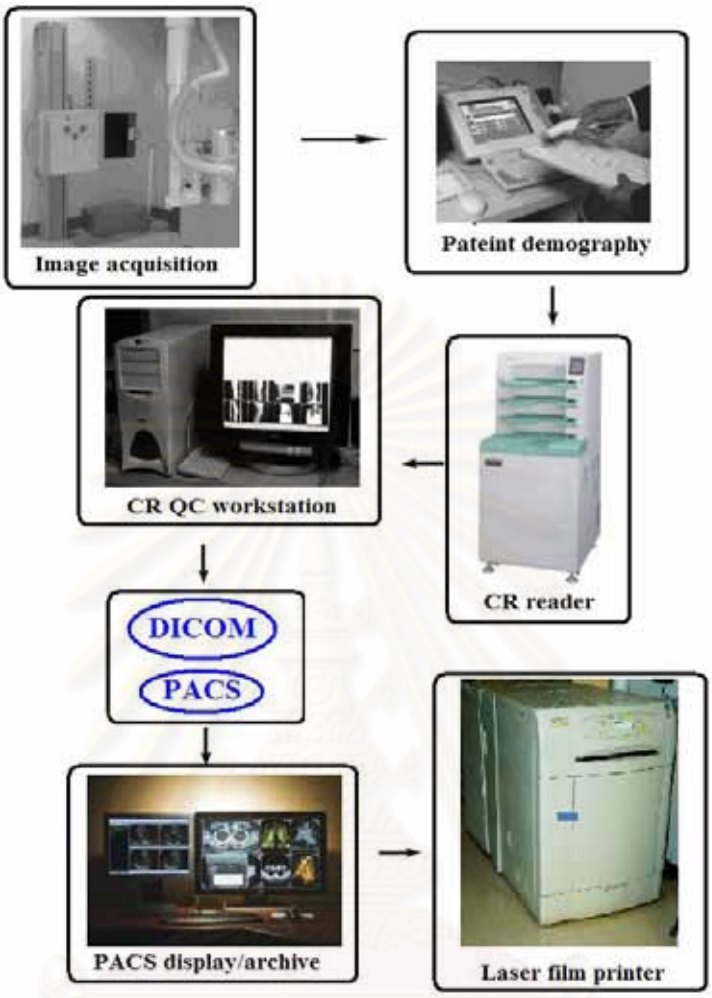

Figure 2.7 The computed radiography system.

2.1.3.3 Photostimulable phosphor (PSP) imaging plate [3] [4]

The PSP material is a barium-fluoro-bromide/iodide (BaFBr/I) compound doped with trace amounts of europium (Eu). The PSP material captures transmitted x-ray flux and creates a transient latent image by the trapping of electrons from the ground state into spatially localized higher-energy-level traps. Proportional number of trapped electron depend on x –ray absorbed. The spatial distribution of trapped electrons represents the unprocessed latent image.

Extraction of the electron latent image requires a simulating light source, which is usually a diode laser (680 nm wavelength), that pumps the electrons out of the trap to a higher energy level within the compound and then immediately to the ground state with only a short lag. As the electrons drop to the valence shell, emission of a blue, ~415 nm photostimulated luminescence (PSL) photon emerges from the phosphor as the visible latent image signal.

The PSP Imaging Plate is a flexible image sensor in which bunches of very small crystals (grain size: about 5 µm) of photo-stimulable phosphor of barium

fluorobromide containing a trace amount of bivalent europium as a luminescence center, formulated as BaFBr: Eu^{2+}, are uniformly coated on a polyester support film. The composite structure of the Imaging Plate is shown in Figure 2.8.

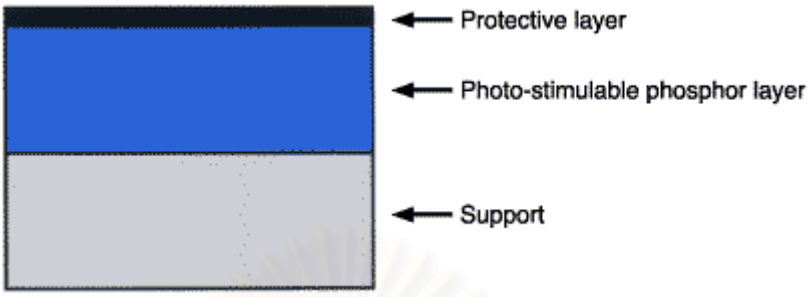

Figure 2.8 Composite structure of the Imaging Plate.

Exposure of samples to the Imaging Plate is performed in a manner similar to that of photo-film. The exposed Imaging Plate is scanned with a laser beam of red light while the plate is being conveyed with high accuracy in a phosphor reader as shown in Figure 2.9

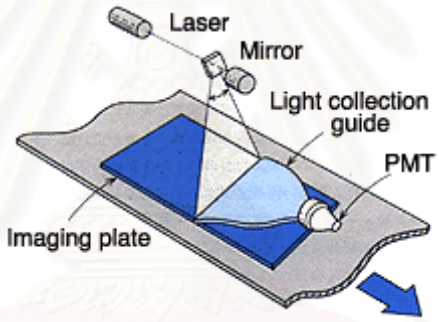

Figure2.9 The exposed Imaging Plate is scanned with a focused laser beam.

Depending on the purpose, the reading density may be selected from 5 to 40 pixels/mm. The reading sensitivity and sensitivity range can also be selected according to the purpose. A bluish purple (400 nm) PSL, released upon laser excitation, is collected through the light collection guide to the photo-multiplier tube (PMT), and converted there to analog electric signals in chronological order. Subsequently, these are converted to digital signals of 8 to 16 bits, again depending on the intended purpose.

Image analysis and data processing are done on the CRT screen. The processed image, if necessary, is printed either as a color or grayscale hard copy. The image or data processing includes those of image density/gradation, spatial frequency, operational reduction or addition between multiple numbers of images, and measurements of radiation dose, length or area. Application calculation processing then becomes possible based on these data. It is a particularly great advantage to quantify the image on the CRT as accurately as the scintillation counter method. The Imaging Plate is reusable after erasing the residual latent image with uniformly irradiated visible light as shown in Figure 2.10.

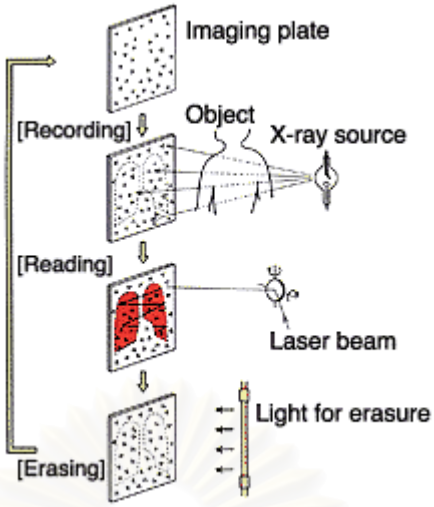

Figure 2.10 Process of recording, reading, erasing and reusing the radiation image by the imaging plate method.

The BaFX: Eu^{2+} (X = Cl, Br or I) crystal is an ionic crystal having a tetragonal structure, shown in figure 2.11, and Ba is replaced with the Eu^{2+} ion to create a solid solution. This crystal, when irradiated by radiation, for example, produces mainly two types of color centers in the crystal where an electron is trapped in an empty lattice of the F or X ion. The color center actually produced mainly depends on the discrepancy between the stoichiometric composition of F and X. The type of color center can be determined by comparing the theoretical value with the measured value from the electron spin resonance (ESR) spectrum by assuming an empty lattice for each anion. Experiments carried out for the composition of X = Br reveal that the spectra of the PSL excitation process produced by visible rays after sufficient X-ray irradiation coincide well with the peak of the optical density, light current, ESR intensity and PSL intensity at the color center. The relative change between the intensity of blue luminescence with the Eu^{2+} ion and that of red luminescence with the Eu^{3+} ion detected in a trace amount is also observed before and after the PSL excitation process.

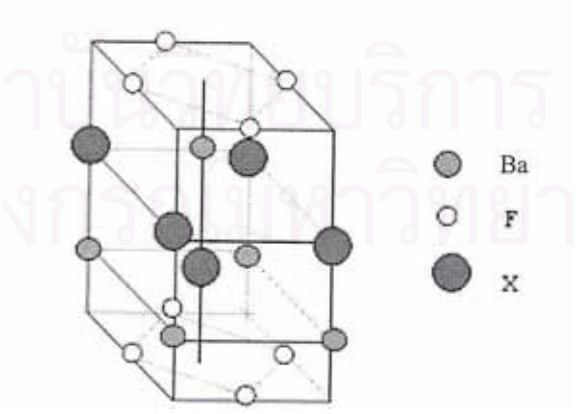

Figure 2.11 Crystal structure of BaFX(X = Cl, Br, I) [5]

From these data, the luminescence mechanism of the BaFBr: Eu^{2+} photo-stimulable phosphor is interpreted as follows. Part of the Eu^{2+} ions become Eu^{3+} ions through the primary excitation by X-rays, for example, with electrons being released

into the conduction band. These electrons are trapped into the Br ion empty lattices of the lattice defects, which are inherently present in the crystal, and color centers of the metastable state are formed. When the PSL excitation light to be absorbed by the color center is irradiated, the trapped electrons are liberated again into the conduction band, or Eu^{3+} ions, becoming an excitation state of the Eu^{2+} ion, to release PSL. It is shown in figure 2.12

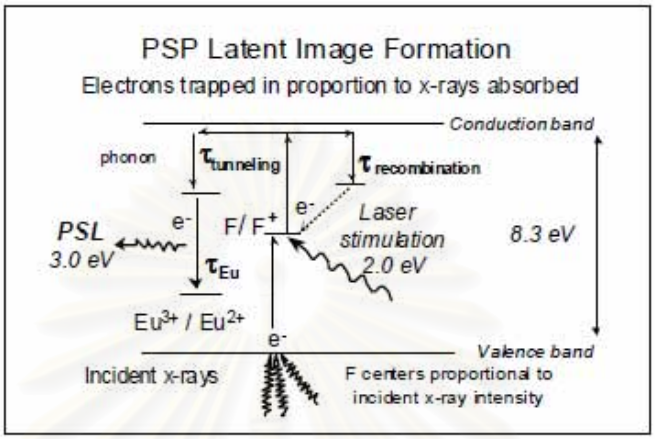

Figure 2.12 Energy diagram of the excitation and photostimulated luminescence processes in BaFBr: Eu^{2+} phosphor. Incident x- ray form and electron latent image in a meta-stable *F* center site that can be processed with a low energy laser beam, producing the desired luminescent signals, τ is decay constant of the indicated process above.[5]

Several techniques have been developed for detecting radiation: the ionization chamber; scintillation counter, and proportional counter tube. However, very few have been established for detecting a radiation image two-dimensionally: photo-film, the two-dimensional proportional counter tube, X-ray image intensifier and X-ray TV. Among these, the means most widely used in various fields is photo-film. The differences between the Imaging Plate and photo-film are clearly illustrated characteristically in Figure 2.13.

A) 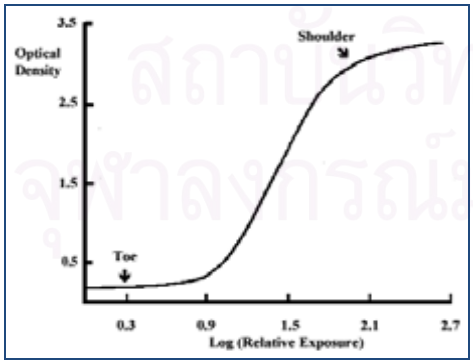

B) 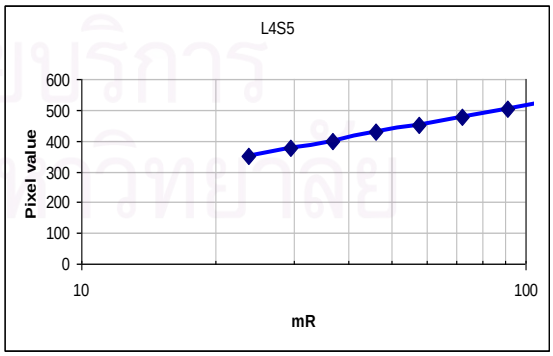

Figure 2.13 Comparison of characteristic between imaging plate and photographic methods A) Photographic film B) imaging plate.

Applications of the Imaging Plate are being widely tried to dramatically improve conventional methods in the medical X-ray diagnostic field as well as in scientific and technological fields requiring radiation image processing. The latter

includes X-ray crystallography, microstructure analyses by electron microscope, and analyses by autoradiography.

2.1.3.4 The CR reader [3]

Because the PSL is of shorter wavelength than the stimulating source, optical filtering can separate these two simultaneous light sources. Collection and amplification of the signal with photosensitive electronic devices followed by digitization of the signal produces the equivalent digital signal.

A) Point scan CR reader

A typical reader is composed of an optical stage, scanning laser beam, IP translation mechanics, light pickup guide(s), photomultiplier tube (PMT), signal transformer/amplifier, and analog-to-digital converter (ADC). The PSP imaging plate is inserted into the reader, and the imaging plate is extracted and translated through an optical stage. The scanning laser beam sweeps across the plate row by row, with a speed that is adjusted according to the luminescent signal decay time constant. The speed of IP translation is set to ensure appropriate coverage by the laser beam as well as to achieve equal sampling in the row and column directions of the output digital image. This sweep is called the scan direction whereas the plate translation represents the sub-scan direction. The PSL captured by the light guide(s) is optically filtered and channeled to the photocathode of the PMT(s), causing emission of electrons and subsequent acceleration and amplification through a series of dynodes. Overall gain of the PMT is controlled by the adjustment of the voltage placed on the dynodes, Current readers use a preset PMT gain that achieves good linearity over clinical exposure ranges of usually 0.1 mR to 100 mR or 0.01 to 10 mR (determined by the preset gain of the PMT) to allow optimal digitization of the PSL signal intensities. Prior to conversion of the PMT signal to a digital value, most CR systems apply a non-linear transformation with a logarithmic or square-root amplifier. Logarithmic conversion provides a linear relationship of incident exposure to output signal amplitude; square-root amplification provides a linear relationship, with the noise associated with the exposure. An illustration of the CR reader components is shown in Figure 2.14.

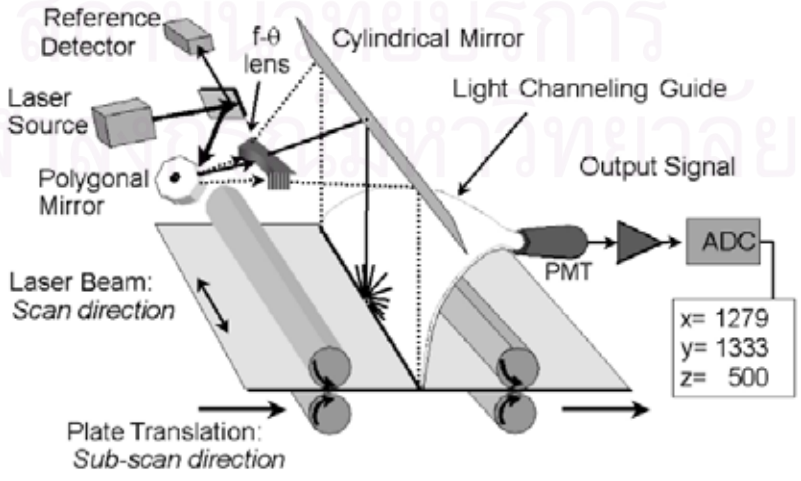

Figure 2.14 Internal components of a conventional point-scan CR reader. Components include the stimulating laser source, a beam splitter, oscillating beam deflector, f-θ lens, stationary reflecting mirror, light collection guide, photomultiplier tube (PMT), and ADC subsystem.

B) Line scan CR reader

A scanning module contains several linear laser units, optical light collection lenses along the length of the scan unit, based on the simultaneous stimulation of the PSP *one line at a time* and the acquisition of the PSL with a charge-coupled-device (CCD) linear array photo detector. An inline high-sensitivity CCD photosensitive array to capture the resultant PSL signals simultaneously, one row at a time. The line scan system has a lens array to focus the light along each point of the stimulated IP to a corresponding point on the CCD array. The module scans of line scans CR reader read is faster than point scan reader with the same detail of performance. The line scan CR reader component is shown in Figure 2.15.

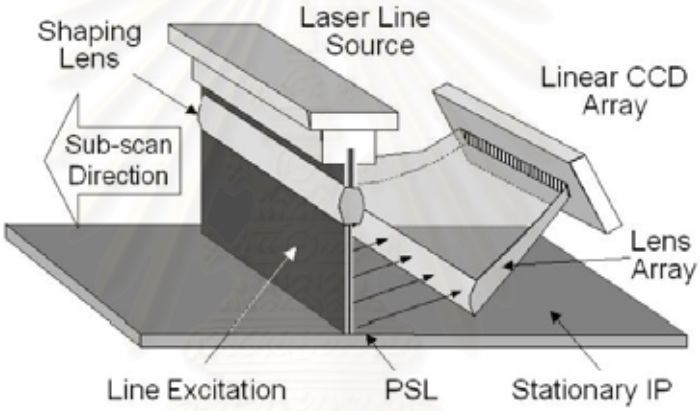

Figure 2.15 Component-level illustration of a line-scan CR detector. The laser source, shaping lens, PSL lens array, and CCD camera assembly move as a unit over the stationary imaging plate.

2.1.3.5 Fuji CR exposure indicators

A) Fuji CR: Latitude number

Expose latitude control the dynamic range of the detector. Varying the latitude (slope) is effect the useful range of the exposure and control the shade of gray of the image. Latitude of Fuji CR images is reported by the system in the *L* parameter associated with the image, where *L* is the $\log_{10}$ of the dynamic range. Decreased the *L* value will give the better contrast, but the dynamic range will be decreased. The optimized protocol is needed for to recognize the latitude of the useful range.

B) Fuji CR: Sensitivity Number

Fuji CR systems use a sensitivity number, *S*, derived from the median value of the anatomy-specific histogram. In the case of underexposure, amplification of the

signals must be increased to map the median value to the mid value of the 10-bit output (code value = 511), and, in the case of an overexposure, amplification must be decreased. The degree of amplification provides an estimate of the incident exposure on the plate for the automatic and semiautomatic modes of operation. Under normal processing conditions, the system sensitivity number is given as

$$S \cong \frac{200}{\text{exposure}\,(mR)} \tag{7}$$

When the system sensitivity number is equal to 200 with the "semi-automatic" or "automatic" exposure data recognizer (EDR) mode, an average photostimulated luminescence within the area sensed by the CR reader can be estimated as 1 mR (80 kVp, no object, and no added filtration other than inherent). For the "fixed" sensitivity mode available with the Fuji CR system, the sensitivity number is independent of the incident exposure on the plate and does not change with exposure.

C) Relationships of pixel value and exposure dose

For the imaging plate we can measure the pixel value of the profile by image processing software, or calculate from their vendor empirical relationships, for FUJI CR imaging plate, the equation is

$$Q(E) = \frac{1024}{L}\log_{10}(k \times S \times E) + 511 \tag{8}$$

- L is the *latitude*
- k is a *calibration constant(1 mR* , 80 kVp, 1 mm. Cu and Al filtration , S = 200)
- S is the *sensitivity*
- E is the *exposure* in mR

When the L number is high, the contrast of the signal decreases, also when the S number is high, the maximum pixel value of the signal increases.

The FWHM was determined based on the pixel value of half of the maximum exposure to the plate. From Eq. (8), this value is

$$Q(\frac{E_{\max}}{2}) = Q(E_{\max}) - \frac{308.25}{L} \tag{9}$$

- $E_{\max}$ is the maximum exposure to the IP (profile peak)
- $Q(E_{\max})$ is the associated pixel value.

For analyzing data, the pixel value was measured and converted to exposure then plotting the CT dose profile, rearranged (8) to provide a determination of exposure.

$$E = \frac{1}{k \times S} 10^{\{\frac{L}{1024}[Q(E)-511]\}} \tag{10}$$

2.1.4 Photographic film

2.1.4.1 General

Photographic film consists of a radiation-sensitive emulsion coated on a transparent polyester base. The emulsion consists of silver halide crystals (typically 95% silver bromide and 5% silver iodide) embedded in gelatin. The exact composition of emulsions varies with the manufacturer and is a closely guarded industrial secret. For protection against mechanical damage, the base is covered with a thin layer of gelatin. When the emulsion is exposed to radiation, excitation and ionization takes place in the silver halide that leads to the formation of a latent image.

Film development is a chemical process, which amplifies the latent image by a factor of millions. This development produces silver grains, i.e. microscopically small irregular aggregates of metallic silver, which cause the film to become opaque. Electron micrographs of some films commonly used in dosimetry reveal a vast difference in grain size and uniformity between the different types of film.

2.1.4.2 Film base and emulsion

The silver halide of a radiographic film is contained in an emulsion coated on a polyester base and protected by a thin gelatin layer for mechanical integrity. Radiographic films are available in different sizes (e.g. 25.4 cm x 30.5 cm), and their radiation dose range is between several mGy and several Gy. They require a wet chemical processing as well as a special device for read out, the densitometer.

It consists of the radiation-sensitive emulsion usually coated on both sides of a transparent sheet of plastic called the base. A thin layer of adhesive provides firm attachment between the emulsion and the film base. The delicate emulsion is protected from mechanical damage by layers known as supercoating. The composition of a dosimetric film is shown in Figure 2.16 [6]

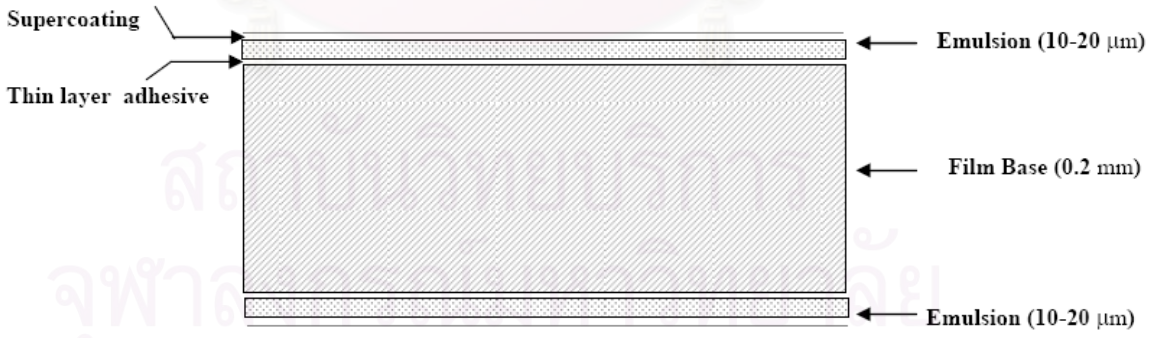

Figure 2.16 Cross-section of a double emulsion X-ray film.

Silver halide is the light-sensitive material in the emulsion. The halide in medical x-ray film is about 90 to 99% silver bromide and about 1 to 10% silver iodide (the presence of AgI produces an emulsion of much higher sensitivity than a pure AgBr emulsion). The production reaction involves the addition of silver nitrate to a soluble halide to form the silver halide:

$$AgNO_3 + KBr \rightarrow AgBr + KNO_3$$

The silver iodo-bromide crystals are precipitated and emulsified in the gelatin under exact conditions of concentration and temperature, as well as the sequence and the rate at which these chemicals are added. The method of precipitation determines the crystal size, and the structural perfection. The silver halide in a photographic emulsion is in the form of very small crystals suspended in the gelatin. The crystal is formed from ions of silver (Ag^+), ions of bromine (Br^-) and ions of iodine (I^-) arranged in a cubic lattice(figure 2.17).

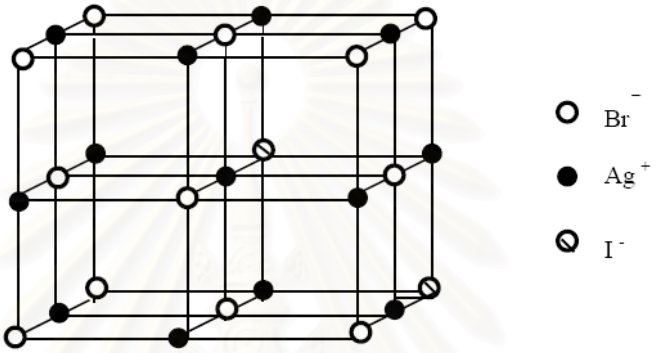

Figure 2.17 The silver iodo-bromide crystal lattice.

The emulsion of an exposed film contains the latent image. The exposed emulsion does not look any different than an unexposed one, but it has been altered. The latent image is recorded as altered chemical bonds in the emulsion, which are not visible, the latent image is render visible during film processing by chemical reduction of silver halide into metallic silver grain. [2]

2.1.4.3 Film processing [2]

For the silver halide crystal have been exposed, the metallic silver atom act as the chemical catalyst for the developer. During the development process, the latent image center catalyzes the reaction, which reduces the remaining silver ions in silver halide crystal into a grain of metallic silver.

Film density is produced by converting silver ion into metallic silver, which causes each processed grain to become black. The process is rather complicated and is illustrated by the sequence of events shown in Figure 2.18, once the chemically developed, the latent image become a manifest image which is visible image.

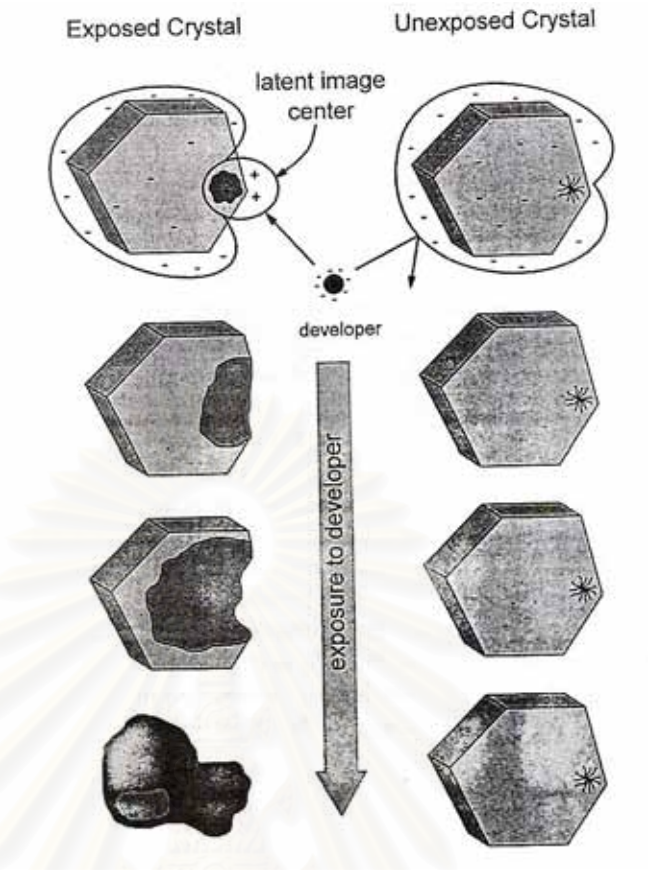

Figure 2.18 Sequence of events that convert a transparent film grain into black metallic silver.

After film development, a small amount of developer remains trapped into emulsion and would continue to cause the development unless neutralized, the fixer is used to arrest the chemical activity of the residual developer. The fixer contains acetic acid to decrease the pH and stop development. The fixer removes the undeveloped silver halide crystal from the emulsion to avoid film blackening.

After fixing, the water bath simply washes residual chemicals out of the film emulsion. Water is continuously cycled through the processor, and the last step is drying. A thermostatically regulated coil heats air blow from power fan, this warm air blows across both surfaces of the film. The film processor component is shown in Figure 2.19.

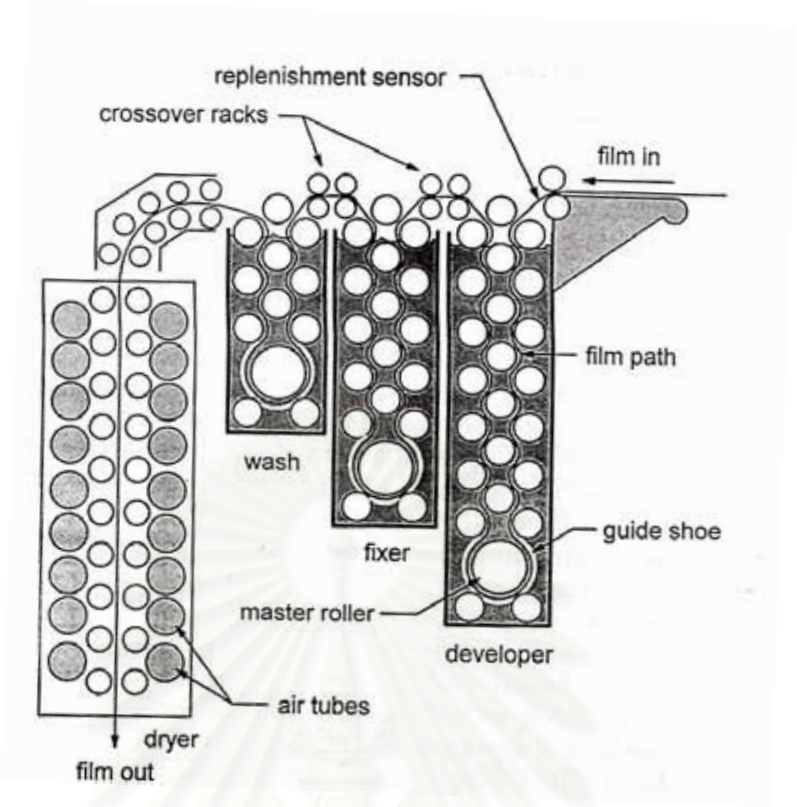

Figure 2.19 The film processor component, film was going through the developer, fixer, wash and dryer.

2.1.4.4 The optical density [7]

The opacity of the developed film can be quantified as an optical density (OD)

$$OD = \log \frac{I_0}{I} \qquad (11)$$

Where I is the transmitted light intensity in a film densitometer and I_0 is the incident light intensity (see in Figure 2.20). This implies that the lower the film opacity, the higher OD is, and vice versa.

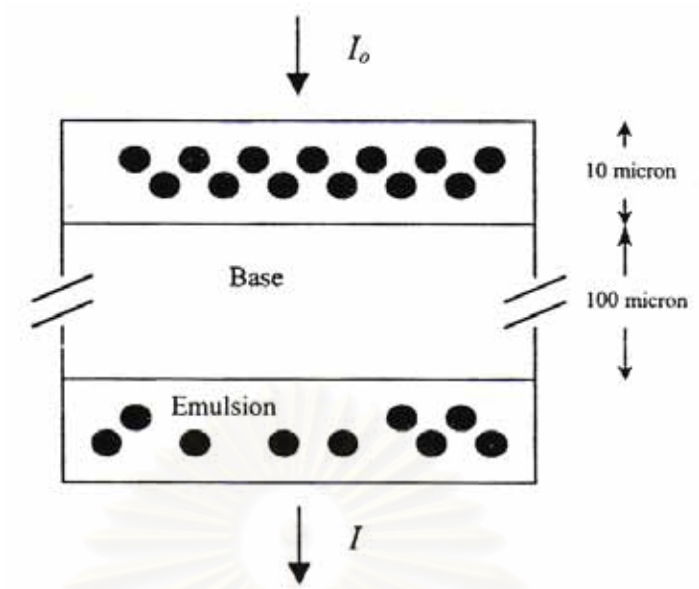

Figure 2.20 Developed radiographic film under film densitometry. Double coating emulsion is typical for verification film. The grain (dark circles) diameter is less than 1 micron, which limits the spatial resolution.

2.1.4.5 The characteristic curve of x – ray film [7]

The characteristic curve of film is generated between the optical density and log exposure as shown in figure 2.21. Each film has its own characteristic curve although all have the same curve. The initial curved part between D_1 and D_2 is the useful range of that film. After passing through D_2, the density is seen to saturate and further exposure produces no further blackening. At very high exposure, the density begins decrease again, call solalization.

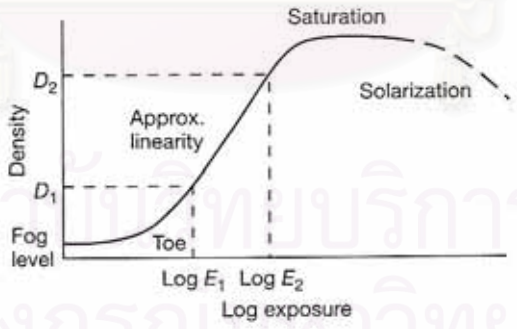

Figure 2.21 The typical characteristic curve for an x- ray film.

The speed of the film is depend on the film gamma, the maximum slope of approximately linear portion of the characteristic curve, defined as

$$\gamma = \frac{D_2 - D_1}{\log E_2 - \log E_1} \qquad (12)$$

The gamma of the film depends on the type of emulsion present, principally the size of silver bromide, and secondly how the film is developed. The fast film has a large gamma; the grain size is bigger than slow film that made the image quality lower than slow film. The slow film has high resolution image but more energy of the photon to generate the image. Shown in figure 2.22

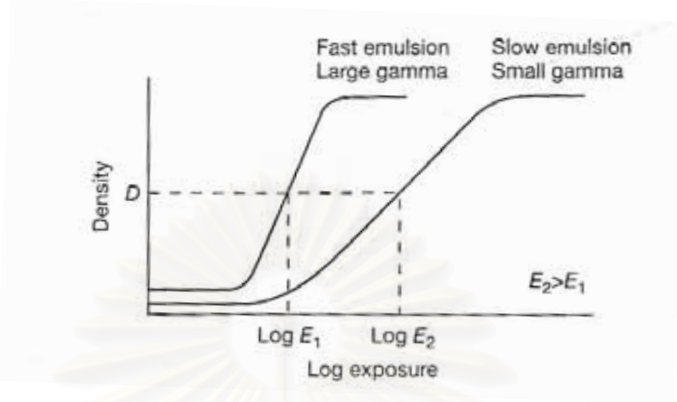

Figure 2.22 Characteristic curves of film with different gamma and speed.

The optimum range of densities for viewing is call latitude, the latitude of film refers to the range of exposure that can be given to the film such that the density produced is within these limits. The higher gamma of the film, the smaller range of exposure it can tolerate and thus the lower latitude. For general radiography a film with reasonably high latitude is used. However because if the gamma of the film is made too small the contrast produced is too small for reasonable evaluation.

2.2 literature review

AAPM report No. 39 described the process for quality control of CT scanner, to determine the nominal beam width of CT collimation setting, by setting the prepatient collimator and exposing the film in axial mode. Then measure the width of the profile and compare with a nominal beam width. Acceptable result is no different from nominal beam width within 2 mm. [1]

R. Sekine, H. Kimura, Y. Muramatsu, T. Murakami, S. Saotome, and N. Moriyama[8] studied the measurement of dose profile from the imaging plate (IP: HR-V type, Fuji), it was placed in its case, X-rayed, and then read with a digital IP reader, which then erased the data in preparation for reuse. The values were then compared with the values obtained with the imaging film. The results obtained for the shape of the beam profile and the FWHM were found to be extremely similar irrespective of the X-ray tube used or individual differences between IPs. However, technical details in English were not available.

Thomson FJ.[9] studied the measurement of the FWHM of the slice thickness radiation dose profile of a CT scanner using a prototype low sensitivity CR imaging plate, as an alternative to the traditional method using envelope-packed industrial film. Using a standard Agfa clinical CR system to acquire the image, the FWHM of the dose profile can be accurately measured using readily available Public Domain software. An Agfa 18 x 24 cm CR cassettes gives a pixel pitch of 113.5 micron, but with interpolation, the measurement accuracy can be less than 1 pixel. For a nominal

10 mm collimation, 15 successive measurements of the FWHM using CR gave an average width of 10.00 mm with a standard deviation of 0.02 mm. This may be compared with 4 successive measurements using film and a dual exposure technique to define the optical density at half peak height, yielding an average width of 9.98 mm with a SD of 0.03 mm. However, this prototype plate is not a commercial product, but a radiotherapy plate with a similar sensitivity is available commercially and should give similar results.

Liu HL, Liu RR, Reeve DM, Shepard SJ, Willis CE.[10] described the procedure for using a Fuji computed radiography (CR) imaging plate (IP) for the measurement of computed tomography (CT) radiation profiles. Two sources of saturation in the data from the IP, signal and quantization, were characterized to establish appropriate exposure and processing conditions for accurate measurements. The IP generated similar profiles compared to those obtained from digitized ready-pack films, except at the profile edges, where the exposure level is low. However, when IP pixel values are converted to exposure, CR and digitized film profiles are in agreement. The full width at half maximum (FWHM) of the CT radiation profile was determined from the relationship between pixel value and exposure and compared to FWHM of the digitized optical density profile from film. To estimate the effect of scattering by the cassette material, radiation profiles were acquired from IPs enclosed in a cassette or in a paper envelope. The presence of the cassette made no difference in the value determined for FWHM. The estimation of the width of the CT radiation profile using Fuji CR is comparable to the measurement from film density described in American Association of Physicists in Medicine (AAPM) Report No. 39. Although their experiment was conducted using Fuji CR, we anticipate that CR plates from other vendors could be successfully used to measure CT beam profiles because of similar empirical relationships between pixel value and exposure.

CHAPTER III

RESEARCH METHODOLOGY

3.1 Research design

This research is observational study design.

3.2 Research design model

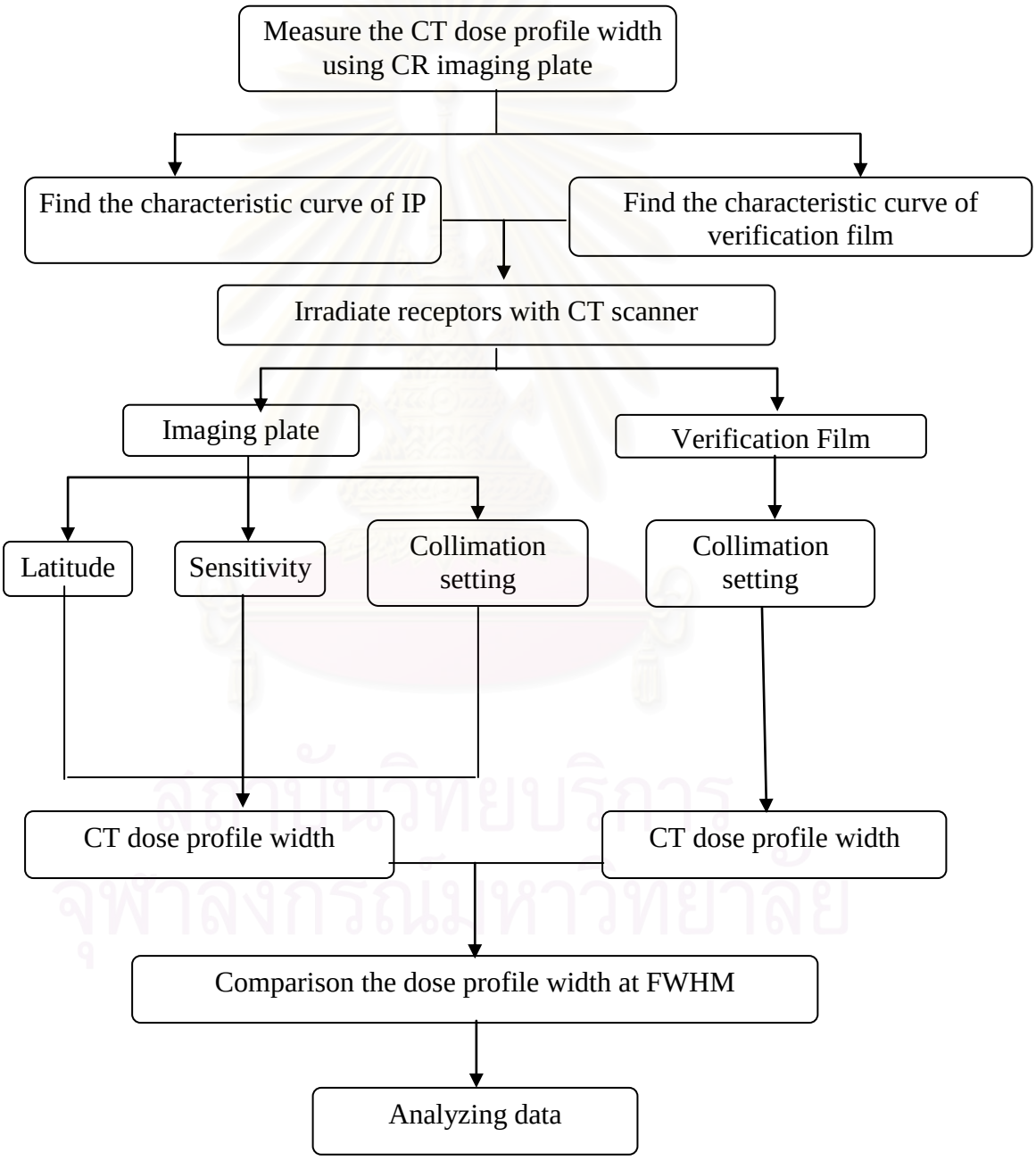

3.3 Conceptual framework

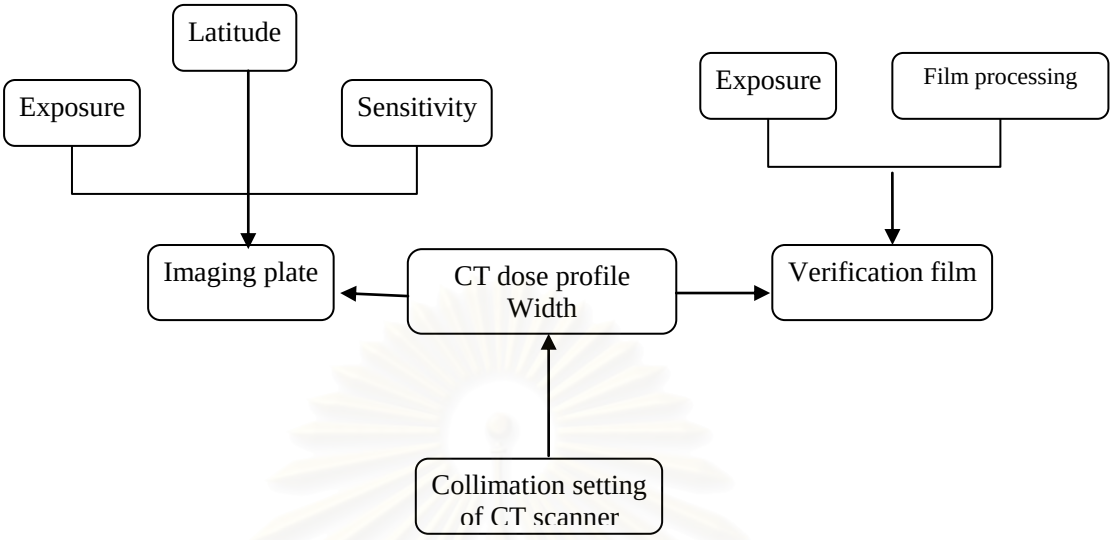

3.4 Key word

- Computed tomography dose profile width
- Computed radiography imaging plate
- Verification film
-

3.5 Research question

3.5.1 Primary question

Can computed radiography imaging plate measure the dose profile width?

3.5.2 Secondary question

How does the difference of computed tomography dose profile width measure by computed radiography compare with verification film?

3.6 Material

3.6.1 Computed radiography imaging plate

The imaging plate is the world's first photostimulable phosphor put to practical use as a recording medium. The imaging plate accurately detects x-ray information and stores it as energy within the phosphor particles. It offers high sensitivity, high sharpness, low noise radiographs for diagnosis by utilizing a high emission photostimulable phosphor, BaFX (X = halogen), in a high-density dispersion image recording layer. In this study the Fuji STVI CR 24 x 30 cm. serial numbers A43279722C was used, it is shown in figure 3.1

Figure 3.1 Fuji Computed radiography imaging plate.

3.6.2 Computed radiography

The Fuji SCR XG5000 reader was designed to a throughput of up to 165 imaging plates (IPs)/ hour. The XG5000 four- cassette stacker and product design allow IPs to be read and erased simultaneously for image preview in a little as 15 seconds and cycle time have short as 30 seconds. It produces high quality image without manipulation to optimize the clinical workflow. It is shown in figure 3.2

Figure3.2 Fuji SCR XG5000.

3.6.3 The ready pack X-Omat V film

The Kodak X-Omat V film is a relatively low speed film designed for verifying the orientation and for approximating patient dosage in radiation therapy procedures. It features the ready pack which eliminates the need for loading cardboard cassettes. It is able in both automated processing cycles and manual processes. Under normal viewing conditions, the film can be used to record the dosages of 0.25 to 1.00 Gy. The film is shown in Figure 3.3

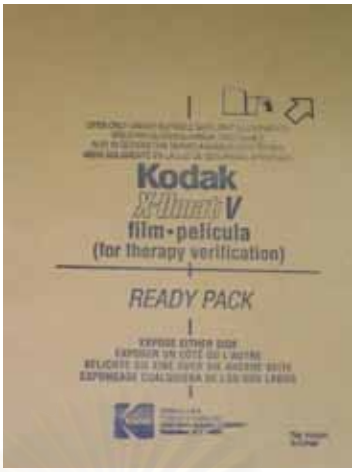

Figure 3.3 Kodak X-Omat V film**.**

3.6.4 Automatic film processor

The automatic film processor is Kodak *RP* X-OMAT (Kodak, USA, Model M6B). The developer temperature is 34.8°c and during the course of processing, the temperature read out is within ± 0.3 °c. The time for whole process is about 90 seconds and this is usually not adjusted. It is shown in figure 3.4.

Figure 3.4 Kodak *RP* X-OMAT automatic film processor.

3.6.5 Vidar VXR-16 Dosimetry Pro and OmniPro IMRT software

The Vidar film digitizer (VXR-16 pro dosimetry, Vidar systems Corp., Herndon, VA) is used to scan the film (figure 3.5). The film scanner operates with a resolution of 142 dots per inch (0.179 mm/pixel) and a depth of 16 bits, offers an optical density range of 0.04-3.65. Two dimensional images are transferred to OmniPro™ IMRT (Scanditronix Wellhofer) software version 1.4.1.0 to read the optical density.

Figure 3.5 Vidar film digitizer (VXR-16 pro dosimetry, Vidar systems Corp., Herndon, VA)

3.6.6 Computed tomography

The GE LightSpeed RT scanner (GE Medical system) has the ability to simultaneously collect 4 rows of scan data .The distance from tube to isocenter is 606 mm. The distance from tube to detector focus is 1062 mm. Bore diameter is 800 mm. The kVp setting is available (80,100,120 and 140 kVp). Exposure techniques range from 10 to 400 mA in 5-mA increments with five scan time setting (1, 2, 3, 4 second). The CT scanner is shown in figure 3.6

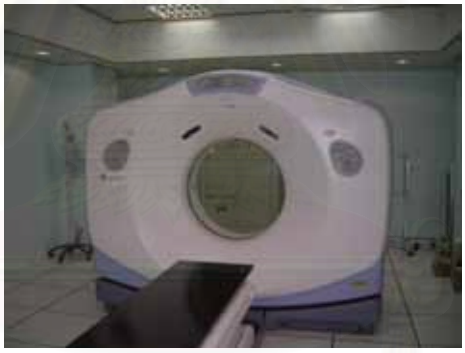

Figure 3.6 GE LightSpeed RT CT scanner.

3.6.7 X-ray machine

The Siemens Polyphos type B3 75040 G2107 (figure 3.7) has a nominal focus of 0.6 and 1.2 mm with total filtration of 1 mm Al at 80 kVp, it is installed with Multix CO with Bucky. The generator has nominal voltage of 150 kVp. The kVp setting is available (40 - 125 kVp) for exposure technique range from 12 to 500 mAs.

Figure 3.7 Siemens Polyphos X-ray machine.

3.6.8 Dosimeter

The Unfors Xi system can simultaneously measure kVp, dose, dose rate, HVL, pulse, pulse rate, dose/pulse, time and waveform.

The basic Unfors Xi configuration consists of two primary components: the Unfors Xi Base Unit and the Unfors Xi Detector. Both can be fully upgraded as new features are introduced. Traditional fragile ion chambers can now be substituted with Unfors small and lightweight solid state detectors to achieve accurate measurements. It is shown in figure 3.8

Figure 3.8 The Unfors Xi solid state detector.

3.6.9 Cerrobend block

Cerrobend is also known as Lipowitz's alloy or Wood's metal, named for American metallurgist B. Wood. It is a fusible alloy that becomes liquid at approximately 70 °C (158 °F). It is a eutectic alloy of 50% bismuth, 26.7% lead, 13.3% tin, and 10% cadmium by weight. Cerrobend uses include making custom-shaped apertures and blocks (for example, electron-beam cutouts and lung blocks) for medical radiation treatment. It is shown in figure 3.9.

Figure 3.9 Cerrobend block.

3.7 Method

The experiments were performed by the following steps:

3.7.1 Quality control of equipment

The quality control of the computed tomography, x-ray machine, film processor and imaging plate were performed base on AAPM protocol. (The result is in Appendices)

3.7.2 Densitometer calibration

The automatic film scanner densitometer of Vidar VXP-16 with the OmniPro IMRT software was calibrated to define the relationship between the densitometer signal and net optical density by step wedge film. The special step wedge film was delivered from manufacture with the range optical density of 0.04 to 3.65. The reference density value for each step of the step film was entered and the signal of the film scanner was read. The graphs of the signal versus the net optical density were plotted.

3.7.3 Calibration of verification film and imaging plate

3.7.3.1 Characteristic curves from x-ray machine

For studying the characteristic of verification film and imaging plate, the Unfors Xi solid-state detector was irradiated by x-ray beams at 100 cm. source image distance, 81 kVp, 10 x 10 cm filed size, 2 - 40 mAs, the exposures were recorded. Then the verification film was irradiated in the same technique and the optical density was measured, the characteristic curve was plotted between exposure and optical density.

The imaging plate was irradiated with x-ray machine at the same techniques as films. The imaging plate was transferred into DICOM file by computed radiography reader. The reading parameters were varied for latitude (L) of 1,2,3 and 4, sensitivity

(S) of 5,50 and 200 in fixed exposure data recognizer (EDR) mode and then the characteristic curve was plotted between pixel values and exposure (mR).

3.7.3.2 Characteristic curves from CT scan

To determine the characteristic curve of 120 kVp of computed tomography that used for this research. The verification film was irradiated by CT scanner at 10 mm. collimation setting, 120 kVp, 10 – 400 mAs.

The imaging plate was irradiated at the same techniques as films to determine the suitable exposure technique that did not cause the saturation. The cerrobend plate which blocks the field to 5×20 cm^2 was prepared to limit the x-ray beam from other directions. The lead sheet was set under imaging plate to filter the radiation from under couch. The set up was shown in figure 3.10

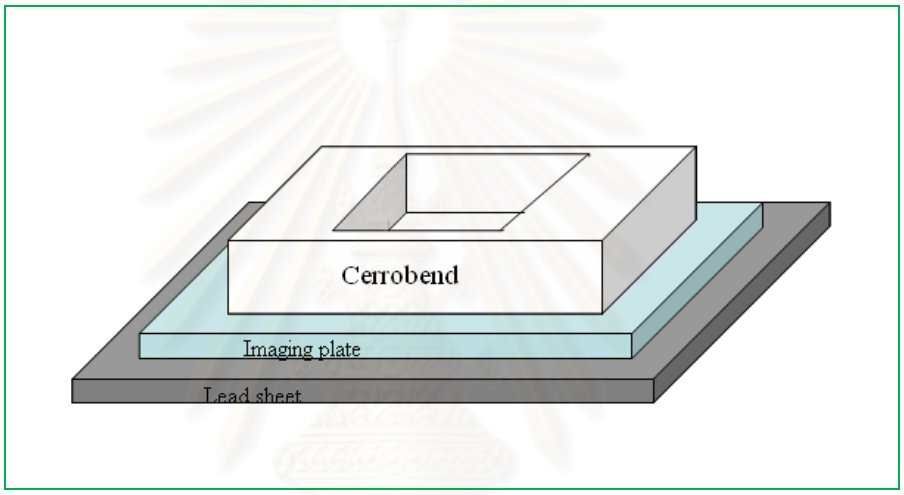

Figure 3.10 The diagram of setting the image plate for filtering the imaging plate.

After exposure, the computed tomography exposure image on imaging plate was transferred into DICOM file by computed radiography reader. The imaging plate parameters were read by varying L number and S number the same as the characteristic studied. The characteristic curve of film and imaging plate were analyzed and the appropriate exposure techniques were defined.

3.7.4 Measurement of computed tomography dose profile width

The verification film was irradiated with computed tomography scanner to collect the computed tomography dose profile width with appropriate exposure techniques depend on their characteristic curve. The computed tomography collimation was set at 5, 10, 15 and 20 mm, the computed tomography dose profile width image was transferred to OmniPro IMRT software by film digitizer. The computed tomography profiles were plotted by optical density and also exposure. The CT dose profile width was measured at the FWHM of the profile.

The imaging plate was scanned with computed tomography scanner to collect the computed tomography dose profile width with appropriate exposure techniques depend on their characteristic curve. The computed tomography collimations are set at 5, 10, 15 and 20 mm. The cerrobend plate combined with lead sheet was used as a

filter material to prevent the signal saturation. The computed tomography radiation image on imaging plate was transferred into DICOM file by computed radiography reader. The imaging plate parameters were changed by varying the L number and S number. The dose profiles were constructed by ImageJ software and transferred the data to Microsoft Excel to determine the computed tomography dose profile width. The computed tomography dose profile was plotted by pixel value and exposure. The pixel values were converted to exposure by equation (10)

$$E = \frac{1}{k \times S} 10^{\{\frac{L}{1024}[Q(E)-511]\}}$$

The profile width was measured at the FWHM for the profiles plotted by exposure.

The point for measured the profile plotted by pixel value was calculated by equation (9):

$$Q(\frac{E_{\max}}{2}) = Q(E_{\max}) - \frac{308.25}{L}$$

The result of computed tomography profile width measured by verification film and imaging plate were compared for both pixel value and exposure plotted.

3.8 Measurement

Independent variable = latitude, sensitivity, collimation setting
Dependent variable = pixel value and CT dose profile width

3.9 Outcome

Computed tomography dose profile width was measured by imaging plate and film. The two methods were compared with the nominal collimator width.

3.10 Data collection

Scan the computed radiography imaging plate and verification film with computed tomography scanner to collect the computed tomography dose profile width. Measure the computed tomography dose profile width at FWHM of the profile by Microsoft Excel.

3.11 Data analysis

The dose profile width from computed radiography imaging plate was compared with the verification film and nominal thickness value. Confirm the acceptance of result with AAPM protocol (± 2 mm).

3.12 Sample size determination

From pilot study, the standard deviation of pixel value measured from imaging plate (81 kVp, 25 mAs, L = 1, S = 50) is 1.928 %, the acceptable error is 3% .Sample size of each parameter was calculated, the result was n = 1.587 with a confidence interval = 95%. The measurement was performed for 2 times for each techniques.

3.13 Benefit of study

- The exposure technique is established to capture the CT dose profile by imaging plate.
- The imaging plate can be used instead of verification film.

3.14 Ethic consideration

This study was performed on the imaging plate and verification film. However, the ethical was approved by Ethics committee, Faculty of medicine, Chulalongkorn University.

CHAPTER IV

RESULTS

4.1. Quality control of equipment

The result of quality control of the film processor, x-ray radiography machine, computed tomography and computed radiography system were shown in Appendix B, C, D and E, respectively.

4.2. Densitometer calibration

The relationship between signal of analog to digital converter (ADC) and optical density from step wedge are shown in table 4.1 and figure 4.1. The densitometer curve showed almost linear relation between signals of ADC and optical density over optical density ranged of 0.2 to 2.3. The saturation of the signal began at optical density of about 2.3. This result suggested that the optical density of the film use should not be more than 2.3.

Table 4.1 The densitometer signal of standard step wedge film for Densitometer calibration

OD	ADC	OD	ADC
0.04	3968	1.85	32867
0.17	5873	1.99	35101
0.33	8439	2.14	37221
0.47	10743	2.29	39578
0.61	13066	2.43	41225
0.78	15734	2.62	43638
0.95	18600	2.75	45154
1.1	21173	2.9	46421
1.25	23645	3.05	47333
1.41	25992	3.2	48718
1.55	28313	3.37	49411
1.69	30446	3.51	49936
		3.65	50865

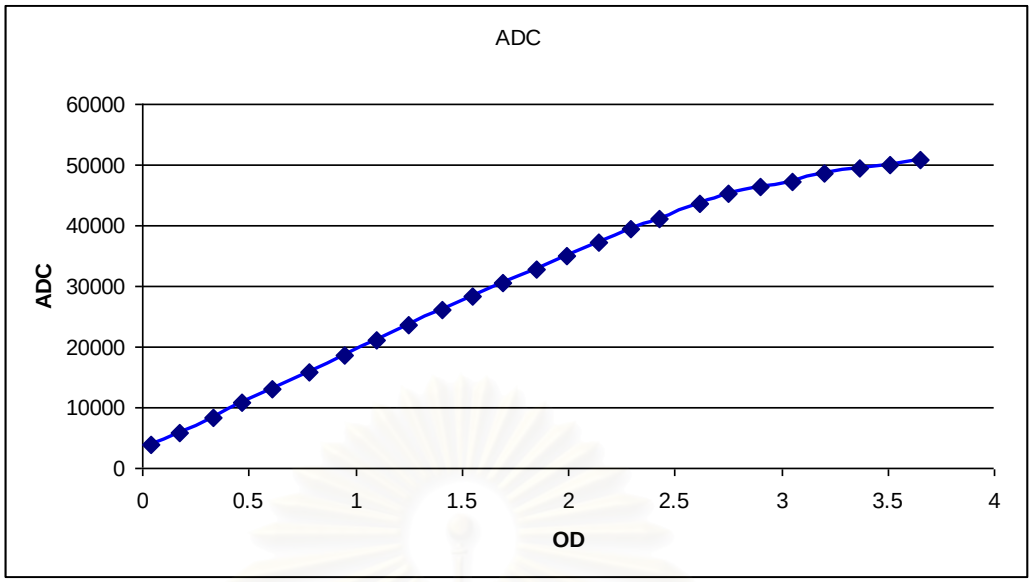

Figure 4.1 The densitometer calibration curve of standard step wedge film.

4.3. Calibration of verification film and imaging plate

4.3.1 Characteristic curves from x-ray machine

The relationship between exposure(mR) and optical density of x-ray generator measured by film at 100 cm. source image distance, 81 kVp, 10 x 10 cm filed size, 2 - 40 mAs are shown in table 4.2 and the characteristic curve is shown in figure 4.2. The optical density plotted with the exposure showed non linearity in the exposure range studied because the exposure was low and the increasing exposure could not be adjusted.

Table 4.2 The relationship of exposure (mR) and optical density. Irradiated by x-ray beams at 100 cm. source image distance, 81 kVp, 10 x 10 cm field size, 2 - 40 mAs.

mAs	mR	average OD
2	23.77	0.112
2.5	29.49	0.1184
3.2	36.74	0.119
4	46.06	0.1202
5	52.52	0.125
6.3	71.91	0.1276
8	91.02	0.1314
10	114.1	0.1402
12.5	142	0.1438
16	180.3	0.1544
20	225.2	0.1674
25	284.3	0.1798
32	356.9	0.2022
40	449.4	0.2278

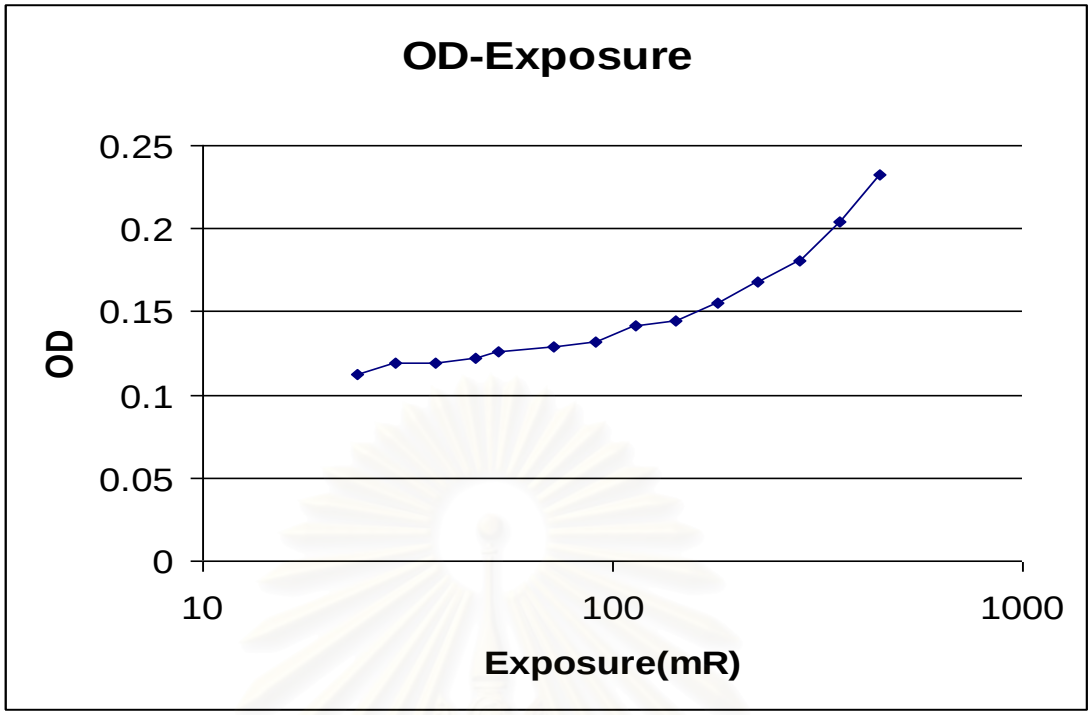

Figure 4.2 X-ray characteristic curve measured by verification film. Irradiated by x-ray beams at 100 cm. source image distance, 81 kVp, 10 x 10 cm field size, 2 - 40 mAs.

The relationship of exposure(mR) and pixel value of imaging plate irradiated by x-ray beams at 100 cm. source image distance, 81 kVp, 10 x 10 cm filed size, 2 - 10 mAs. are shown in table 4.3 and the characteristic curves plotted in semi- log scales between exposure in log scale and pixel value in linear scales are shown in figure 4.3 A) to 4.3 D) for various L and S parameters of L = 1, S = 5, 50 and 200, L = 2, S = 5, 50 and 200, L = 3, S = 5, 50 and 200, L = 4, S = 5, 50 and 200, respectively. The graphs showed the non quantization limited at L = 1; S = 5, L =2; S =5, L = 3; S = 5 and 50, and for L = 4 for all S values . After 10 mAs exposure, all parameter setting showed the saturation.

Table 4.3 The relationship of exposure(mR) and pixel value irradiated by x-ray beams at 100 cm. source image distance, 81 kVp, 10 x 10 cm filed size, 2 - 10 mAs. Imaging plate was saturated after 10 mAs.

mAs	mR	L1			L2			L3			L4		
		S5	S50	S200	S5	S50	S200	S5	S50	S200	S5	S50	S200
2	23.77	0	900	1020	185	704	1012	296	640	840	352	608	760
2.5	29.49	0	1008	1020	244	760	1020	336	672	876	376	632	788
3.2	36.74	80	1020	1020	292	804	1020	364	708	912	400	656	812
4	46.06	184	1020	1020	340	860	1020	400	740	944	428	684	836
5	57.52	280	1020	1020	396	908	1020	432	772	976	452	708	864
6.3	71.91	380	1020	1020	448	960	1020	468	808	1016	476	736	888
8	91.02	492	1020	1020	500	1012	1020	504	844	1020	504	760	916
10	114.1	592	1020	1020	552	1020	1020	540	876	1020	532	788	940

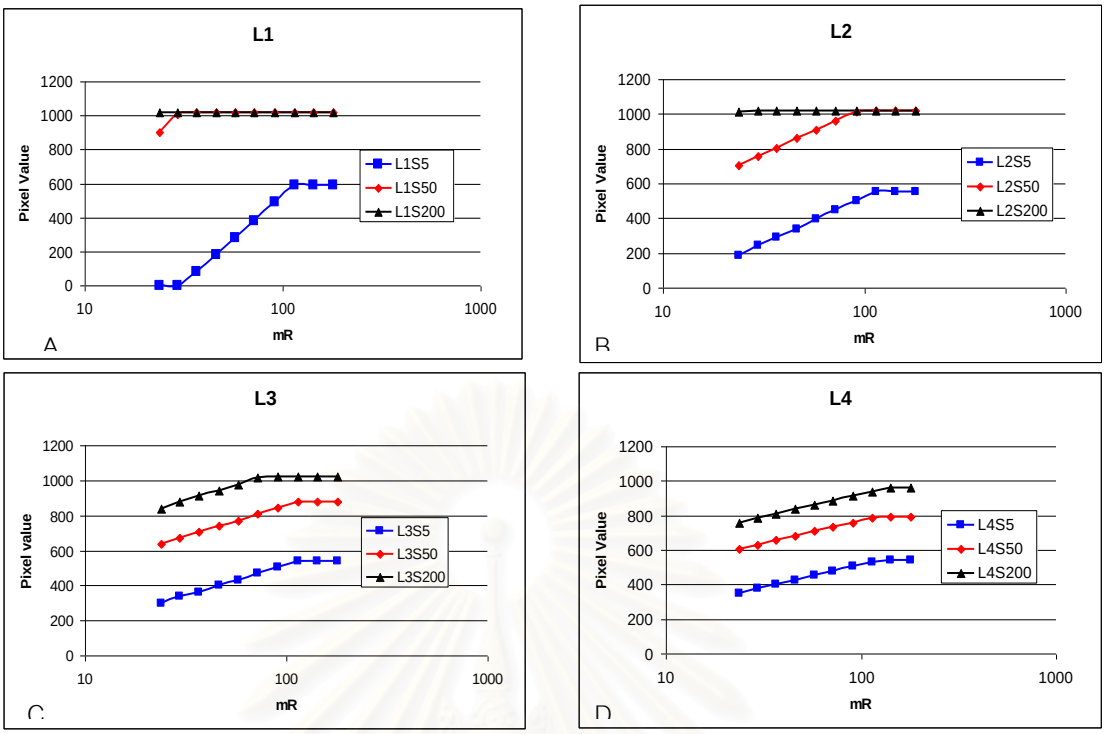

Figure 4.3 X-ray characteristic curve measured by imaging plate, irradiated by x-ray beams at 100 cm. source image distance, 81 kVp, 10 x 10 cm filed size, 2 - 10 mAs.
A) L = 1, S = 5, 50 and 200.
B) L = 2, S = 5, 50 and 200.
C) L = 3, S = 5, 50 and 200.
D) L = 4, S = 5, 50 and 200.

4.3.2 Characteristic curves from CT scan

The relationship of CT exposure (mR) and optical density of CT generator measured by film are shown in table 4.4 and the characteristic curve plotted in semi- log scales between exposure in log scale and optical density in linear scales is shown in figure 4.4. The optical density plotted with the exposure showed linearity in the exposure range of 3500 to 9700 mR (150 to 400 mAs).

Table 4.4 the relationship of CT exposure(mR) and optical density . irradiated film by CT scanner at 10 mm. collimation setting, 120 kVp, 10 – 400 mAs.

mAs	Exposure(mR)	OD
10	230.7	0.168
20	461.92	0.229
50	1159.4	0.388
100	2306.5	0.615
150	3459.9	0.808
200	4608.2	0.978
300	7285.7	1.277
400	9695.6	1.513

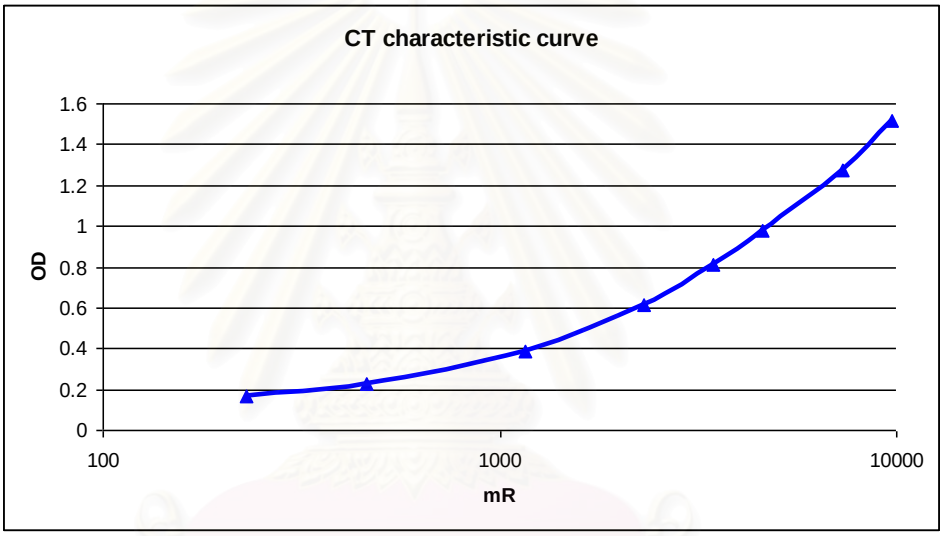

Figure 4.4 The characteristic curve measured by film, irradiated by CT scanner at 10 mm. collimation setting, 120 kVp, 10 – 400 mAs.

For imaging plate, we cannot plot the characteristic curve of CT scanner because the signal was saturated at 10 mAs. After the imaging plate was filtered by using cerrobend block combine with lead sheet, the signal is saturated at 20 mAs. At S = 50, the signal from L = 1 and 2 were quantization, but at S = 200, only parameter setting with L = 4 can be measured without saturation.

4.4 .Measurement of computed tomography dose profile width

CT dose profile measured by verification film at 120 kVp, 10 mAs with the collimations setting of 5, 10, 15 and 20 mm. plotted by optical density were 7.7, 11.7, 17.1, and 20.5 mm, respectively, and plotted by exposure were 6.9, 11.3, 16.5, and 20 mm, respectively. The results including the difference from collimation setting are shown in table 4.5 and the graphs are plotted in figure 4.5 to figure 4.8 for 5, 10, 15 and 20 mm. collimation setting, respectively. The beam width difference from the collimation setting was higher for the profile obtained from optical density than from

exposure. The lower part of the profile showed higher value from optical density than from exposure.

Table 4.5 CT dose profile width measured by film in optical density and exposure.

Collimation setting (mm.)	Profile width (mm.)		Difference from Collimation setting (mm.)	
	OD	exposure	OD	exposure
5.00	7.7	6.9	2.70	1.90
10.00	11.7	11.3	1.70	1.30
15.00	17.1	16.5	2.10	1.50
20.00	20.5	20	0.50	0.00

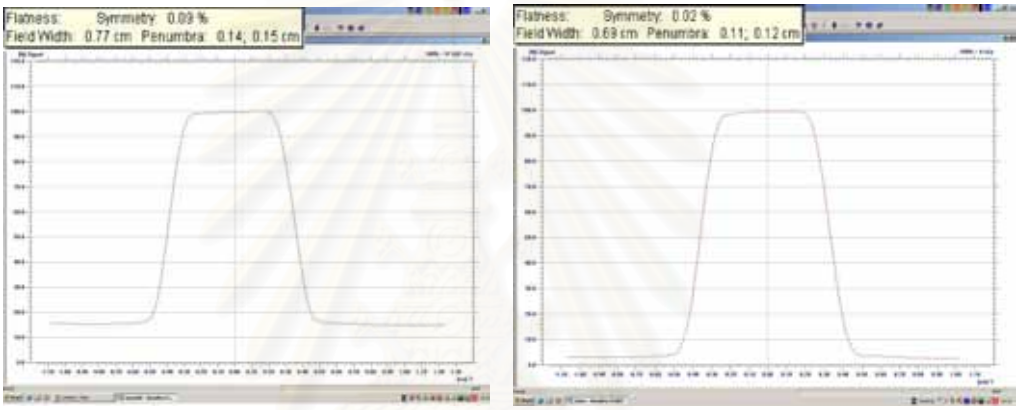

A) Optical density plotted B) Exposure plotted

Figure 4.5 The profile measured by film of 5 mm. collimation. A) Plotted by OD, the profile width is 7.7 mm. B) Plotted by exposure, the profile width is 6.9 mm.

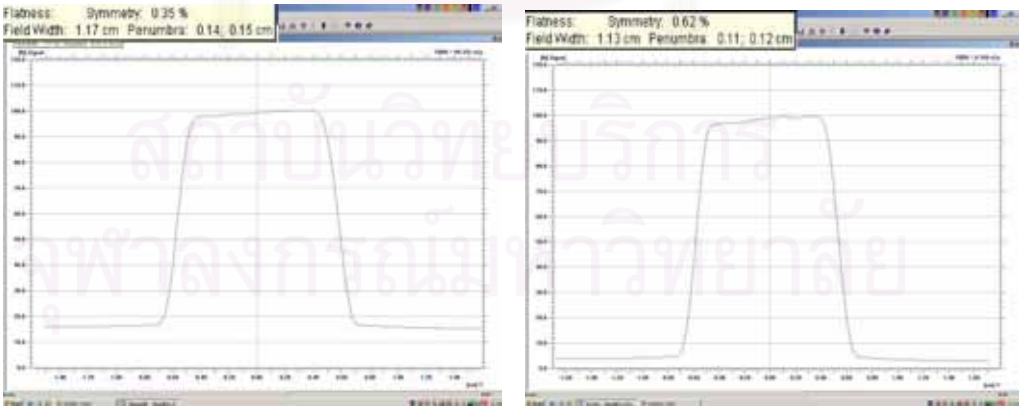

A) Optical density plotted B) Exposure plotted

Figure 4.6 The profile measured by film of 10 mm. collimation. A) Plotted by OD, the profile width is 11.7 mm. B) Plotted by exposure, the profile width is 11.3 mm.

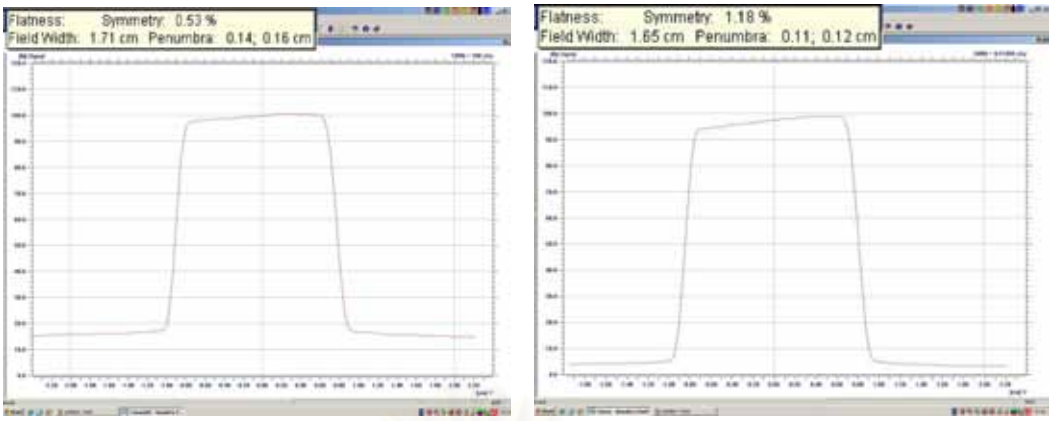

A) Optical density plotted B) Exposure plotted

Figure 4.7 The profile measured by film of 15 mm. collimation. A) Plotted by OD, the profile width is 17.1 mm. B) Plotted by exposure, the profile width is 16.5 mm.

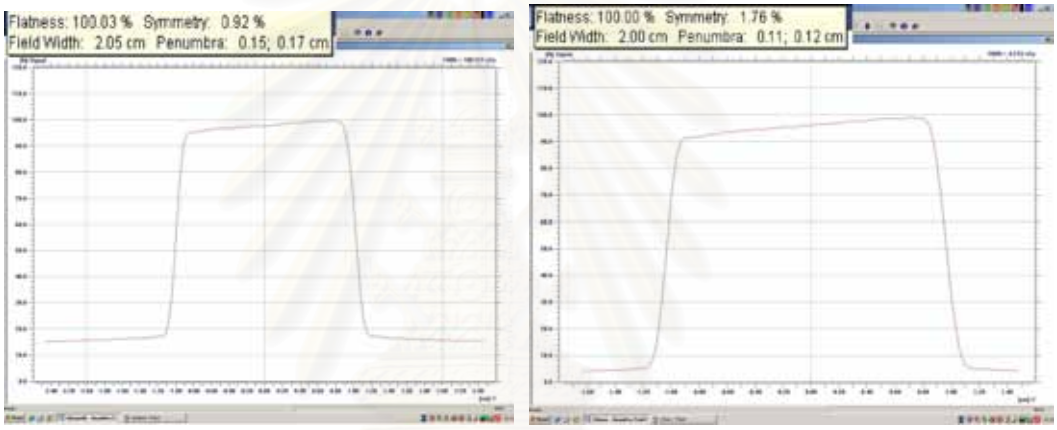

A) Optical density plotted B) Exposure plotted

Figure 4.8 The profile measured by film of 20 mm. collimation. A) Plotted by OD, the profile width is 20.5 mm. B) Plotted by exposure, the profile width is 20 mm.

The CT dose profile width measured by imaging plate in pixel values and exposures are shown in table 4.6 to table 4.12 and the graph are plotted in figure 4.9 to 4.15 for 5, 10, 15 and 20 mm. collimations setting for various L and S parameters of L = 1, S = 5, L = 2, S = 5, L = 3, S = 5 and 50, L = 4, S = 5, 50 and 200, respectively.

The profile measured by imaging plate plotted in pixel value, compared with profile measured by film in optical density, for L = 1, the profile width of both methods were closer than L = 2, 3 and 4. While the CT dose profile width measured by imaging plate plotted in exposure was agreeable to CT dose profile measured by film in exposure value for most of collimation setting except the 5 mm which the imaging plate dose profile was wider than the film dose profile measured for all parameters of CR reading. When L was fixed and S value was increased, dose profile was narrower, but there was no effect for 5 mm collimation setting.

The dose profile measured by imaging plate in pixel value had the different shape depend on parameter setting. When the dose profile was converted from pixel value to exposure, each of dose profile shape for all readout parameters was similar for the same collimation setting.

Table 4.6 CT profile width measured by imaging plate and the difference from collimation setting and film in pixel value and exposure for parameter setting of L = 1; S =5.

L=1; S=5

Collimation setting (mm.)	Profile width (mm.)		Difference from collimation setting (mm.)		Difference from film (mm.)	
	pixel value	exposure	pixel value	exposure	OD/pixel value	exposure
5.00	7.80	7.35	2.80	2.35	-0.1	-0.45
10.00	11.55	11.25	1.55	1.25	0.15	0.05
15.00	16.95	16.43	1.95	1.43	0.15	0.075
20.00	20.10	19.73	0.10	-0.27	0.4	0.275

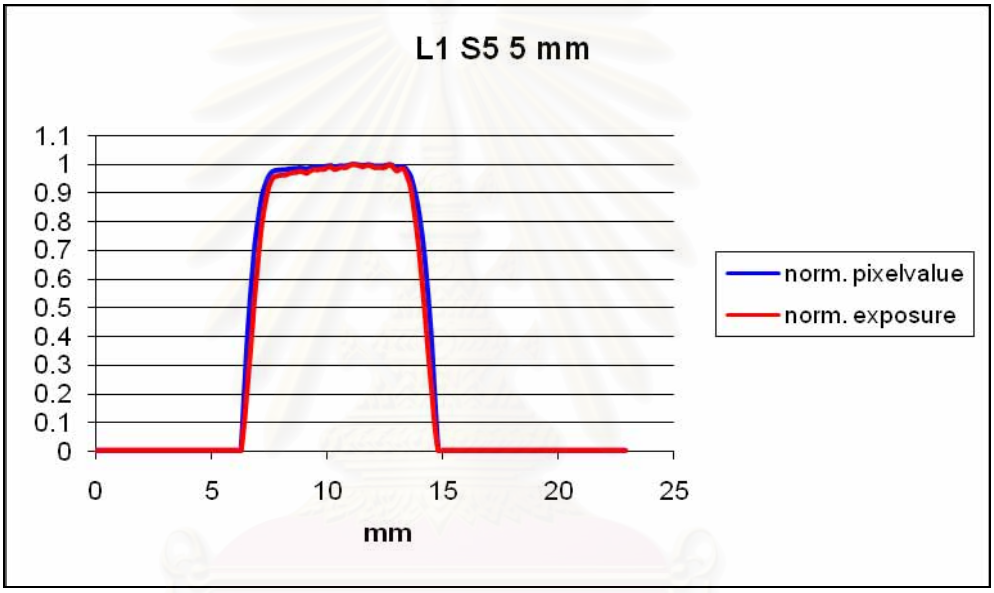

A) 5 mm. collimation setting.

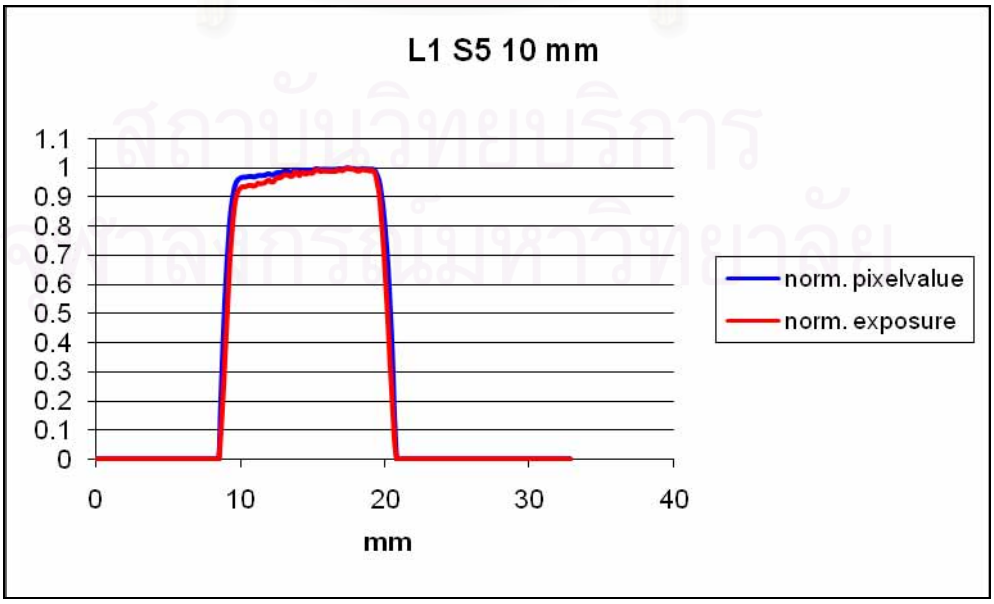

B) 10 mm. collimation setting.

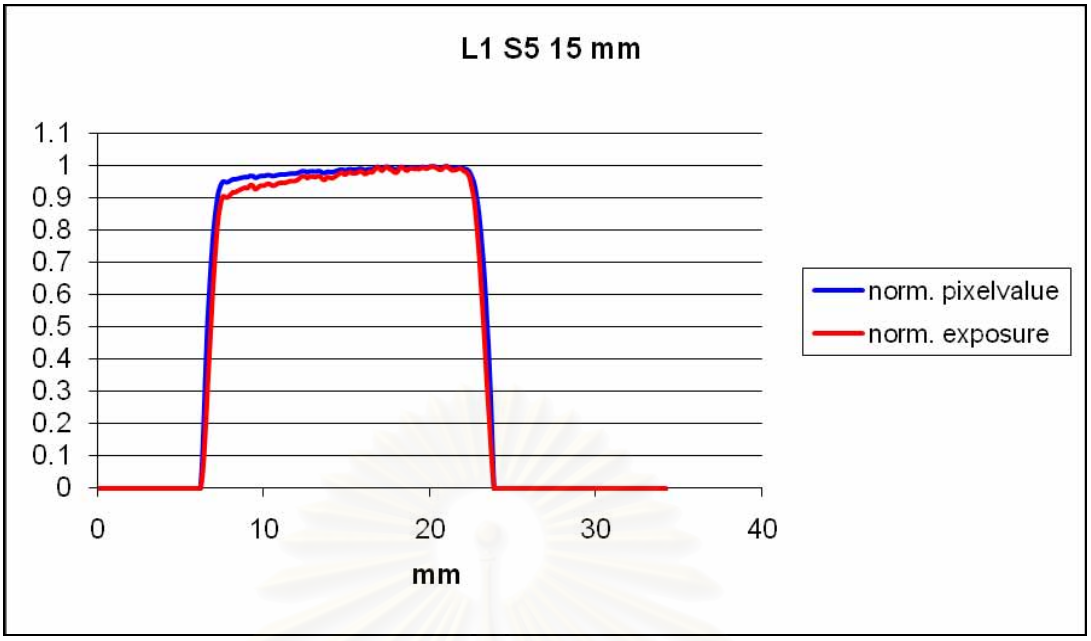

C) 15 mm. collimation setting.

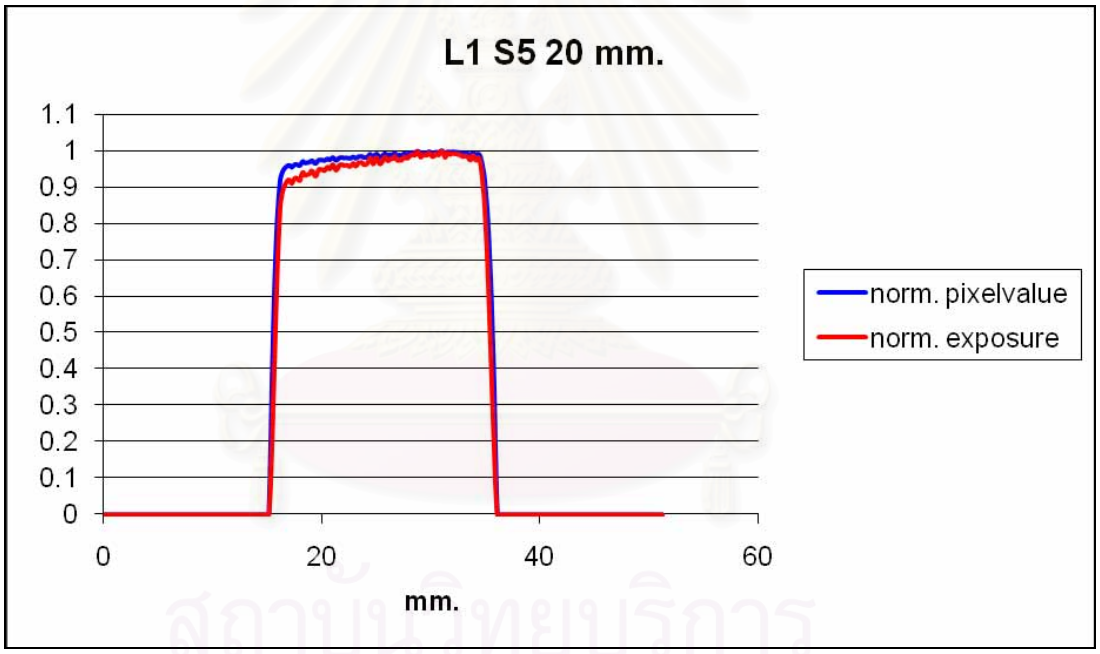

D) 20 mm. collimation setting.

Figure 4.9 The profile measured by imaging plate of L = 1; S = 5 plotted by pixel value and exposure.
A) The 5 mm. collimation setting.
B) The 10 mm. collimation setting.
C) The 15 mm. collimation setting.
D) The 20 mm. collimation setting.

Table 4.7 CT profile width measured by imaging plate and the difference from collimation setting and film in pixel value and exposure for parameter setting of L = 2; S =5.

L=2; S=5

Collimation setting (mm.)	Profile width (mm.)		Difference from collimation setting (mm.)		Difference from film (mm.)	
	pixel value	exposure	pixel value	exposure	OD/pixel value	exposure
5.00	7.80	7.60	2.80	2.60	-0.10	-0.70
10.00	11.63	11.33	1.63	1.33	0.07	-0.02
15.00	16.73	16.65	1.73	1.65	0.38	-0.15
20.00	20.15	19.88	0.15	-0.13	0.35	0.13

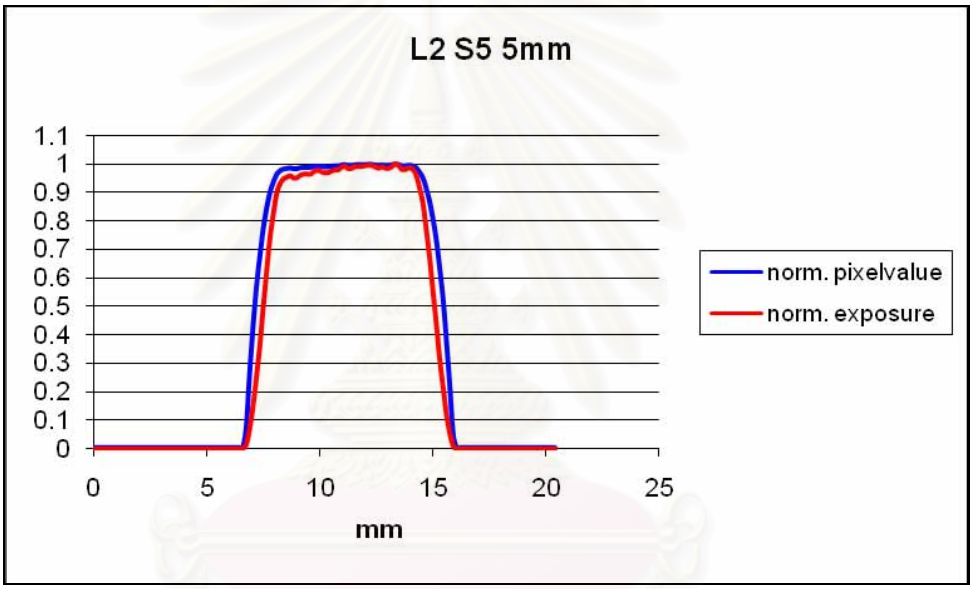

A) 5 mm. collimation setting.

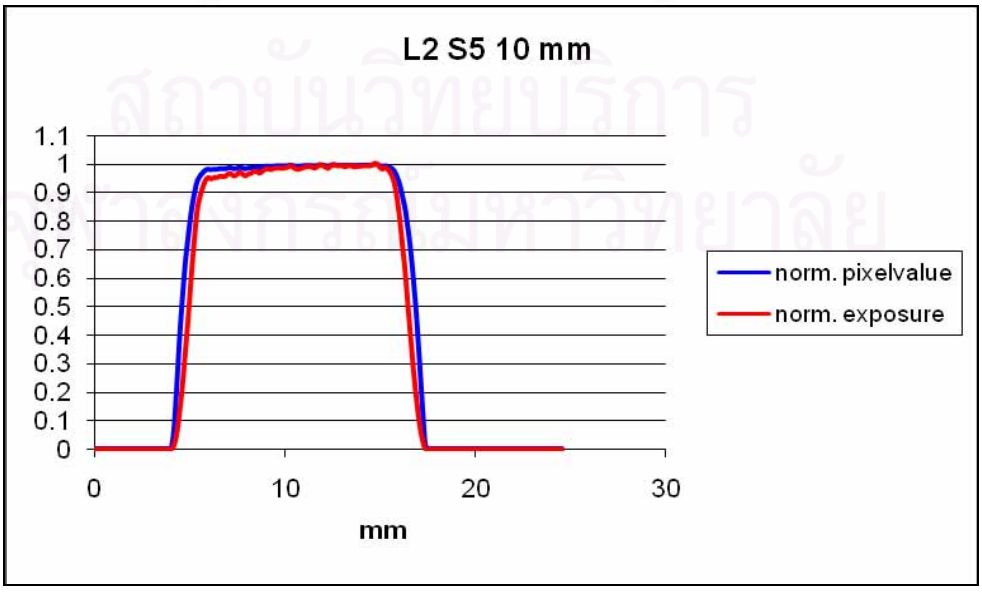

B) 10 mm. collimation setting.

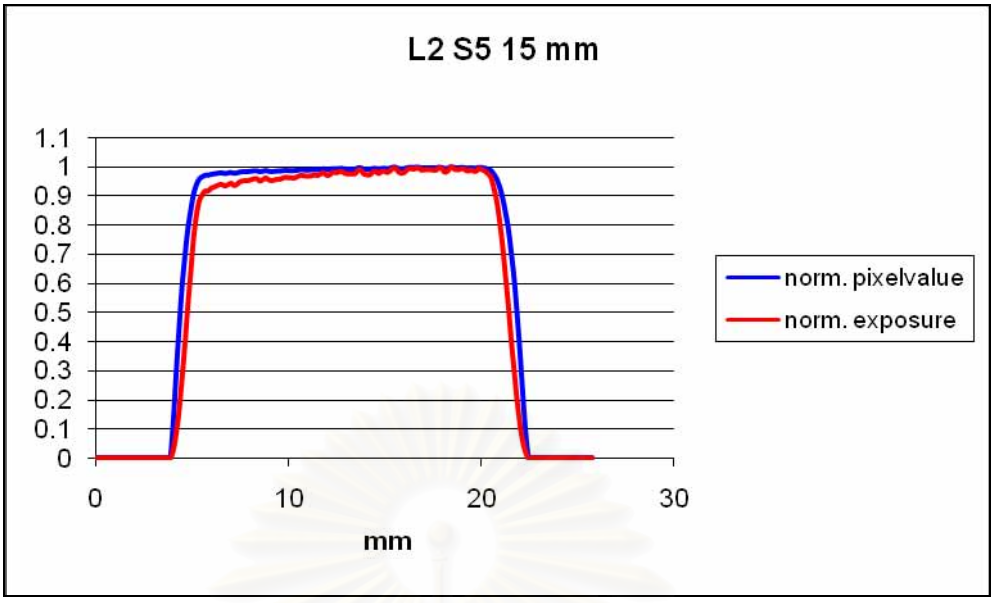

C) 15 mm. collimation setting.

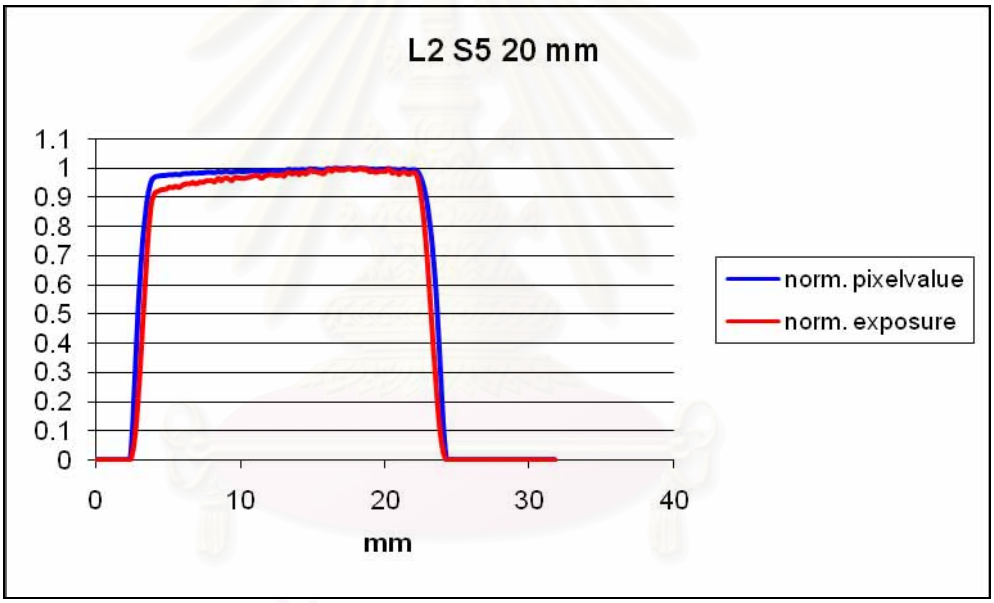

D) 20 mm. collimation setting.

Figure 4.10 The profile measured by imaging plate of L = 2; S = 5 plotted by pixel value and exposure.
A) The 5 mm. collimation setting.
B) The 10 mm. collimation setting.
C) The 15 mm. collimation setting.
D) The 20 mm. collimation setting.

Table 4.8 CT profile width measured by imaging plate and the difference from collimation setting and film in pixel value and exposure for parameter setting of L = 3; S =5.

L=3; S=5

Collimation setting (mm.)	Profile width (mm.)		Difference from collimation setting (mm.)		Difference from film (mm.)	
	pixel value	exposure	pixel value	exposure	OD/pixel value	exposure
5.00	8.25	7.65	3.25	2.65	-0.55	-0.75
10.00	12.00	11.55	2.00	1.55	-0.30	-0.25
15.00	17.40	16.73	2.40	1.73	-0.30	-0.22
20.00	20.48	19.95	0.48	-0.05	0.03	0.05

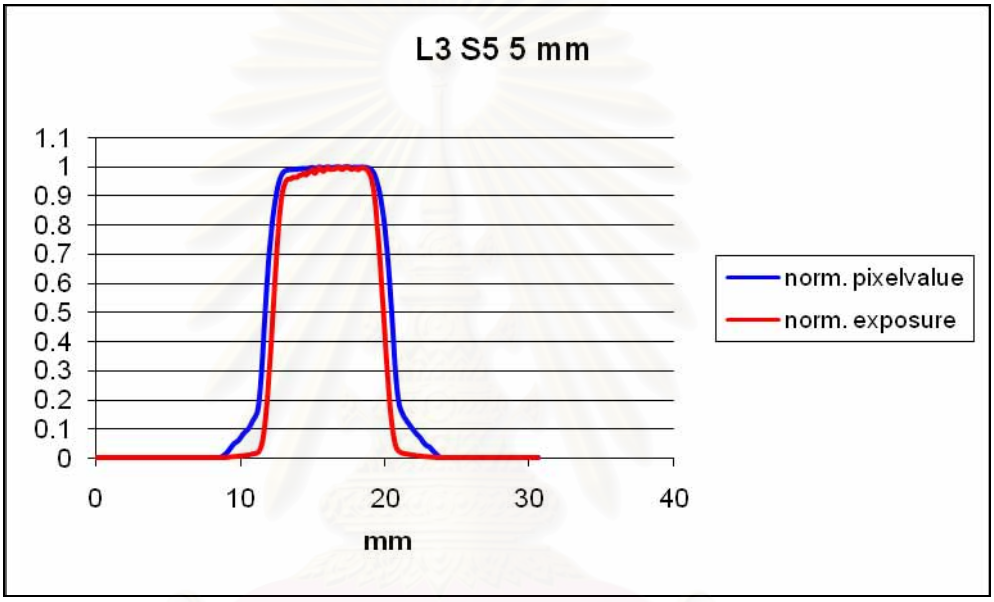

A) 5 mm. collimation setting.

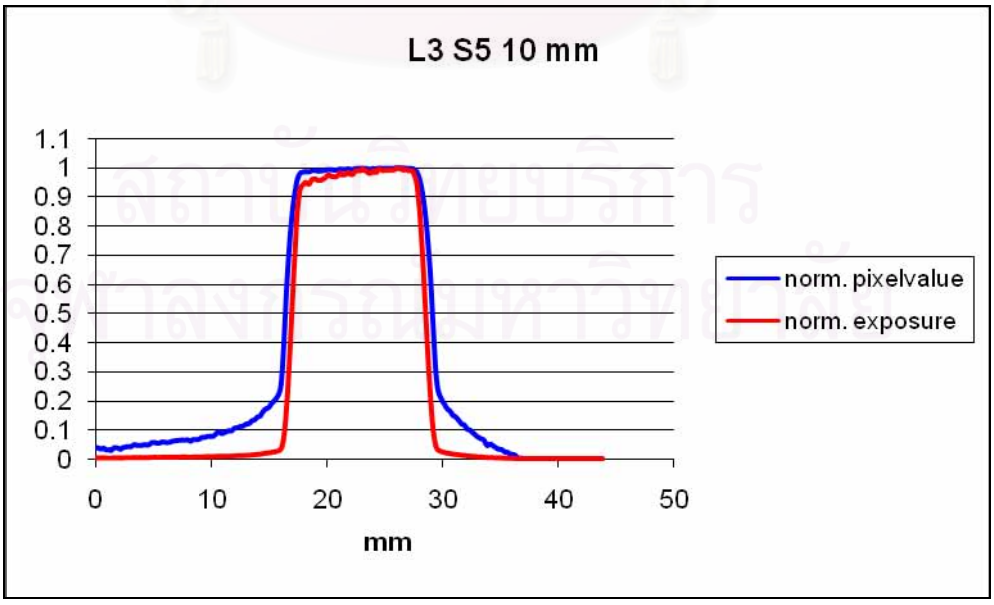

B) 10 mm. collimation setting.

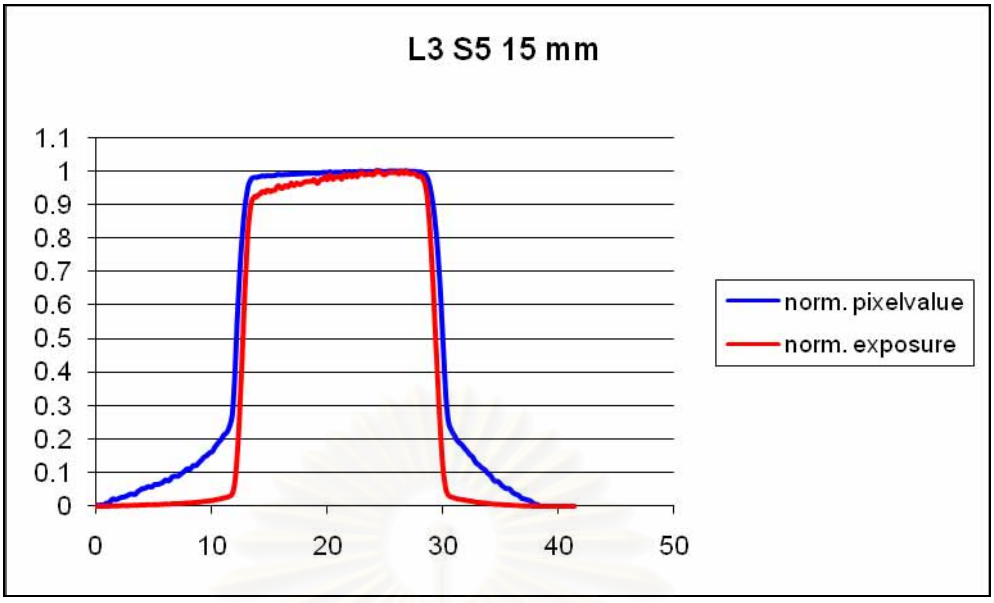

C) 15 mm. collimation setting.

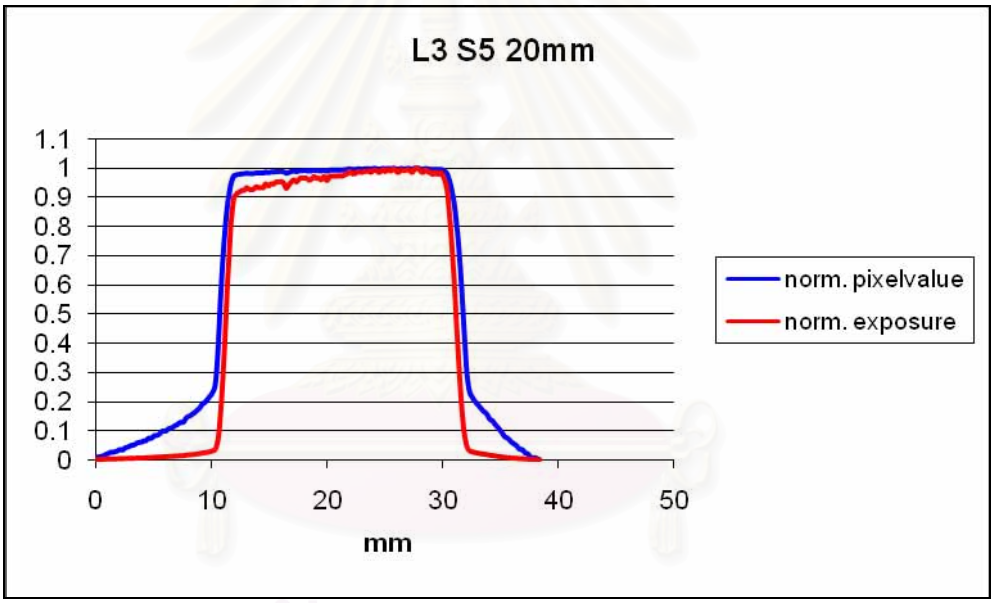

D) 20 mm. collimation setting.

Figure 4.11 The profile measured by imaging plate of L = 3; S = 5 plotted by pixel value and exposure.
A) The 5 mm. collimation setting.
B) The 10 mm. collimation setting.
C) The 15 mm. collimation setting.
D) The 20 mm. collimation setting.

Table 4.9 CT profile width measured by imaging plate and the difference from collimation setting and film in pixel value and exposure for parameter setting of L = 3; S =50.

L=3; S=50

Collimation setting (mm.)	Profile width (mm.)		Difference from collimation setting (mm.)		Difference from film (mm.)	
	pixel value	exposure	pixel value	exposure	OD/pixel value	exposure
5.00	8.40	7.65	3.40	2.65	-0.70	-0.75
10.00	12.00	11.40	2.00	1.40	-0.30	-0.10
15.00	17.10	16.50	2.10	1.50	0.00	0.00
20.00	20.55	19.95	0.55	-0.05	-0.05	0.05

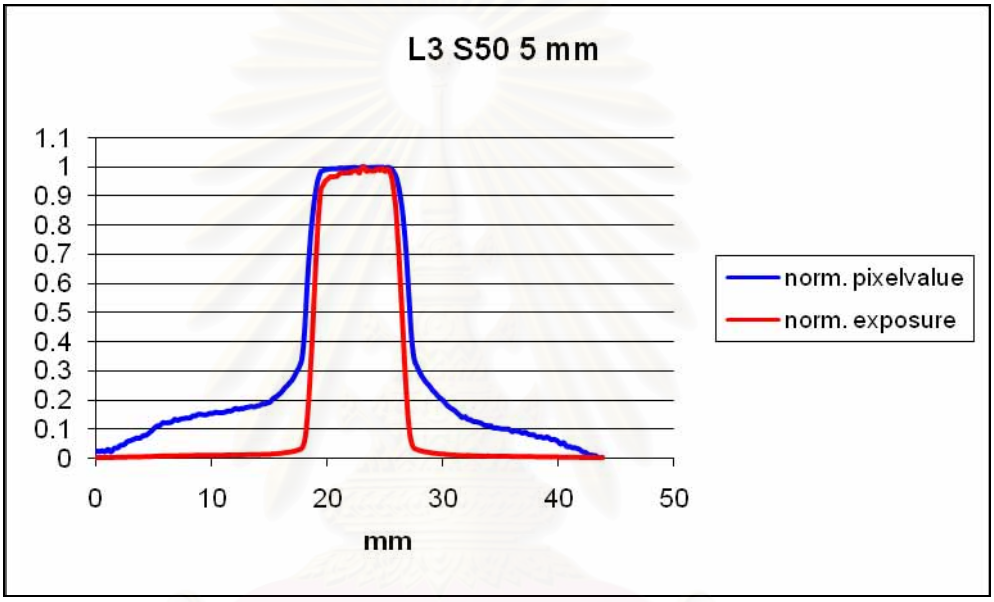

A) 5 mm. collimation setting.

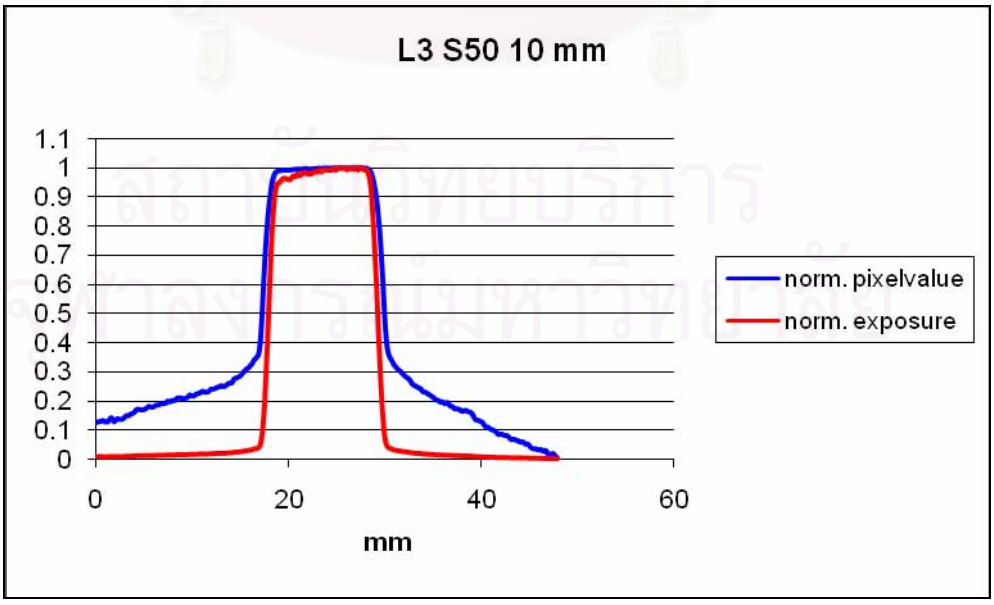

B) 10 mm. collimation setting.

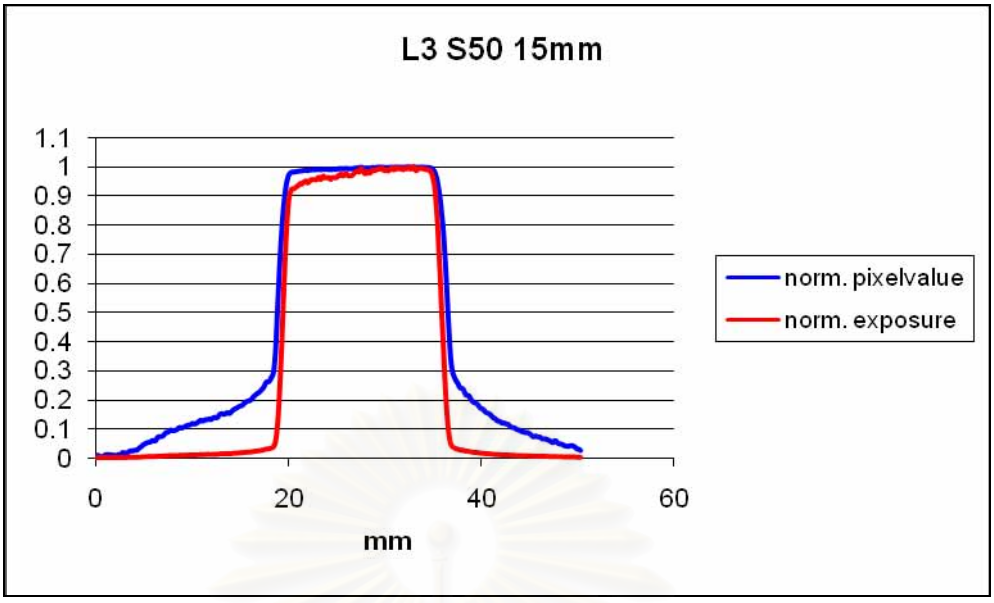

C) 15 mm. collimation setting.

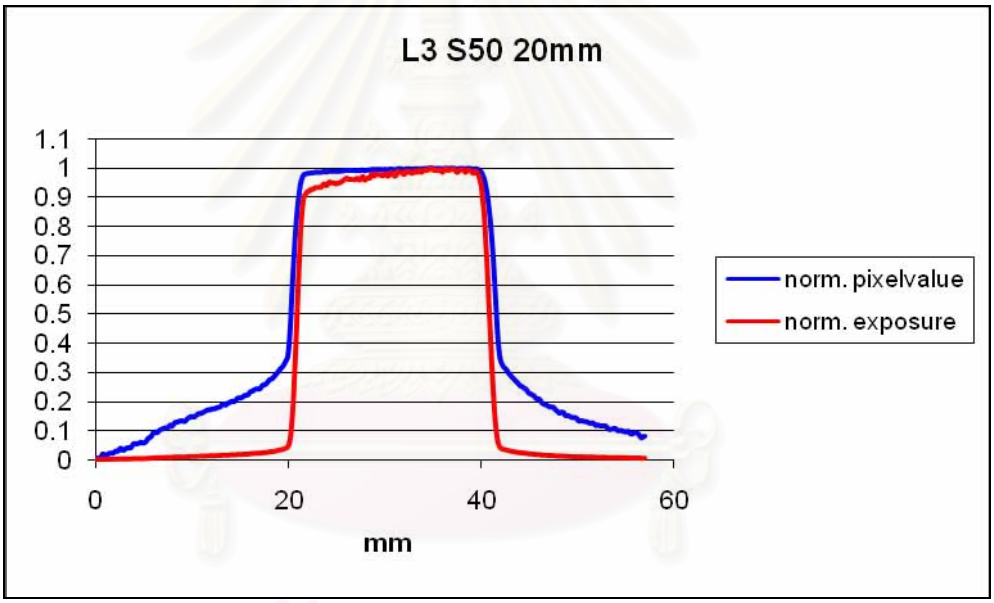

D) 20 mm. collimation setting.

Figure 4.12 The profile measured by imaging plate of L = 3; S = 50 plotted by pixel value and exposure.
A) The 5 mm. collimation setting.
B) The 10 mm. collimation setting.
C) The 15 mm. collimation setting.
D) The 20 mm. collimation setting.

Table 4.10 CT profile width measured by imaging plate and the difference from collimation setting and film in pixel value and exposure for parameter setting of L = 4; S =5.

L=4; S=5

Collimation setting (mm.)	Profile width (mm.)		Difference from collimation setting (mm.)		Difference from film (mm.)	
	pixel value	exposure	pixel value	exposure	OD/pixel value	exposure
5.00	8.40	7.65	3.40	2.65	-0.70	-0.75
10.00	12.16	11.48	2.16	1.48	-0.45	-0.18
15.00	17.43	16.73	2.43	1.73	-0.33	-0.23
20.00	20.65	20.03	0.65	0.02	-0.15	-0.02

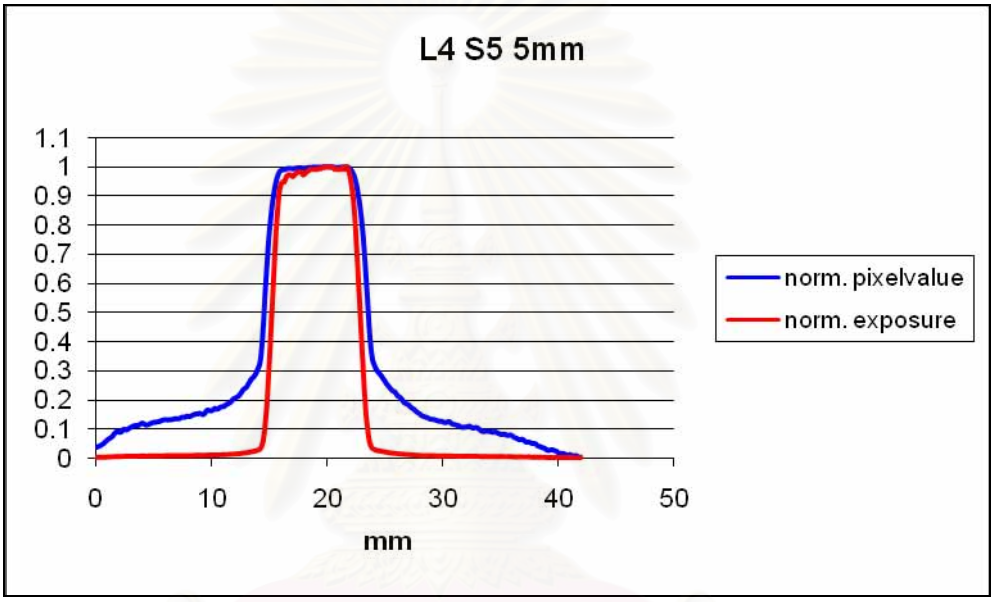

A) 5 mm. collimation setting.

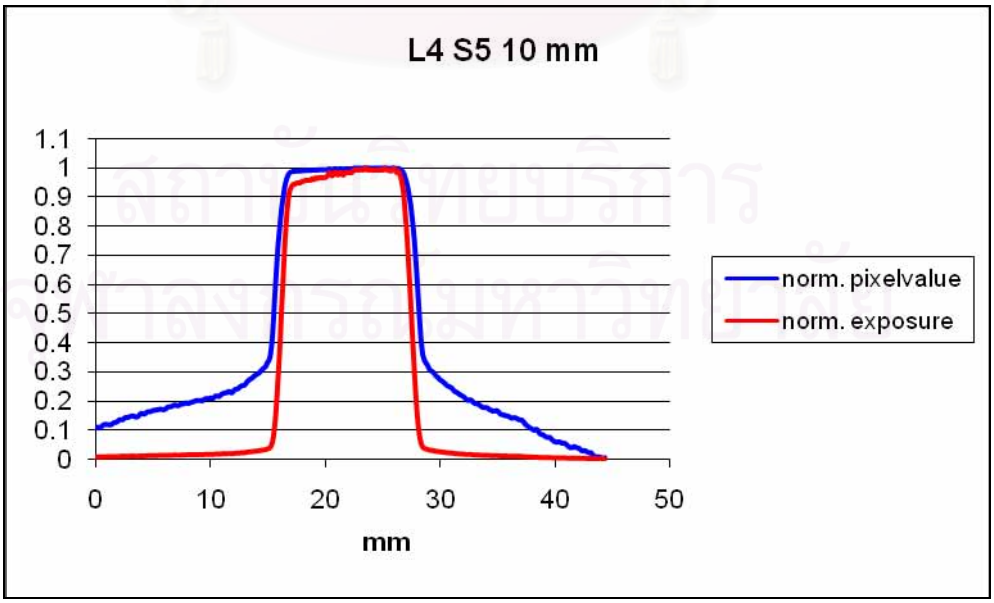

B) 10 mm. collimation setting.

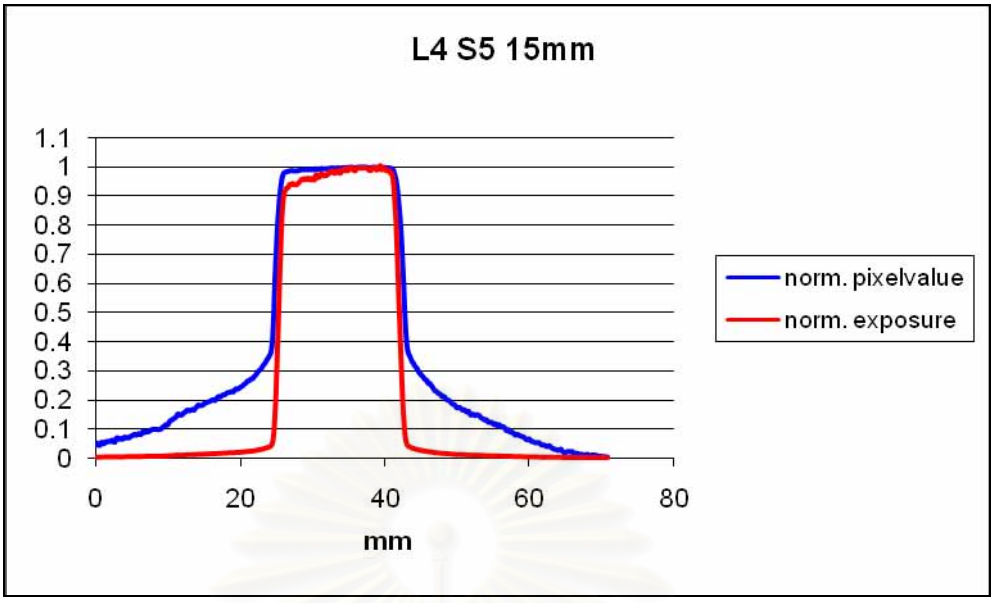

C) 15 mm. collimation setting.

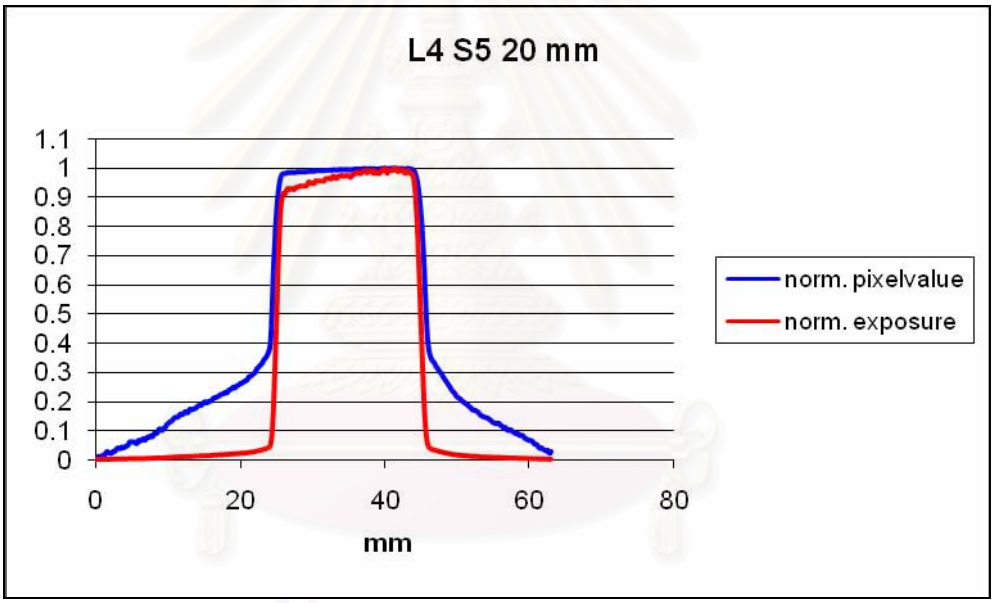

D) 20 mm. collimation setting.

Figure 4.13 The profile measured by imaging plate of L = 4; S = 5 plotted by pixel value and exposure.
A) The 5 mm. collimation setting.
B) The 10 mm. collimation setting.
C) The 15 mm. collimation setting.
D) The 20 mm. collimation setting.

Table 4.11 CT profile width measured by imaging plate and the difference from collimation setting and film in pixel value and exposure for parameter setting of L = 4; S =50.

L=4; S=50

Collimation setting (mm.)	Profile width (mm.)		Difference from collimation setting (mm.)		Difference from film (mm.)	
	pixel value	exposure	pixel value	exposure	OD/pixel value	exposure
5.00	8.33	7.65	3.33	2.65	-0.62	-0.75
10.00	12.00	11.33	2.00	1.33	-0.30	-0.02
15.00	17.10	16.50	2.10	1.50	0.00	0.00
20.00	20.55	19.95	0.55	-0.05	-0.05	0.05

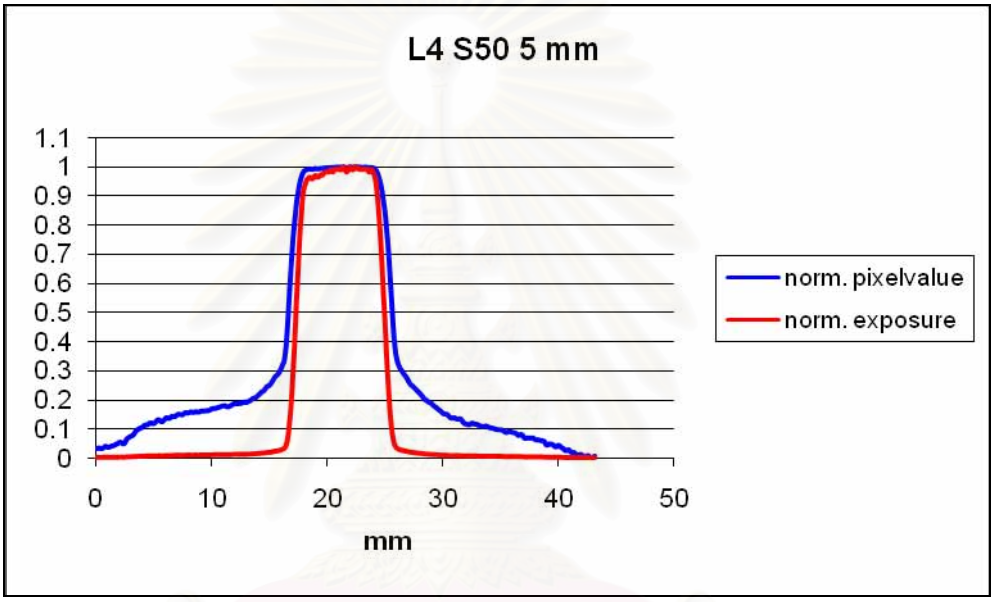

A) 5 mm. collimation setting.

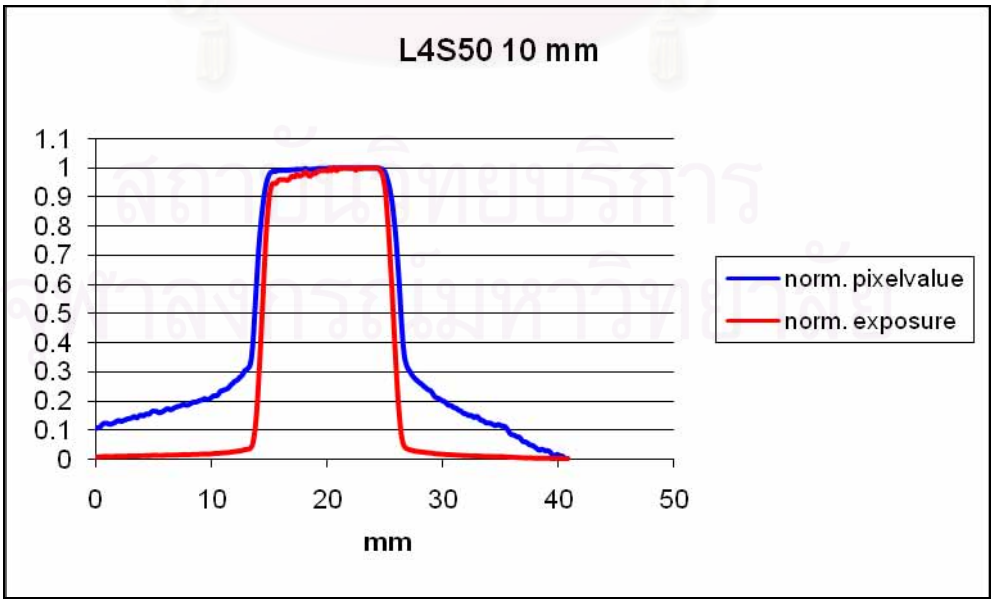

B) 10 mm. collimation setting.

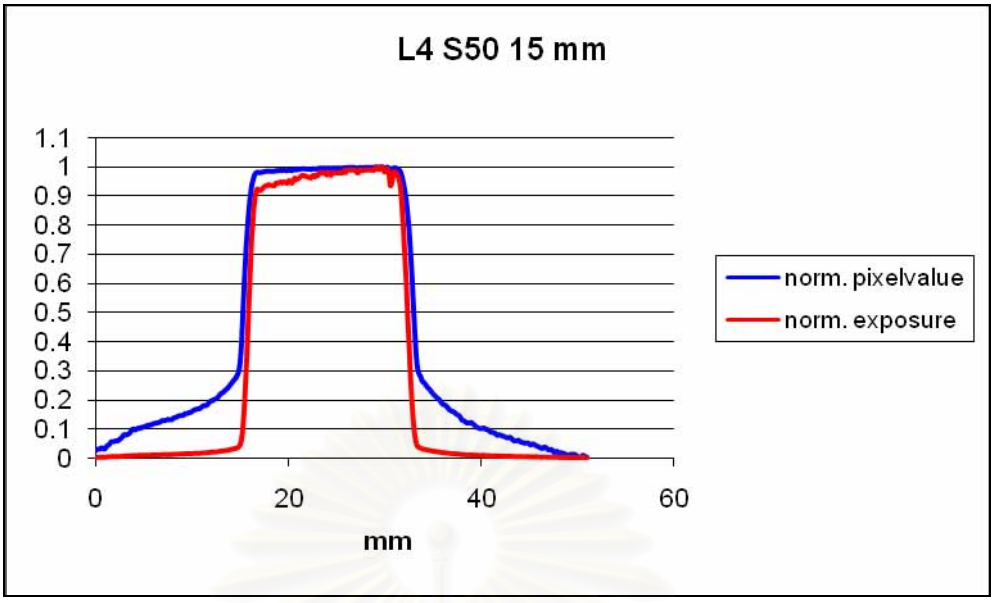

C) 15 mm. collimation setting.

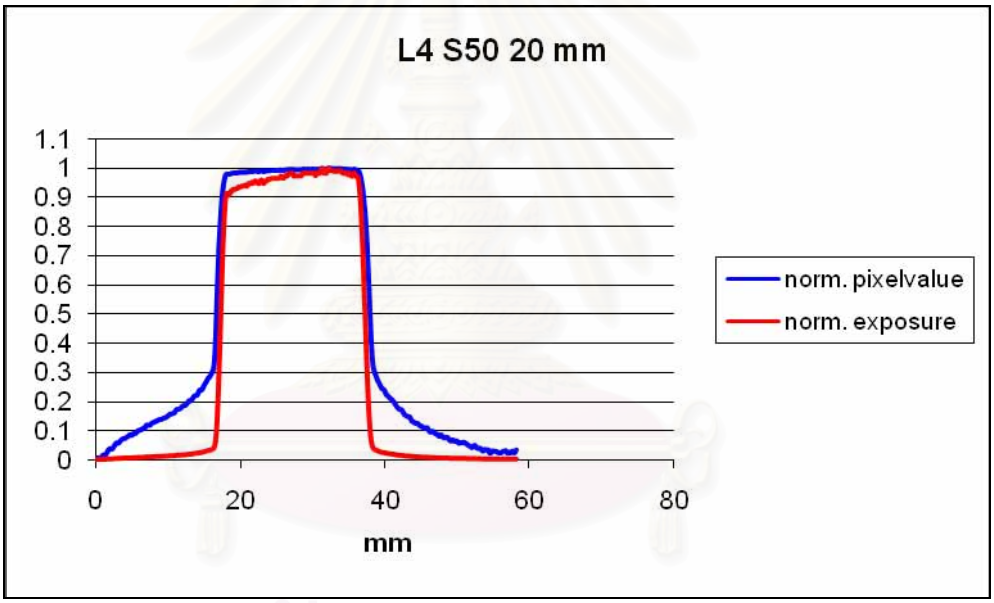

D) 20 mm. collimation setting.

Figure 4.14 The profile measured by imaging plate of L = 4; S = 50 plotted by pixel value and exposure.
A) The 5 mm. collimation setting.
B) The 10 mm. collimation setting.
C) The 15 mm. collimation setting.
D) The 20 mm. collimation setting.

Table 4.12 CT profile width measured by imaging plate and the difference from collimation setting and film in pixel value and exposure for parameter setting of L = 4; S =200.

L=4; S=200

Collimation setting (mm.)	Profile width (mm.)		Difference from collimation setting (mm.)		Difference from film (mm.)	
	pixel value	exposure	pixel value	exposure	OD/pixel value	exposure
5.00	8.40	7.65	3.40	2.65	-0.7	-0.75
10.00	12.08	11.30	2.08	1.30	-0.375	0
15.00	17.10	16.50	2.10	1.50	0	0
20.00	20.55	19.95	0.55	-0.05	-0.05	0.05

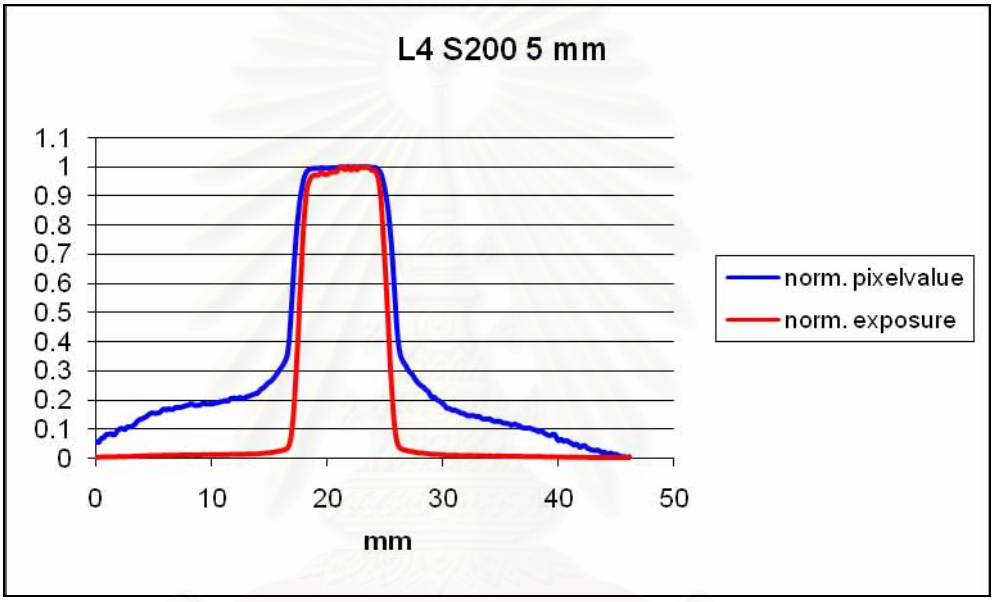

A) 5 mm. collimation setting.

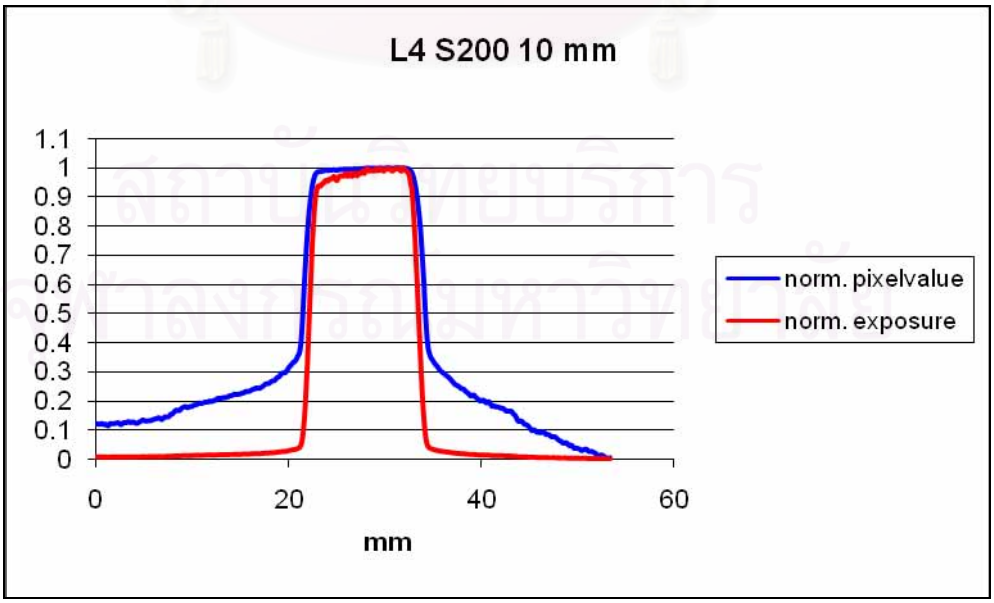

B) 10 mm. collimation setting.

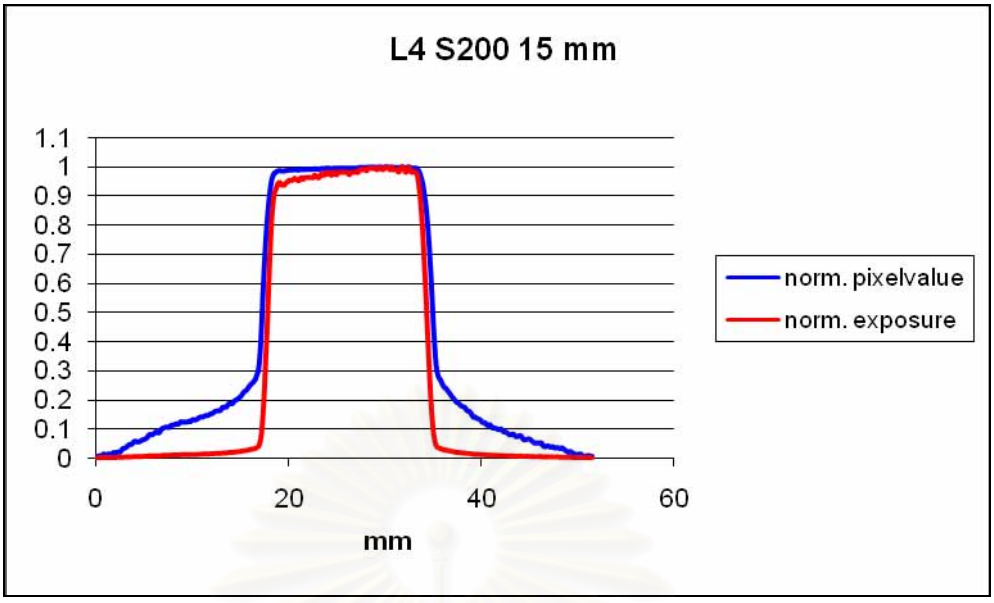

C) 15 mm. collimation setting.

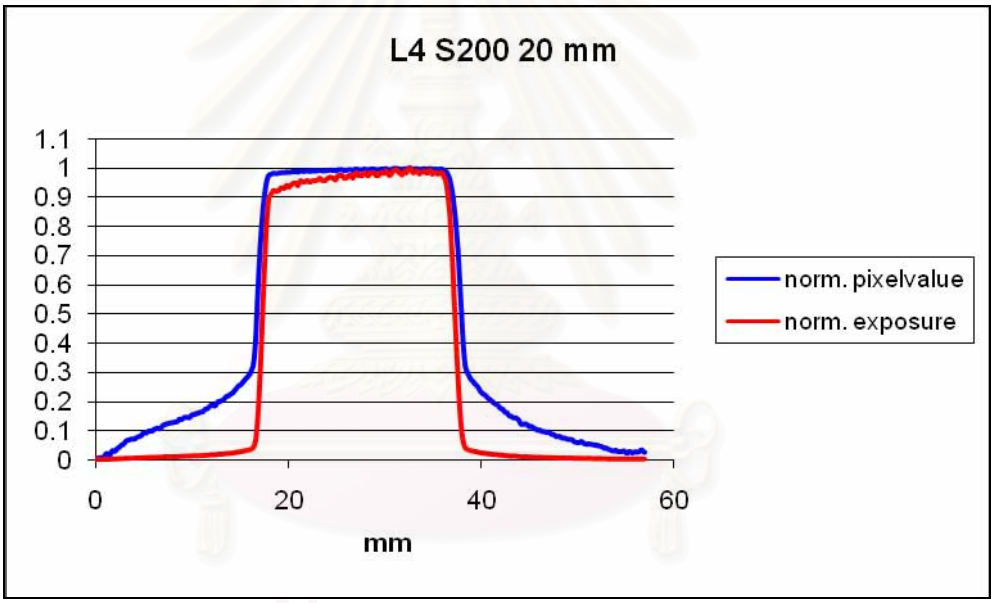

D) 20 mm. collimation setting.

Figure 4.15 The profile measured by imaging plate of L = 4; S = 200 plotted by pixel value and exposure.
A) The 5 mm. collimation setting.
B) The 10 mm. collimation setting.
C) The 15 mm. collimation setting.
D) The 20 mm. collimation setting.

Figure 4.16 shows the histogram of the comparable of the dose profile width of film and imaging plate for L = 1; S = 5. The agreement was demonstrated for both plotted by pixel value and exposure, because the profiles plotted by pixel value were more easily to measure directly at FWHM . The point of FWHM for both calculated according to equation (9) and measured directly were slightly different.

Figure 4.17 shows the histogram of the comparable of the dose profile width of film and imaging plate for L = 4; S = 200. The agreement was demonstrated for both plotted by pixel value and exposure, but the profiles plotted by pixel value were more complex to defined because the FWHM of profiles were not located at the half maximum. We used equation (9) to estimate the half maximum.

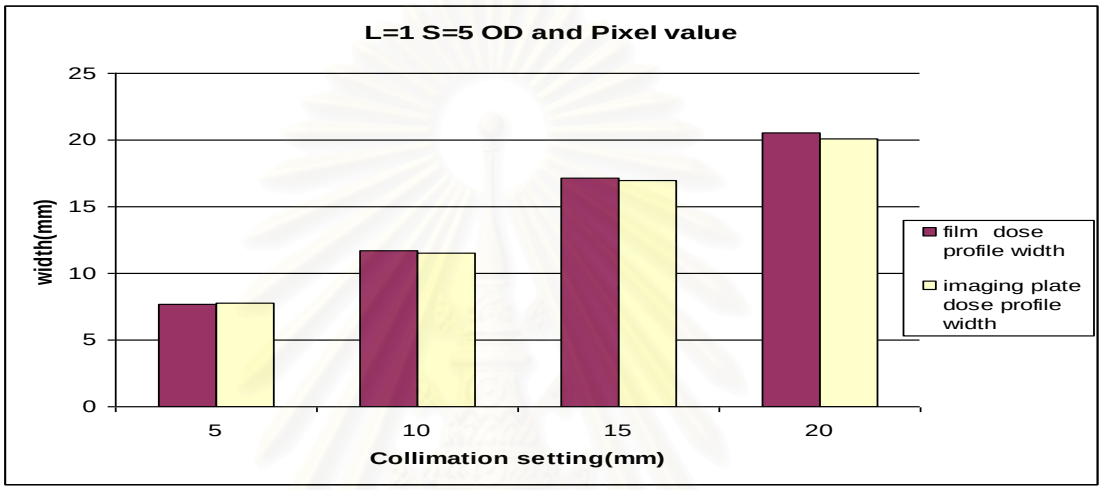

A) Dose profile width of film plotted by OD and imaging plate plotted by pixel value.

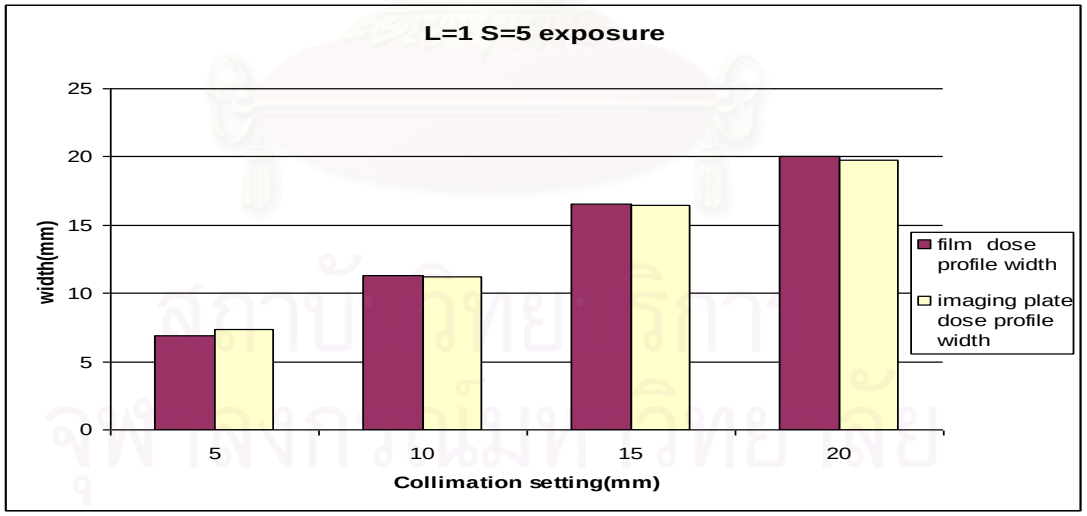

B) Dose profile width of film and imaging plate plotted by exposure.

Figure 4.16 Comparison between dose profile width of film and imaging plate of L = 1; S =5 A) Dose profile width of film plotted by OD and imaging plate plotted by pixel value B) Dose profile width of film and imaging plate plotted by exposure.

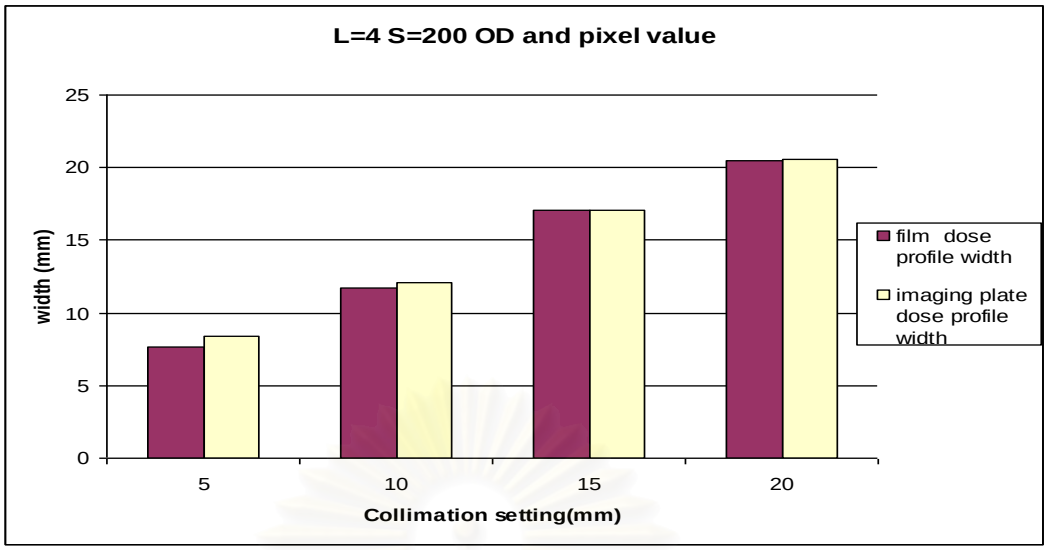

A) Dose profile width of film and imaging plate plotted by optical density and pixel value.

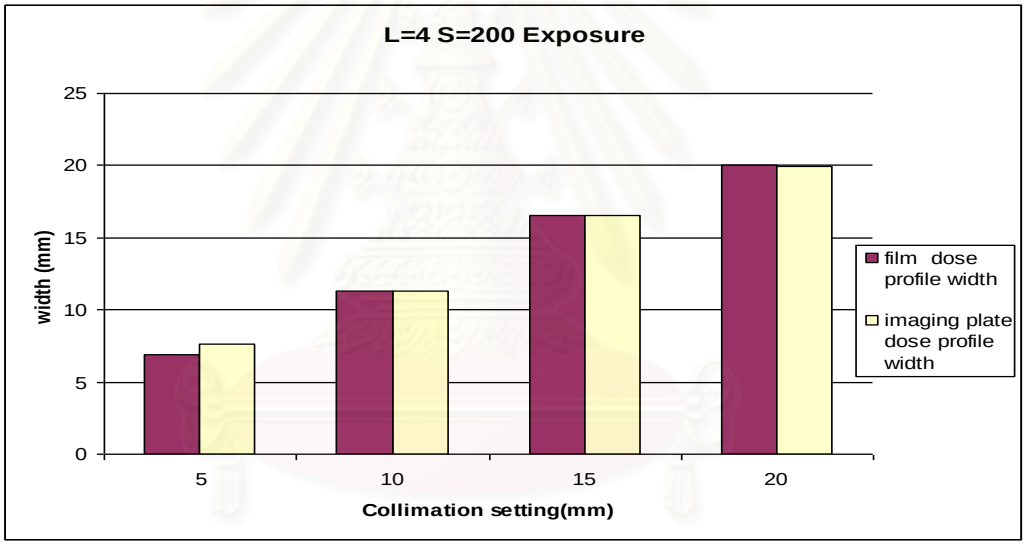

B) Dose profile width of film and imaging plate plotted by exposure.

Figure 4.17 Comparison between dose profile width of film and imaging plate of L = 4; S =200. A) Dose profile width of film and imaging plate plotted by optical density and pixel value. B) Dose profile width of film and imaging plate plotted by exposure.

CHAPTER V

DISCUSSION AND CONCLUSION

5.1 Discussion

The film characteristic curve was shown less slope and non linearity relationship in semi- log scale between exposure of x-ray beam and optical density in the low dose region, small change in optical density give rise to more change in exposure. This resulted in higher plotted by optical density than plotted by exposure in the low region of dose profile. While the imaging plate characteristic curves showed linearity between pixel value and exposure for semi – log scale but the quantization occur for lower value of L and S. these were due to the limited pixel value presented in the imaging plate reader (10 bits).

The characteristic curves irradiated with computed tomography scanner plotted in semi- log scales between exposure and pixel value showed linearity for film in the high exposure range, but the saturation was occurred for imaging plate when the exposure was equal or more than 10 mAs, this was due to the high radiation when the CT tube was rotated. The cerrobend block and lead sheet was used for blocking the beam came from other direction except from the vertical beam.

The computed tomography dose profile width measured by imaging plate was mostly narrower than film if latitude (L) was too low, because the signal from low energy beam wasn't detected. Increase the S value may cause the pixel value higher. If S value was high enough, the low energy beam such as scatter radiation could be detected. That will change the shape and the width of the profile. But when varied S value too high, the signal may be quantization.

Computed tomography dose profile width measured by imaging plate with parameter setting L = 1 S = 5 plotted in pixel value is close to the profile width measured by film plotted in optical density, because this parameter is high contrast and the scatter radiation didn't detect in this parameter, this is shown in the characteristic curves of both film and imaging plate in figure 5.1 A. Only high energy beam can be measured, and the difference between half maximal pixel value and FWHM is not significant, shown in figure 5.1 B. But when we converted this profile into exposure, the profile width from imaging plate is too narrow because some signal was lost. But the result still in the acceptable limitation (± 2 mm.) except 5 mm. width.

At the parameter setting L = 4 S = 200, the computed tomography dose profile width measured by imaging plate could detect each energy of CT scan irradiated, this is shown in the characteristic curves of both film and imaging plate in figure 5.2 A. When we converted to exposure, the computed tomography dose profile width was close to the computed tomography dose profile width measured by film, but in pixel value, this parameter gave too wide profile because the imaging plate had high response to low energy beam and had a big different between half-maximal pixel value and FWHM, shown in figure 5.2 B.

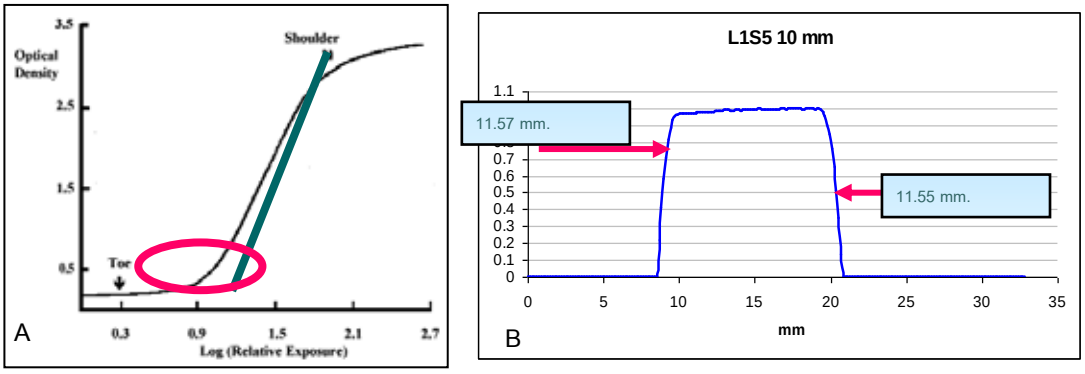

Figure 5.1 The reason to explain why it had a small difference between half-maximal pixel value and FWHM A) The characteristic curves of film and imaging plate at L =1; S = 5, this parameter is high contrast and the scatter radiation didn't detect in this parameter. B) The difference between half maximal pixel value and FWHM.

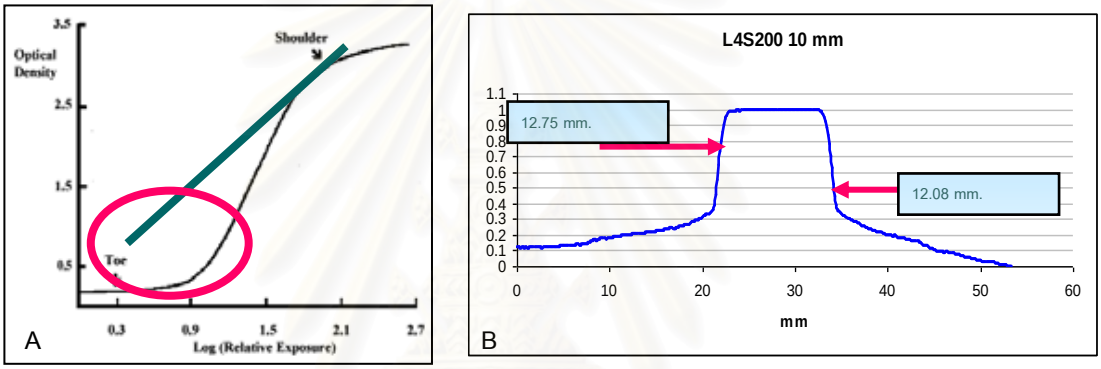

Figure 5.2 The reason to explain why it had a big difference between half-maximal pixel value and FWHM. A) The characteristic curves of film and imaging plate at L =1; S = 5, this parameter could detect each energy of CT scan irradiated B) The difference between half maximal pixel value and FWHM is significant.

The heel effect affected to the profile shape, especially the profile plotted by exposure, it made the slope at the off axis of the dose profile, the high intensity was shown in the profile at the cathode side of CT x – ray tube.

As compare to the result of related literature(*Liu HL, 2005*)[10], our study illustrated the narrower profiles and more accurate, because we used the same kVp to irradiate film and imaging plate (related literature used 80 kVp to avoid signal saturated), but *Liu HL's* result was more consistency even the parameters were changed. This is shown in table 5.1

Table 5.1 Comparison between Liu HL and this study for 10 mm. collimation setting, scan with 80 kVp (Liu HL) and 120 kVp (this study).

Collimation (mm)	Parameter		Result (mm)		Different from film (mm)	
	L	S	Liu HL	This study	Liu HL	This study
10	1	5	11.9	11.25	0.3	0.05
10	4	5	11.9	11.48	0.3	0.18
10	4	50	11.9	11.33	0.3	0.02
10	4	200	11.9	11.30	0.3	0.00

To prevented the saturation of imaging plate due to high exposure, this study employed the cerrobend block for limiting the direction of beam and lead sheet for filtering the beam from under cough, so the exposure was reduced. Dose from equation(10) was the dose given to the imaging plate, which was between 48 to 52 mR.In case of cerrobend plate was not available, the lead sheet about 2 mm thickness was also useful. The two lead sheets were placed on the imaging plate making 1 - 3 cm slit as shown in figure 5.3. Then the image plate could be exposed without saturation.

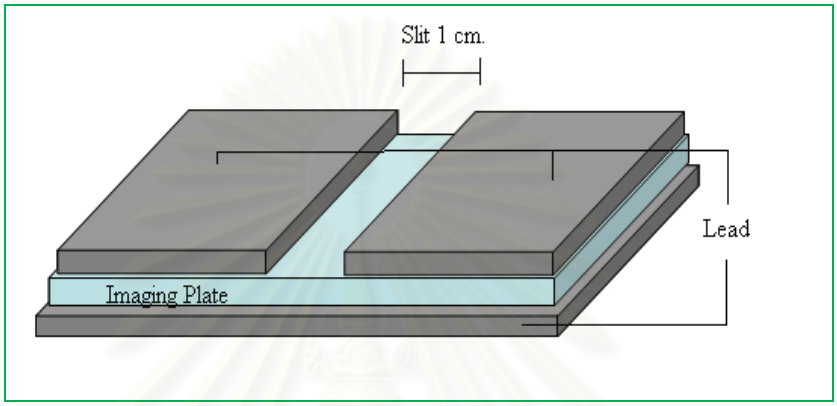

Figure 5.3 Setting of lead sheet for filtering the radiation from another direction except from above.

5.2 Conclusion

Before using film and imaging plate measured the dose profile width, the characteristic curve of film and imaging plate were studied for both x – ray beam and computed tomography beam, by plotting between optical density and exposure for film, and between pixel value and exposure by the imaging plate in semi – log scale. The characteristic curves of film irradiated with x – ray showed non linearity because low exposure were used and computed tomography scanner showed linearity in the exposure range of 3500 – 9700 mR. The characteristic curves of imaging plate plotted in semi- log scales between exposure and pixel value showed linearity but the saturation were occurred when the exposure with the x –ray was more than 10 mAs at 81 kVp.

Then the suitable exposure technique of this study for irradiated verification film and imaging plate were observed by computed tomography scanner. The cerrobend block and lead sheet were used for filtering and limiting beam direction when irradiated imaging plate. The suitable exposure technique was 120 kVp, 10 mAs.

The full width at half maximum of the dose profile measured by film of 5, 10, 15 and 20 mm. collimator beam were 7.7, 11.7, 17.1, and 20.5 mm, respectively, for the plotted of optical density, when changing the optical density to exposure, the full width at half maximum were 6.9, 11.3, 16.5, and 20 mm, respectively.

The suitable parameters for measuring the imaging plate computed tomography dose profile width plotted by pixel value were L = 1; S = 5. Dose profile width was 7.8, 11.6, 16.95 and 20.1 mm. The result was closer to the film profile width plotted by optical density.

For measuring the computed tomography dose profile width plotted by exposure, the suitable parameter of imaging plate was L = 4; S= 200, Dose profile width was 7.65, 11.3, 16.5 and 19.95 mm. the width was comparable to the film dose profile width. The difference from collimator setting of film width and IP width were mostly the same for all nominal collimation setting except 5 mm collimator setting.

From this study, the image plate could be used for the quality assurance of the CT dose profile width comparable to film. However, the parameters for the exposure and the computed radiography reader should be checked before implementing this technique into the department.

REFERENCES

[1] American Association of Physicists in Medicine, AAPM Report No. 39, Specification and acceptance testing of computed tomography scanners New York, American Institute of Physics (1993).

[2] Jerrold TB. The essential physics of medical imaging. 2nd ed. USA. Lippincott Williams & Wilkins (2002): 176 - 81, 255 - 83, 326 - 72, 344 - 46.

[3] Seibert JA. Computed radiography technology 2004. MMP AAPM (2004): 153 – 175.

[4] FUJIFILM Corporation. What is imaging plate? http://www.fujifilm.com/products/life_science/si_imgplate/img_plate.html .

[5] Suwanpradit P. Quality Control Program of the Computed Radiography System. Thesis for the Degree of Master Science in Medical Imaging, Faculty of Medicine, Chulalongkorn University, 2004: 7 – 9,44 – 51.

[6] Christensen EE, Curry T S, James N, chapter 10. An introduction to the physics of radiology(1972), The science of photography, Vol. 2. London, Fountain press(1967).

[7] Dendy PP, Heaton B. Physics for diagnostic radiology. 2nd ed. UK, 1999: 89 – 93

[8] R. Sekine, H. Kimura, Y. Muramatsu, T. Murakami, S. Saotome, and N. Moriyama. Reusable imaging plate (IP) for swift and automatic measurement of x-ray CT dose profiles. Nippon Igaku Hoshasen Gakkai Zasshi 60 (2004): 69–70. Abstract in English.

[9] Thomson FJ. Measurement of CT scanner dose profiles in a filmless department. Australas Phys Eng Sci Med 28 (2005): 179-83.

[10] Liu H.L., Liu R.R., Reeve D.M., Shepard S.J., Willis C.E. Measurement of CT radiation profile width using CR imaging plates. Med Phys 32(2005) :2881-7.

APPENDICES

APPENDIX A

REPORT OF FILM PROCESSOR QUALITY ASSURANCE

The reference H&D curve for automatic film processor Kodak M6B were plotted, the optical density were read from the 21 steps of standard step wedge film for 3 days. The average of 3 consecutive days was determined and used for plotting the graph. The graph gave the high density (HD), low density (LD), medium density (MD) or speed index of 1.25, density difference (DD) or contrast index of 1.56, base+fog of 0.25 and temperature index of 35.03°C. These values were used as the reference for the QA of the film processor.

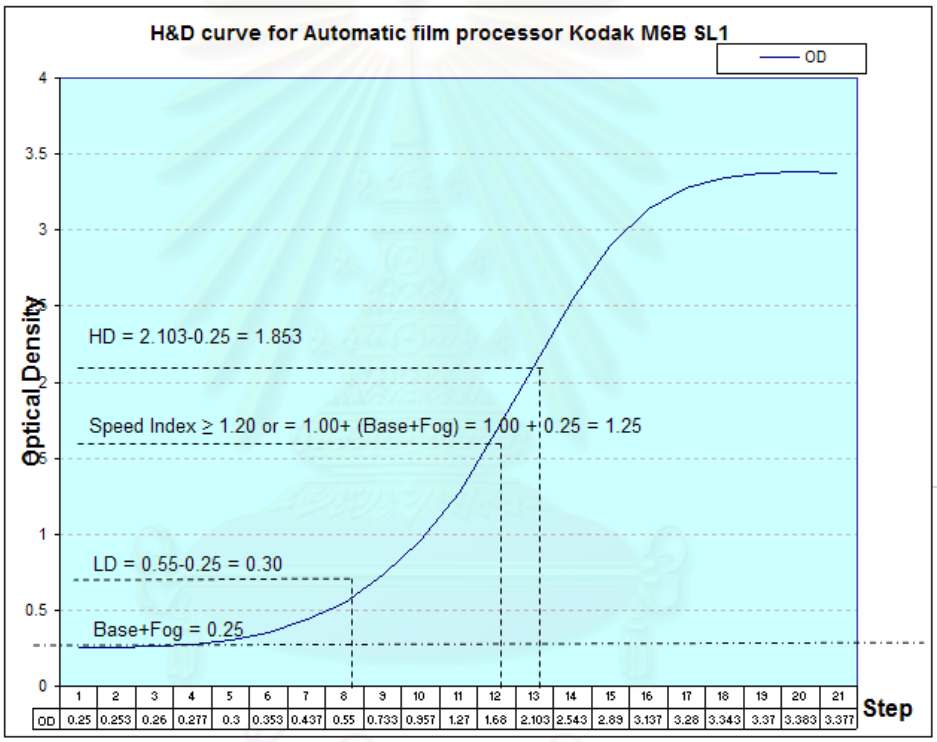

The processing control chart was constructed and was used to record and monitor the processor performance parameters. These parameters were measured before the first film was developed, with the tolerance of speed index 1.25 ± 0.2, contrast index 1.553 ± 0.2, base+fog 0.25 ± 0.03, and temperature index 34.93 ± 0.3 to provide the consistent of processor performance. The graphs were plotted for 3 times of measurement. The result showed the good performance of the film processor, all the parameters were in the limit.

Date	Temp.	B+F	Speed Index	Contrast Low step	Contrast High step	Contrast Index
				8	13	HD-LD
22/04/2008	35	0.25	1.25	0.56	2.12	1.56
23/04/2008	35	0.26	1.26	0.55	2.1	1.55
24/04/2008	35.1	0.24	1.24	0.54	2.09	1.55

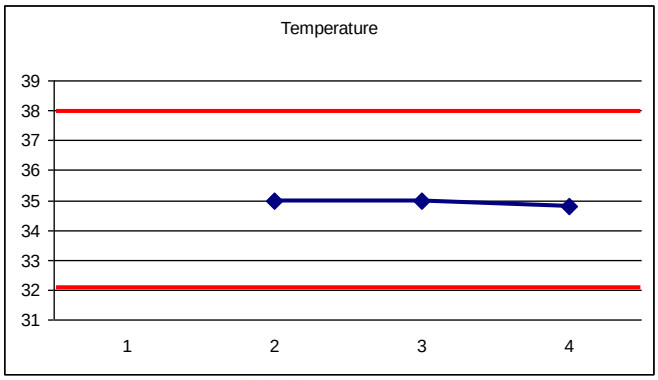

Temperature Index ±0.3

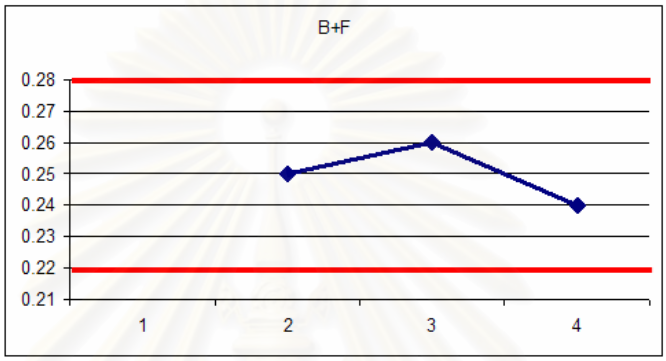

Base+Fog ± 0.03

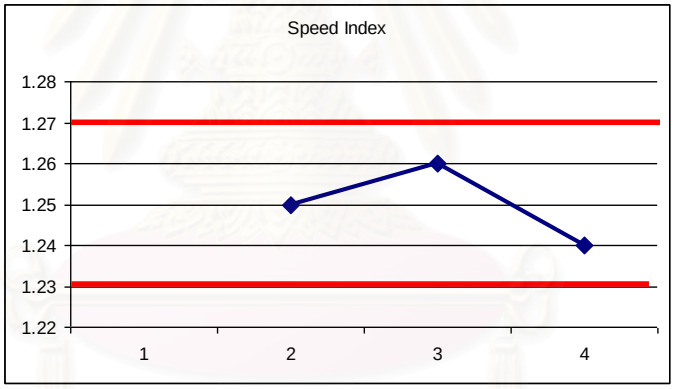

Speed Index ± 0.2

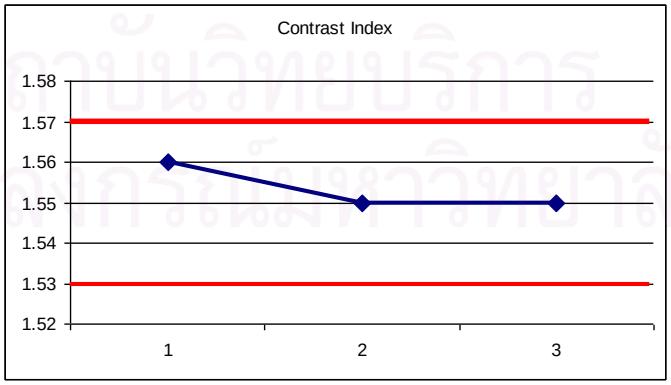

Contrast Index ± 0.2

APPENDIX B

REPORT OF RADIOGRAPHIC SYSTEM PERFORMANCE

LOCATION:	**BBR 4th floor, room 3**
DATE:	**10/03/08**
ROOM NUMBER:	**3**
MANUFACTURE:	**Seimens Polyphose, october 1988**
MODEL NUMBER	**8375040 G 2107**
SERIAL NUMBER	**01465-S01**

P	**GENERAL MECHANICAL CONDITIONS**
P	**ALL INDICATOR LAMPS AND "BEAM ON INDICATOR"**
N/A	**DEAD MAN SWITCH**
P	**SOURCE IMAGE DISTANCE INDICATOR (SID)**
P	**MECHANICAL MOTION TEST**
N/P	**FIELD SIZE INDICATION**
P	**LIGHT VRS RADIATION CONGRUENCE**
P	**CROSS HAIR CENTERING**
N/A	**AUTOMATIC COLLIMATION (PBL)**
N/A	**PHTO TIMER REPRODUCIBILTY AND DENSITY COMPENSATION**
P	**EXPOSURE REPRODUCIBILTY**
P	**LINEARITY OF EXPOSURE WITH mA/mAs**
N/A	**TIMER ACCURACY**
P	**BEAM QULITY (HVL)**
P	**KVP ACCURACY**
N/A	**ENTRANCE SKIN EXPOSURE (ESE)**

P	**PASS**
F	**FAIL**
N/A	**NOT APPLICABLE**
N/P	**NOT PERFORMED**
NOTE	**RECOMMENDATION SUGGESTED**

GENERAL CONDITION OF MECHANICAL AND ELECTRICAL COMPONENTS

n	Are there any frayed or exposed electrical wires?
n	Could the electrical wires interfere with the use of the unit?
n	Is there a play in the couch when it is locked?
y	Does it have the freedom of movement it was designed for?
N/A	Is the couch level in the tube and perpendicular directions?
n	Is there a play in the tube when it is locked?
y	Does it have the freedom of movement it was designed for?
y	Does the visual and/or beam-on indicator function properly?
N/A	Is the "dead-man" switch installed properly?
y	Are all the indicator lamps functioning and properly?

comments:

SOURCE IMAGE RECEPTOR DISTANCE ACCURACY CHECK

Allowable limits	**2% of SID**	
Indicated SID	100.0	**Cm/In**
Measured SID	99.5	**Cm/In**
SID to table top or Bucky		
% Deviation	0.5	
Pass/fail	**PASS**	

Motion and Lock Test

Tube longitudinal	**OK**
Tube rotate	**OK**
Tube transverse	**OK**
Tube vertical	**OK**
Tube angulate	**OK**
Collimator jaws	**OK**
Collimator rotation	**OK**

comments:

Field Size Indication

The purpose of this test is to ensure that the radiographer can set the optical field size within 2% of SID for all field sizes. It is checked for two selected field sizes.

		SID	100			
Field size set		**Measured**		**%Deviation**		
A-c Axis	**Perp Axis**	**A-c Axis**	**Perp Axis**	**A-c Axis**	**Perp Axis**	**Pass/Fail**
10	10					PASS
20	20					PASS

Congruence of Light vrs Radiation Filed

The purpose of this test is to verify that the radiation field is aligned with the light field within 2% of SID for all field sizes. It is checked for two selected field sizes.

Light Field		**Radiation Fld**		**%Deviation**		
A-c Axis	**Perp Axis**	**A-c Axis**	**Perp Axis**	**A-c Axis**	**Perp Axis**	**Pass/Fail**
10	10	9.8	9.65	0.20	0.35	PASS
20	20	19.6	19.9	0.40	0.10	PASS

Cross-hair Centering

The purpose of this test is to verify that the center of optical and radiation fileds are within 2% of SID.

Deviation between the centers	**0.52**	cm
% Deviation	**0.52**	

comments:

Positive beam limiting device (PBL) test

N/A	Does the PBL system collimate within 5 seconds?
N/A	Does it collimate to larger than the cassette size?
N/A	Does its collimate to smaller than the casstette size?
N/A	Is there an over ride key?
N/A	With the key removed, is PBL automatically activated?

Cassette size		Light Field		%Deviation		
A-c Axis	Perp Axis	A-c Axis	Perp Axis	A-c Axis	Perp Axis	Pass/Fail
10.0	8.0	**N/A**	**N/A**	10.00	8.00	**N/A**
12.0	10.0	**N/A**	**N/A**	12.00	10.00	**N/A**

comments:

Photo Timer Performance Test

The purpose of this test is to verify that the Coeff. Of Variation of phototimed exposures is within 0.05 and the exposure increases and decreases with the density control function. Use 3.4 mm Cu at approximately 80 Kvp. Select center cell.

Kvp	70

Density	mAs/O.D.
N	**N/A**
N	**N/A**
N	**N/A**
N	**N/A**
-1	**N/A**
1	**N/A**

Mean of Normal Exposures	**N/A**
Standard Deviation	**N/A**
Coefficient of Variation	**N/A**
Pass/Fail	**N/A**

Reproducibility of Exposure

The purpose of this test is to verify that radiation exposure at 80 Kvp is reproducible with a CV of 0.05 or less. Select mid current and 1/10 of a second on mA and S or elsle select about 25 mAs on mAs only option machines. Select SCD=26".

	mA	Sec	mAs
			25

mR1	mR2	mR3	mR4
284.5	284.2	284.5	284.2

Mean Exposure	284.35
Standard Deviation	0.173
Coefficient of Variation	0.001
Pass/fail	PASS

comments:

mA or mAs Linearity

The purpose of this test is to verify that mR/mAs measured at two adjacent mA stations or mAs settings are linear and retains a COV of less than 0.1. Select around 80 Kvp

kVp	mA	Sec	mAs	mR	mR/mAs	COV
81	2.22	0.9	2.0	23.8	11.89	
81	2.25	1.11	2.5	29.5	11.80	0.004
81	2.32	1.38	3.2	36.7	11.48	0.014

Timer Accuracy

The purpose of this test is to verify that the measured time is within 10% of the set time. A set of three typical times are used for this test.

Set Time		Measured	% Dev
Fraction	**Decimal**		
N/A			
N/A			
N/A			
N/A			

comments:

Beam Quality (HVL) Measurement

The purpose of this test is to verify that there is minimum of 2.3 mm of Al HVL in the beam at 80 kVp.

Filter Thickness mm of Al	Exposure mR
0.0	291.3
2.0	188.4
3.0	157.1

50% of open 145.7

HVL	3.37	**mm of Al**

Kvp Accuracy and mR/mAs Test

The purpose of this test is to verify that the average kVp is within 10% of set kVp and mR/mAs at 40" is within the norms published in NCRP #33

Select SCD of 26"

kVp							
Set	**Measured**	**mR**	**mA**	**Sec**	**mAs**	**mR/mAs**	**% KvP Deviation**
40	38.7	34.59	23	1.07	25	1.384	3.23
50	46.3	80.58	28	0.89	25	3.223	7.42
60	56.3	139.7	32	0.78	25	5.588	6.25
70	64.6	202.5	28	0.903	25	8.100	7.76
81	76.3	284.3	23	1.064	25	11.372	5.77
90	85.0	356.7	21	1.196	25	14.268	5.53
102	97.6	467.5	18	1.383	25	18.700	4.35

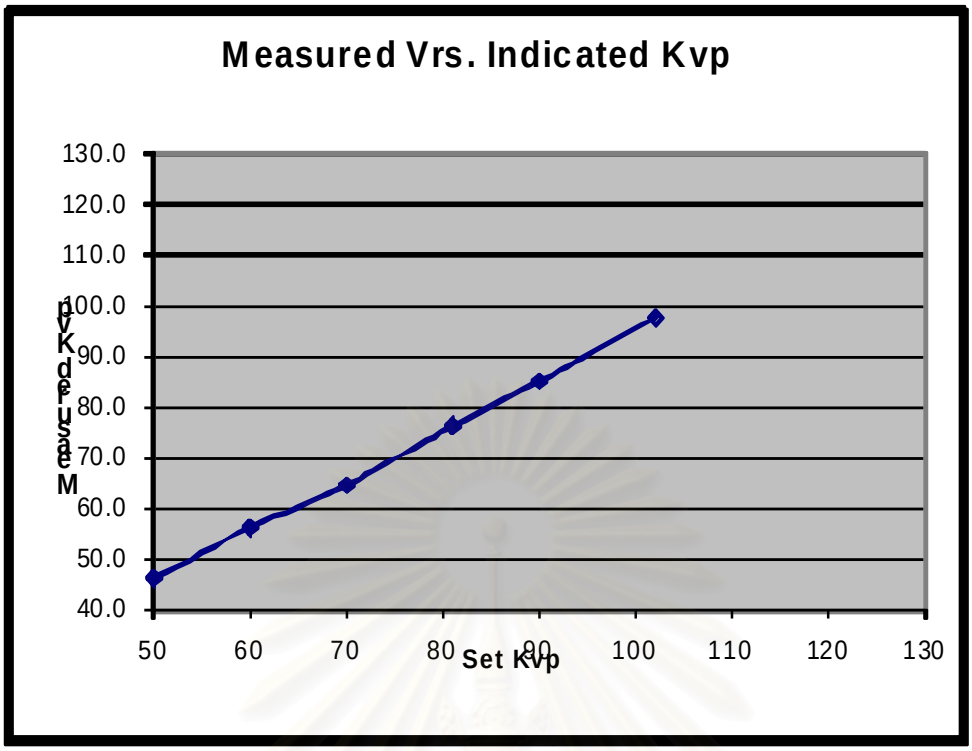
Measured Vrs. Indicated Kvp
130.0
120.0
110.0
100.0
90.0
80.0
70.0
60.0
50.0
40.0
50
60
70
80
90
100
110
120
130
Set Kvp

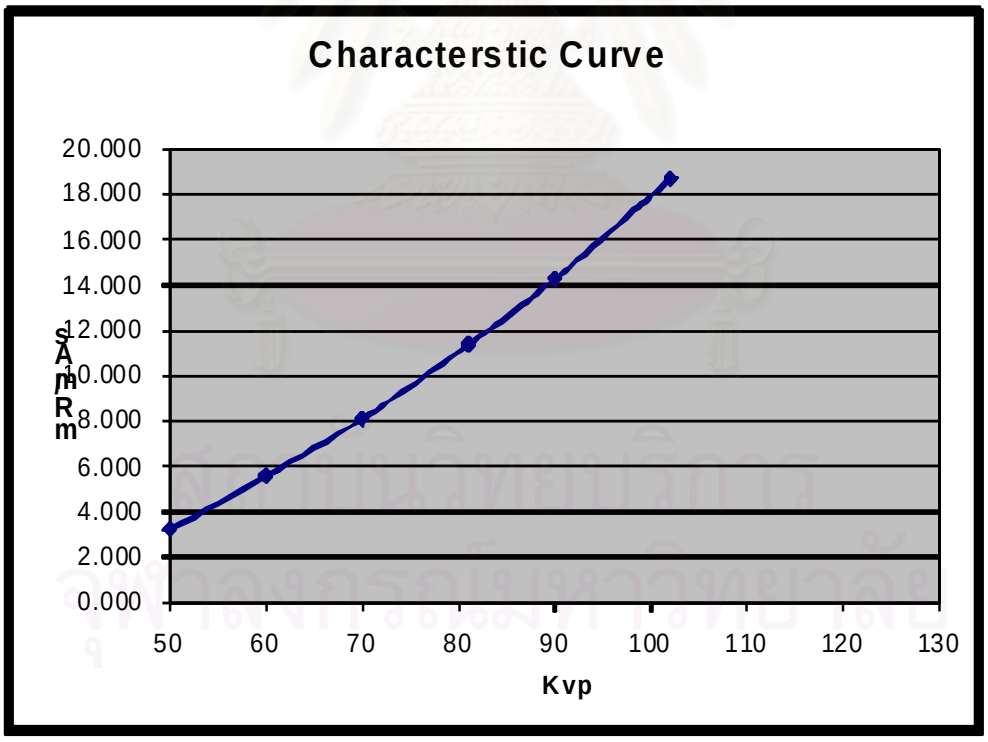
Characterstic Curve
20.000
18.000
16.000
14.000
12.000
10.000
8.000
6.000
4.000
2.000
0.000
50
60
70
80
90
100
110
120
130
Kvp

FOCAL SPOT SIZE

The purpose of this test is determine the focal spot using siemens star with a view to monitor blooming of the focal spot over time. The same technique has to be used each year.

	Set kVp:	44	Set mA: 2.5	Set time:	1
Degree of Star:		2	Large or Small Focal Spot:		S
Star dimension:					
Actual:	5.5		Radiographic:	10.83	
Blurr:	14.985		Manufacturer specification:		

Computed Focal Spot Size: **0.540** Meets NEMA:

	Set kVp:		Set mA:	Set time:	
Degree of Star:			Large or Small Focal Spot:		
Star dimension:					
Actual:			Radiographic:		
Blurr:			Manufacturer specification:		

Computed Focal Spot Size: Meets NEMA:

Comments:

PHOTO TIMER CONSTANCY

Set kVp:	**N/A**	Phantom:	**N/A**
mAs:	**N/A**	O.D.:	**N/A**
Mean:	**N /A**	Mean:	**N/A**
Std. Dev.:	**N/A**	Std. Dev.:	**N/A**
C.V.:	**N/A**	C.V.:	**N/A**

APPENDIX C

REPORT OF COMPUTED TOMOGRAPHY SYSTEM PERFORMANCE

LOCATION	**Alizabeth building**
DATE	23/04/2008
ROOM NUMBER	**CT simulator room**
MANUFACTURER	**GE LightSpeed RT**
M/N AND S/N	**2374681-2 / 35179CN1**

N/P	**Scan Localization Light Accuracy**
P	**Alignment of Table to Gantry**
P	**Table Increments Accuracy**
N/P	**Slice Increment Accuracy**
N/P	**Gantry Tilt**
P	**Radiation Profile Width**
	Beam Alignment
P	**C.T. # Position Dependence and S/N**
P	**Reproducibilty of C.T. Numbers**
P	**mAs Linearity**
P	**Multiple Scan Average Dose**
P	**Linearity of C.T. Numbers**
P	**High Contrast Resolution**
	Low Contrast Resolution

Scan Localization Light Accuracy

Purpose: To test congruency of scan localization light and scan plane

Method : Tape Localization film to the backing plate making sure that the edges of the film are parallel to the plate edge. Place the film vertically along the midline of the couch aligned with its longitudinal axis. Raise the table to the head position. Turn the alignment light. Mark both internal and external light with unique pin pricks along the midline of the light. Expose the internal light localization using the narrowest slice setting at 120-140 Kvp, 50-100 mAs. For external light increment table to light position under software control and expose the film. The centre of the rradiation field from the pin pricks should be less than 2 mm.

Results:	Measured Deviation	External	**N/P**	mm
		Internal	**N/P**	mm

Comments:

Alignment Of Table To Gantry

Purpose: To ensure that long axis of the table is horizontally aligned with a verical line passing through the rotational axis of the scanner

Method: Locate the table midline using a ruler and mark it on a tape affixed to the table. With the gantry untitled, extend the table top into gantry to tape position. Measure the horizontal deviation between the gantry aperture centre and the table midline. The Deviation should be within 5 mm

Results:

	Table	Bore
Distance from Right to Centre:	20.5	39.5
Distance from Centre to Left:	20.5	40
Measured Deviation:	0	0.25

Comments:

Table Increment Accuracy

Purpose: To determine accuracy and reproducibilty of table longitudinal motion

Method: Tape a measuring tape at the foot end of the table. Place a paper clip at the center of the tape to function as an indicator. Load the table uniformly with 150 lbs. From the initial position move the table 300, 400 and 500 mm into the gantry under software control (+ ve). Record the relative displacement of the pointer on . the ruler. Reverse the direction of motion (-ve) and repeat. Repeat the measurements four times. Positional errors should be less than 3 mm. At 300 mm position.

Results:

Indicated	Measured	Deviation
300	300	0
400	400.5	0.5
500	500.5	0.5
-300	-300	0
-400	-400	0
-500	-500	0

Comments:

Slice Increment Accuracy

Purpose: To Determine the accuracy of the slice increment.

Method: Set up as you would for beam profile measurement. Select 120 Kvp, 100 mAs, smallest slit width. Perform several scans with different programmed slice seperations under auto control. Scan the film with a densitometer and measure the distance between the peaks

Slice Sep in mm	Measured Sep in mm	Deviation
20	**N/P**	**N/P**
30	**N/P**	**N/P**
50	**N/P**	**N/P**

Comments:

Gantry Angle Tilt

Purpose: To determine the limit of gantry tilt and the accuracy of tilt angle indicator

Method: Tape a localization film to the backing plate making sure that the edges of the film are parallel to the edges of the backing plate. Place the film vertically along the midline of the couch aligned with its longitudinal axis. Raise the table to the head position. Move the table into the gantry. Center plate to alignment light.

Expose the film at inner light location using narrowest slit, 120-140 kVp, 50-100 mAs. Tilt the gantry to one extreme from the console. Record the indicated gantry angle. Expose the film using the above technique. Measure the clearence from the closest point of gantry to midline of the table.

Tilt the gantry to it's extreme in the opposite direction. Record clearence and repeat the exposure. Measure the tilt angles from the images on the film. Deviation between indicated and measured tilt angles <= 3^0 . Gantry clearence should be >= 30 cm.

Results:

	Away	**Towards**
Indicated Angle	**N/P**	**N/P**
Measured Angle	**N/P**	**N/P**
Deviation	**N/P**	**N/P**
Clearence	**N/P**	**N/P**

Comments:

Position Dependence And S/N Ratio Of C.T. Numbers

Method: Position the C.T. head phantom centered in the gantry. Using 1 cm slice thickness , obtain one scan using typical head technique. Select a circular region of interest of approximately 400 sq. mm. And record the mean C.T. number and standard deviation for each of the positions 1 through 5

Technique:

Kvp	120	**mA**	250	**Seconds**	1

Results:

Position	**Mean C.T. #**	**S.D.**	**C.V.**
1	0.21	3.11	14.810
2	0.69	3.26	4.725
3	0.87	3.22	3.701
4	1.00	3.19	3.190
5	0.19	3.52	18.526

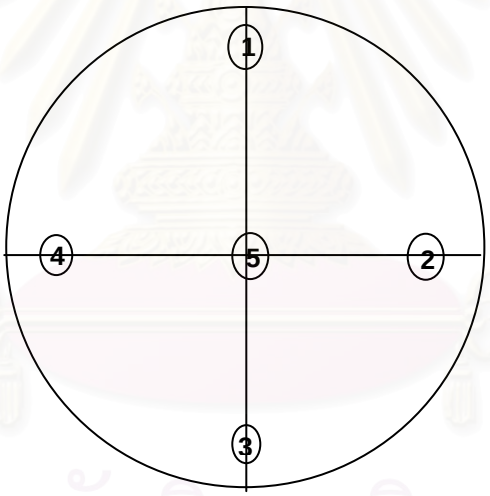

Comments:

Reproducibilty of C.T. Numbers.

Method: Using the same set up and technique as position dependence, obtain three scans. Using the same ROI as position dependence in location 5, which is the center of the phantom, obtain mean C.T. numbers for each of the four scans. The coefficient of variation of mean C.T. numbers of the four scans should be less than 0.002

Results:

Run Number	**1**	**2**	**3**	**4**
Mean C.T. #	0.19	0.25	0.34	0.48

Mean Global C.T. Number	0.315
Standard Deviation	0.126
Coefficient Of variation	0.400

mAs Linearity

Method: Set up the same as position dependence and insert 10 cm long pencil chamber in the center slot of the C.T. dose head phantom. Select the same kvp and time as used for head scan. Obtain four scans in each of the mA stations normally used in the clinic. For each mA station record the exposure in mGy for each scan. Scans should be performed in the increasing order of mA. Compute mGy/mAs for each mA setting.

Technique: **kVp** 120 **Sec** **1** **FOV** 92.89

	Exposure in mGy					
mA	**Run 1**	**Run 2**	**Run 3**	**Run 4**	**mR/mAs**	**C.V.**
10	2.021	2.03	2.02		0.20	
20	4.046	4.055	4.055		0.20	0.001
50	10.14	10.1	10.19		0.20	0.001
100	20.22	20.23	20.25		0.20	0.001
150	30.36	30.34	30.35		0.20	0.000
200	40.4	40.45	40.42		0.20	0.001
300	85.06	85.04	85.05		0.28	0.168

Comments:

Linearity Of C.T. Numbers

Method: Set up the mini C.T. performance phantom as described in beam alignment. Select the section containing the test objects of different C.T. numbers. Select the head technique and perfrom a single transverse scan. Select a region of interest (ROI) of sufficient size to cover the test objects. Place the ROI in the middle of each test object and record the mean C.T. number.

Technique:

kVp:	120	**mA:**	250
Sec:	1	**FOV:**	92.89
Slice Thickness in mm:	10 mm		

Results:

Material	**Expected CT #**	**Measured CT #**
LPDE	-100	-86.66
PMP	-200	-174.56
AIR	-1000	-958.67
TEPLON	990	940.05
DELRIN	340	350.84
ACYLIC	120	125.22

Note: **Expected C.T. numbers are either the predicted ones or the ones obtained during the previous annual measurement.**

Comments:

High Contrast Resolution:

Method: Set up the mini C.T. performance phantom as described in beam alignment. Select the section containing the high resolution test objects. Select the head technique. Perform a single transverse scan. Select the area containing the high resolution test objects and zoom as necessary. Select appropriate window and level for the best visualization of the test objects. Record the smallest test object visualized on the film.

Technique:

kVp: 120	**mA:** 250
Sec: 1	**FOV:**

Results:

Slice Thickness in mm	Resolution lp/cm
10	6
7.5	4
5	4
3.75	4
2.5	3
1.25	4

Comments:

Low contrast Resolution:

Method: Select the section containing the low resolution test objects in the mini phantom. Perform a single transverse scan utilizing the same technique as high resolution

Technique:

kVp:	**mA:**
Sec:	**FOV:**

Results:

	Resolution	
Slice Thickness in mm		
10	2.0	3.0
7.5	3.0	5.0
5	3.0	3.0
3.75	5.0	5.0
2.5	5.0	5.0
1.25	6.0	9.0

Multiple Scan Average Dose

Skull Technique		Run Number	Exposure in mR
kVp		1	
mA		2	
Scan Time Sec		3	
Slice Thickness	10 mm	4	
Slice Increment	0	Mean Exposure	

MSAD=(E x f x K x L)/T
E=Average exposre reading
f= Factor to convert exposure in air
to absorbed dose
f=0.00078 rad/mR
K=Calibration factor of radiation
measuring system K=1
L= Effective length(mm) of radiation
measuring system
T= Tomographic slice thickness
in mm

Mean Exposure	
S.D.	
C.V.	

f=	L=

Calculated MSAD	rad

Slice Thickness Accuracy

Purpose: To Determine the accuracy of the slice thickness.

Method: Set up as you would for beam profile measurement. Select 120 kVp, 100 mAs, smallest slit width. Perform several scans with different programmed slice thicknesses under auto control. Scan the film with a densitometer and measure the full width at half maximum distance.

Slice Thick in mm	Measured Thick in mm	Deviation
5	6.9	**1.9**
10	11.3	**1.3**
15	16.5	**1.5**
20	20	**0**

Comments:

APPENDIX D

CR SYSTEM CALIBRATION

Result	Calibration test	Criteria
P	**Monitor & laser printer setup**	5% on 0% and 95% on 100% should be visible. Horizontal and vertical resolution should not differ by greater than 20 %
P	**Dark noise**	Artifact free should be expect
P	**Erasure cycle efficiency**	Absence of a ghost image of the first exposure in the re – exposed image.
F*	**Sensitivity index calibration**	Indicated exposure should be agreed within 20% from measured exposure.
N/P	**Sensitivity index consistency**	No different of indicated exposure between plate greater than 20%
P	**Uniformity**	Variation should be less than 10%
P	**Scaling error**	Measured distance should be agree within 3%
P	**Blurring**	No blurring.
P	**Limiting spatial resolution**	45^0 direction > 1.2/2p Scan and sub scan direction > 0.85/2p (p is pixel dimension in mm.)
N/P	**Threshold contrast detail delectability**	Compare with another QA test
P	**Laser beam function**	The edge should be continues across the full length of the image. No aliasing of the edge.
N/P	**Moire pattern**	No Moire pattern should be visible

P = pass
F = fail
N/P = not perform

* = This test couldn't perform with calibration protocol because the x – ray machine cannot set parameter that made 1 μGy irradiated. We test with 11.35 μGy

Monitor & laser printer setup

Purpose: to test that device used to view the image data are sufficient quality to maximize the information available to the observer.

Result: 5% on 0% and 95% on 100% detail are clearly visible. All of Horizontal and vertical resolution bar are clearly visible.

Dark noise

Purpose: to assess the level inherent noise of the system

Result: No artifact displayed on the image.

Erasure cycle efficiency

Purpose: to test that minimal residual signal (ghosting) remains on a plate after readout and erasure.

Result: No ghost image from re –exposed image.

Sensitivity index calibration

Purpose: To assess the accuracy of the plate exposure values calculated using exposure indicators.

Result:

µGy	11.35	kVp	81
mAs	25	SID	150 cm

Sensitivity	113	
indicated exposure	15.39823	µGy

tolerance	0.35	FAIL

Note: the QC protocol use 1 µGy, but we used 11.35 µGy because system limitation.

Sensitivity index consistency

Purpose: to assess the variation of sensitivity between plates, and set a baseline for monitoring system sensitivity for future QA testing.

Result: Not Perform, we have only 1 QC imaging plate

Uniformity

Purpose: to assess the uniformity of the recorded signal from uniformly exposed plate. A non uniform response could affect image quality.

Result:

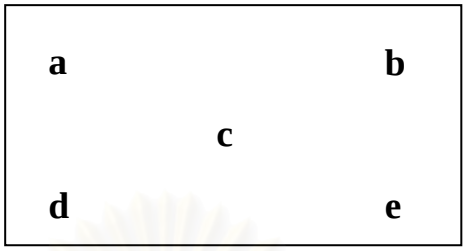

L	1	S	200

a	b	c	d	e	average	SD
1012	1012	1012	1004	1004	1008.8	3.919184

PASS

Scaling error

Purpose: to assess the accuracy of software distance indicators and check for distortion.

Result:

expected	measurement	
1	1.01	-1.00%
2	1.99	0.50%
3	3.02	-0.67%
4	3.99	0.25%
5	4.98	0.40%
0.5	0.51	-2.00%

PASS

Blurring

Purpose: to test for any localized distortion or blurring the image.

Result: no blurring of the image.

Limiting spatial resolution

Purpose: To test the high contrast limit of systems ability to resolve detail.

Direction	pattern	lp/mm.
Scan	18	3.55
sub-scan	18	3.55
45^0	17	3.15

Result: Pass

Threshold contrast detail delectability

Purpose: To monitor image quality by assessing the visibility of low contrast detail.

Result: Not perform.

Laser beam function

Purpose: To assess laser beam scan line integrity and jitter

Result: each edges of the image are uniform across full length of the image. The most sharpen edge of the image is result on “scan” direction.

Moire pattern

Purpose: To test the presence of Moire pattern artifacts caused by grids

Result : Not perform.

VITAE

NAME:	Mr. Sirapath Sirarojnkul
DATE OF BIRTH:	May 30, 1984
PLACE OF BIRTH:	Bangkok, Thailand
INSTITUTIONS ATTENDED:	Thamasart University, 2005: Bachelor of Science (Physics) Chulalongkorn University, 2009: Master of Science (Medical Imaging)
HOME ADDRESS:	325/11 Ramintra 5, Anusaovaree, Bangkhen, Bangkok, 10220